US010984075B1

(12) **United States Patent**
Liang et al.

(10) **Patent No.: US 10,984,075 B1**
(45) **Date of Patent: Apr. 20, 2021**

(54) **HIGH DIMENSIONAL TO LOW DIMENSIONAL DATA TRANSFORMATION AND VISUALIZATION SYSTEM**

(71) Applicant: **SAS Institute Inc.**, Cary, NC (US)

(72) Inventors: **Yu Liang**, Cary, NC (US); **Arin Chaudhuri**, Raleigh, NC (US); **Haoyu Wang**, Cary, NC (US)

(73) Assignee: **SAS Institute Inc.**, Cary, NC (US)

(*) Notice: Subject to any disclaimer, the term of this patent is extended or adjusted under 35 U.S.C. 154(b) by 0 days.

(21) Appl. No.: **17/069,293**

(22) Filed: **Oct. 13, 2020**

Related U.S. Application Data

(60) Provisional application No. 63/057,141, filed on Jul. 27, 2020, provisional application No. 63/047,111, filed on Jul. 1, 2020.

(51) **Int. Cl.**
G06F 17/16 (2006.01)
G06F 16/28 (2019.01)
(Continued)

(52) **U.S. Cl.**
CPC ***G06F 17/16*** (2013.01); ***G06F 16/283*** (2019.01); ***G06F 16/287*** (2019.01);
(Continued)

(58) **Field of Classification Search**
None
See application file for complete search history.

(56) **References Cited**

U.S. PATENT DOCUMENTS

5,835,901 A * 11/1998 Duvoisin G06K 9/627 706/19
6,035,057 A * 3/2000 Hoffman G01S 7/12 382/159

(Continued)

OTHER PUBLICATIONS

Wen Li, Ying Zhang, Yifang Sun, Wei Wang, Wenjie Zhang, Xuemin Lin "Approximate Nearest Neighbor Search on High Dimensional Data—Experiments, Analyses, and Improvement", Oct. 8, 2016 arXiv:1610.02455 (Year: 2016).*

(Continued)

Primary Examiner — Polina G Peach
(74) *Attorney, Agent, or Firm* — Bell & Manning, LLC

(57) **ABSTRACT**

A computer transforms high-dimensional data into low-dimensional data. A distance is computed between a selected observation vector and each observation vector of a plurality of observation vectors, a nearest neighbors are selected using the computed distances, and a first sigmoid function is applied to compute a distance similarity value between the selected observation vector and each of the selected nearest neighbors where each of the computed distance similarity values is added to a first matrix. The process is repeated with each observation vector of the plurality of observation vectors as the selected observation vector. An optimization method is executed with an initial matrix, the first matrix, and a gradient of a second sigmoid function that computes a second distance similarity value between the selected observation vector and each of the nearest neighbors to

(Continued)

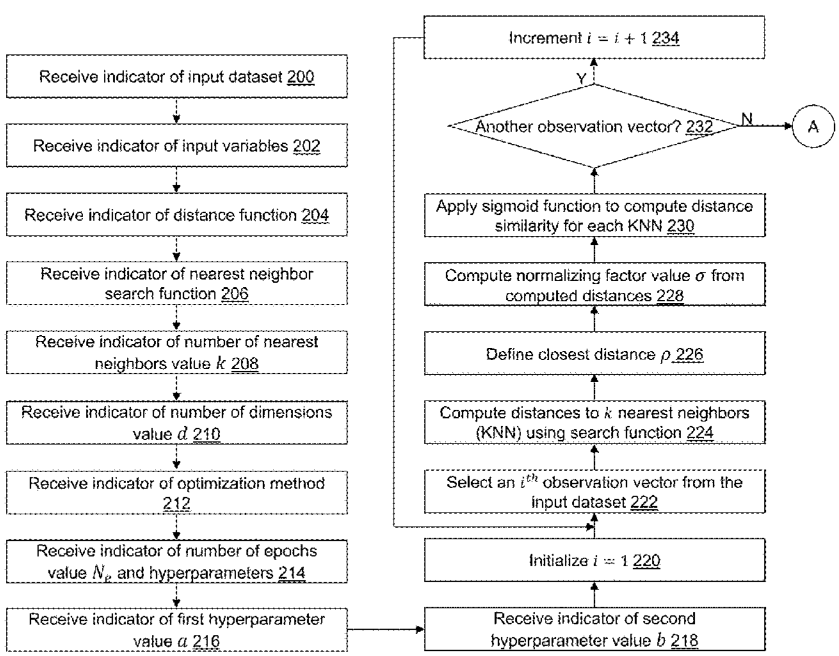

transform each observation vector of the plurality of observation vectors into the low-dimensional space.

30 Claims, 47 Drawing Sheets
(36 of 47 Drawing Sheet(s) Filed in Color)

(51) **Int. Cl.**
G06N 20/00 (2019.01)
G06F 17/17 (2006.01)
G06K 9/62 (2006.01)
(52) **U.S. Cl.**
CPC ***G06F 17/175*** (2013.01); ***G06K 9/6276*** (2013.01); ***G06N 20/00*** (2019.01)

(56) **References Cited**

U.S. PATENT DOCUMENTS

7,010,167	B1 *	3/2006	Ordowski	G06K 9/6267 345/644
7,043,514	B1 *	5/2006	Achlioptas	G06K 9/6247 708/401
7,230,973	B2 *	6/2007	Brunel	H04B 1/71057 375/130
9,665,405	B1 *	5/2017	Goodnight	G06Q 10/0635
9,893,742	B1 *	2/2018	Noma	H03M 7/40
10,148,680	B1 *	12/2018	Segev	H04L 63/1425
10,504,005	B1 *	12/2019	Walters	G06K 9/6267
10,824,603	B2 *	11/2020	Sastry	G06F 16/211
2007/0118297	A1 *	5/2007	Thayer	G16H 50/70 702/21
2010/0094611	A1 *	4/2010	Sankaranarayanan	G01R 31/318357 703/22
2010/0274539	A1 *	10/2010	Virkar	G06K 9/6254 703/2
2014/0108324	A1 *	4/2014	Chen	G06N 20/00 706/52
2015/0160098	A1 *	6/2015	Noda	G05B 23/024 702/35
2015/0248458	A1 *	9/2015	Sakamoto	H04L 9/3236 707/719
2017/0091637	A1 *	3/2017	Chae	G06N 5/003
2018/0089762	A1 *	3/2018	Lopez de Prado	G06N 5/003
2018/0182412	A1 *	6/2018	Kleijn	G10L 21/028
2018/0268015	A1 *	9/2018	Sugaberry	G06N 5/003
2018/0285459	A1 *	10/2018	Soni	G06N 5/02
2018/0341720	A1 *	11/2018	Bhatia	G06N 5/003
2019/0251467	A1 *	8/2019	Lokare	G06F 17/16
2020/0097997	A1 *	3/2020	Li	G06K 9/6251
2020/0311542	A1 *	10/2020	Wang	G06N 3/04
2020/0337650	A1 *	10/2020	Calhoun	A61B 5/165

OTHER PUBLICATIONS

H Jegou et al: "Product Quantization for Nearest Neighbor Search", IEEE Transactions on Pattern Analysis and Machine Intelligence, vol. 33, No. 1, Jan. 1, 2011 (Jan. 1, 2011), pp. 117-128 (Year: 2011).*

Mikolov, T., Sutskever, I., Chen, K., Corrado, G. S., and Dean, J. (2013). "Distributed Representations of Words and Phrases and Their Compositionality." In Advances in Neural Information Processing Systems, 3111-3119. La Jolla, CA: Neural Information Processing Systems Foundation.

Tang, J., Liu, J., Zhang, M., and Mei, Q. (2016). "Visualizing Large-Scale and High-Dimensional Data." In Proceedings of the 25th International Conference on World Wide Web, 287-297. Geneva: International World Wide Web Conferences Steering Committee.

McInnes, L., Healy, J., and Melville, L. (2018). "UMAP: Uniform Manifold Approximation and Projection for Dimension Reduction." arXiv preprint, arXiv:1802.03426.

Ceriotti, M., Tribello, G. A., and Parrinello, M. (2011). "Simplifying the Representation of Complex Free Energy Landscapes Using Sketch-Map." Proceedings of the National Academy of Sciences 108:13023-13028.

Radu Horaud, "A Short Tutorial on Graph Laplacians, Laplacian Embedding and Spectral Clustering," 2009—csustan.csustan.edu, 41 pages.

* cited by examiner

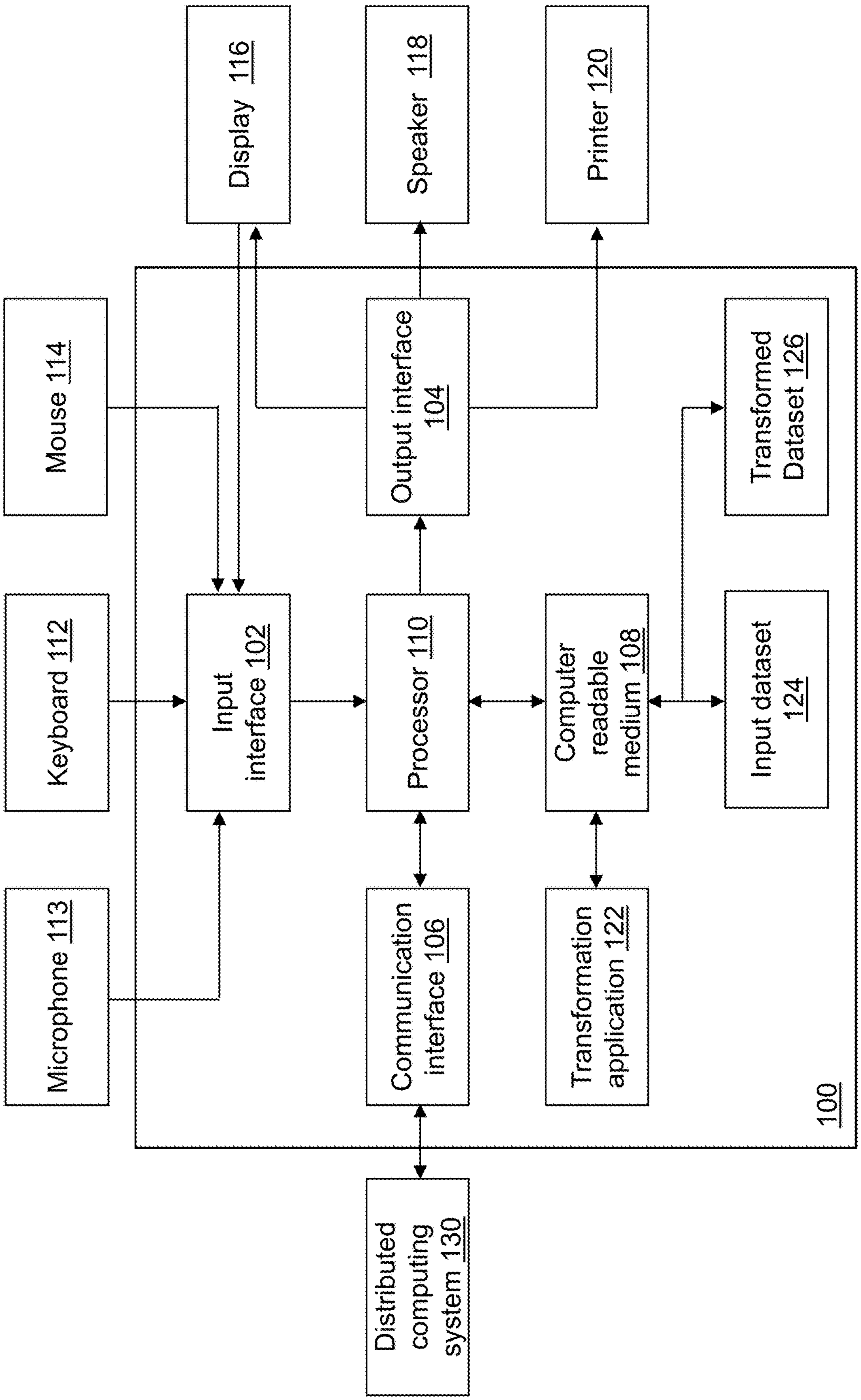
Display 116
Speaker 118
Printer 120
Mouse 114
Output interface 104
Transformed Dataset 126
Keyboard 112
Input interface 102
Processor 110
Computer readable medium 108
Input dataset 124
Microphone 113
Communication interface 106
Transformation application 122
100
Distributed computing system 130

FIG. 1

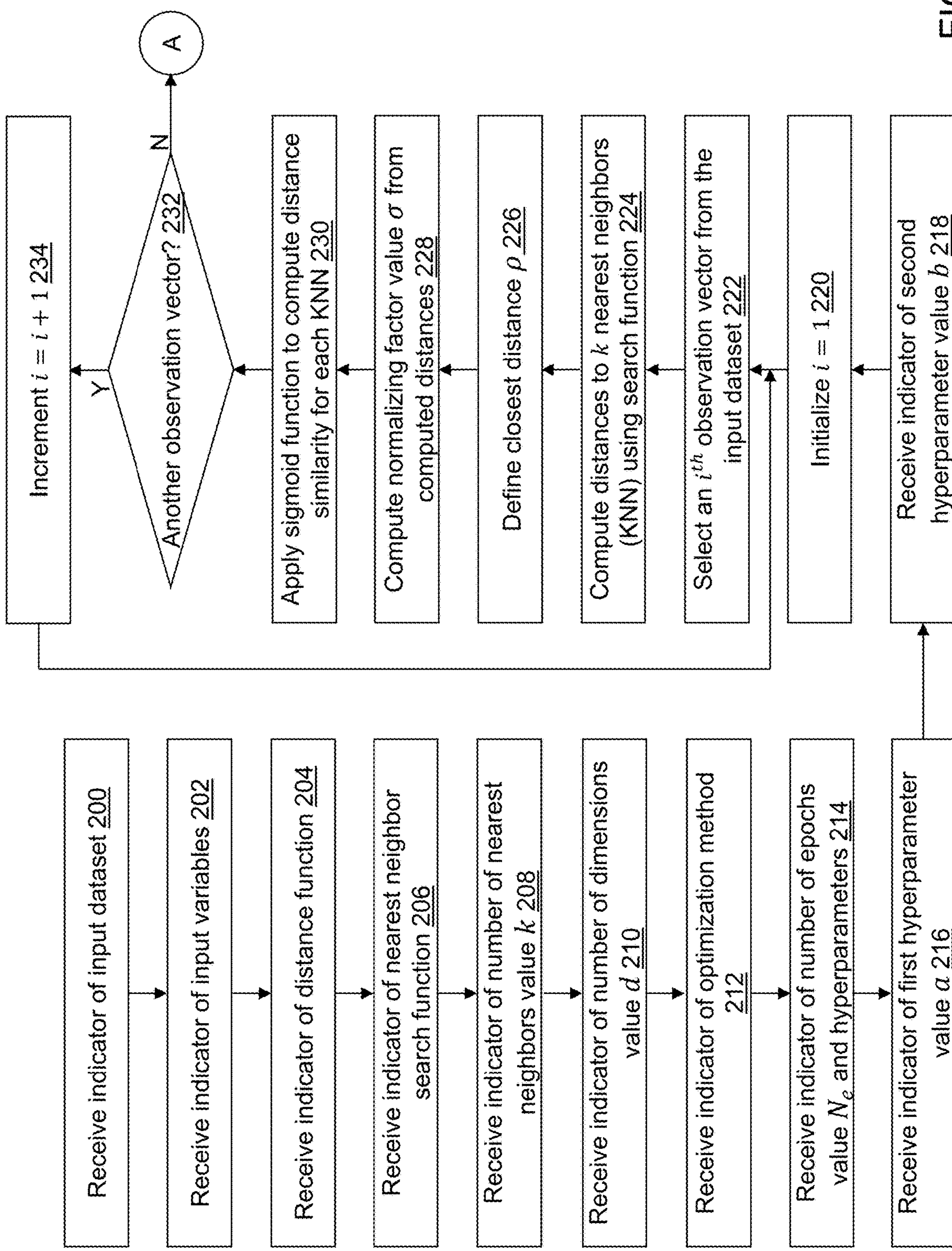
Receive indicator of input dataset 200
Receive indicator of input variables 202
Receive indicator of distance function 204
Receive indicator of nearest neighbor search function 206
Receive indicator of number of nearest neighbors value k 208
Receive indicator of number of dimensions value d 210
Receive indicator of optimization method 212
Receive indicator of number of epochs value N_e and hyperparameters 214
Receive indicator of first hyperparameter value a 216
Receive indicator of second hyperparameter value b 218
Initialize $i = 1$ 220
Select an i^{th} observation vector from the input dataset 222
Compute distances to k nearest neighbors (KNN) using search function 224
Define closest distance ρ 226
Compute normalizing factor value σ from computed distances 228
Apply sigmoid function to compute distance similarity for each KNN 230
Another observation vector? 232
Y
N
Increment $i = i + 1$ 234
A

FIG. 2A

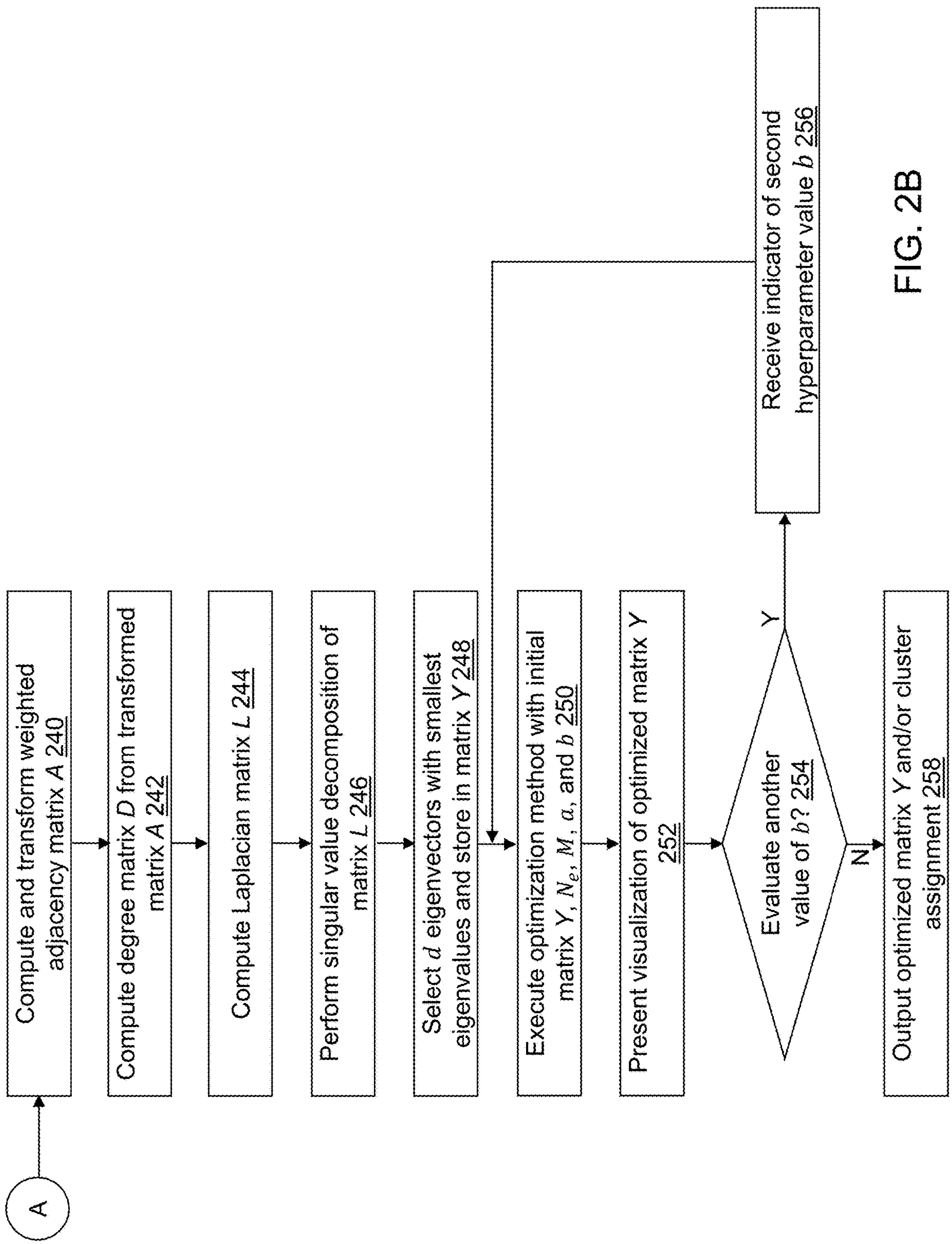
A
Compute and transform weighted adjacency matrix A 240
Compute degree matrix D from transformed matrix A 242
Compute Laplacian matrix L 244
Perform singular value decomposition of matrix L 246
Select d eigenvectors with smallest eigenvalues and store in matrix Y 248
Execute optimization method with initial matrix Y, N_e, M_i, a, and b 250
Present visualization of optimized matrix Y 252
Evaluate another value of b? 254
Y
N
Receive indicator of second hyperparameter value b 256
Output optimized matrix Y and/or cluster assignment 258

FIG. 2B

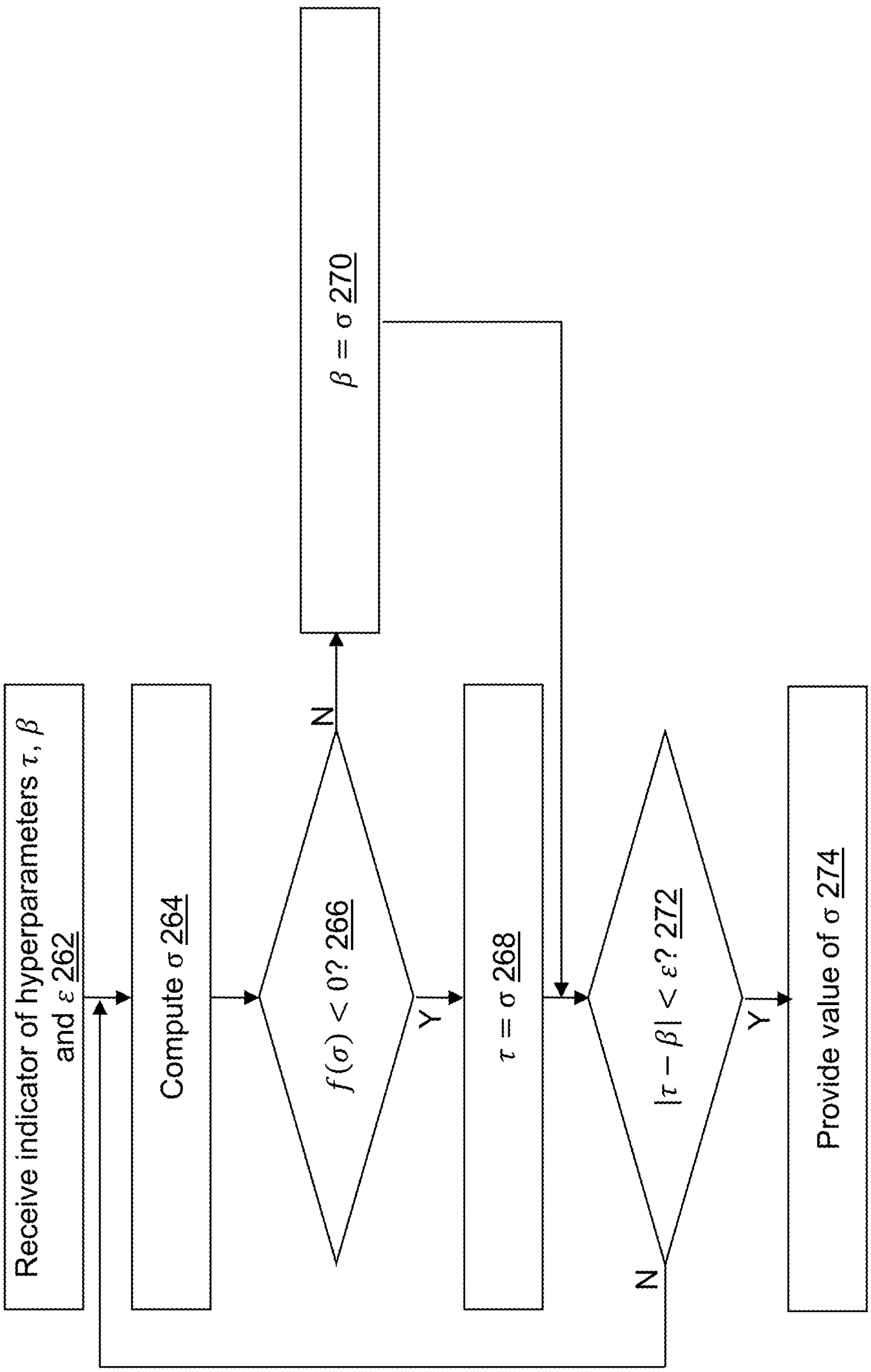
Receive indicator of hyperparameters τ, β and ε 262
Compute σ 264
$f(\sigma) < 0$? 266
N
Y
$\beta = \sigma$ 270
$\tau = \sigma$ 268
$|\tau - \beta| < \varepsilon$? 272
N
Y
Provide value of σ 274

FIG. 2C

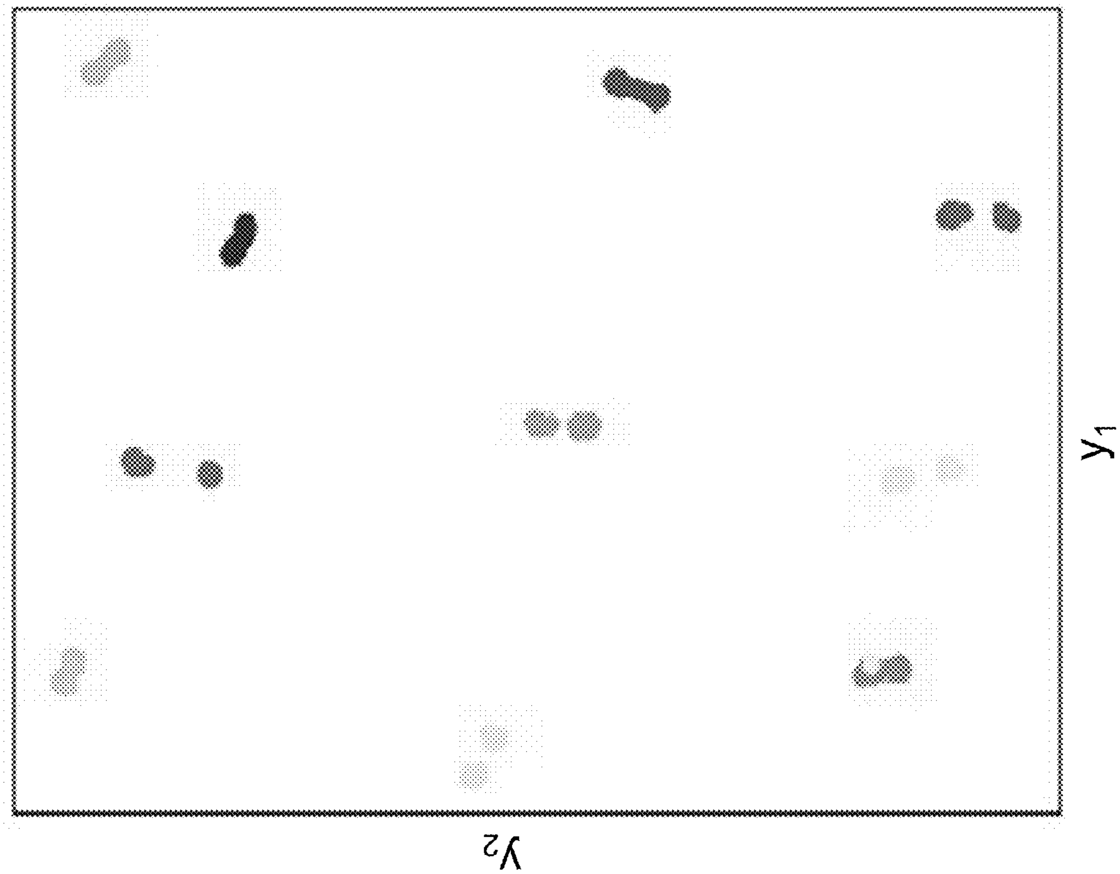

FIG. 3B

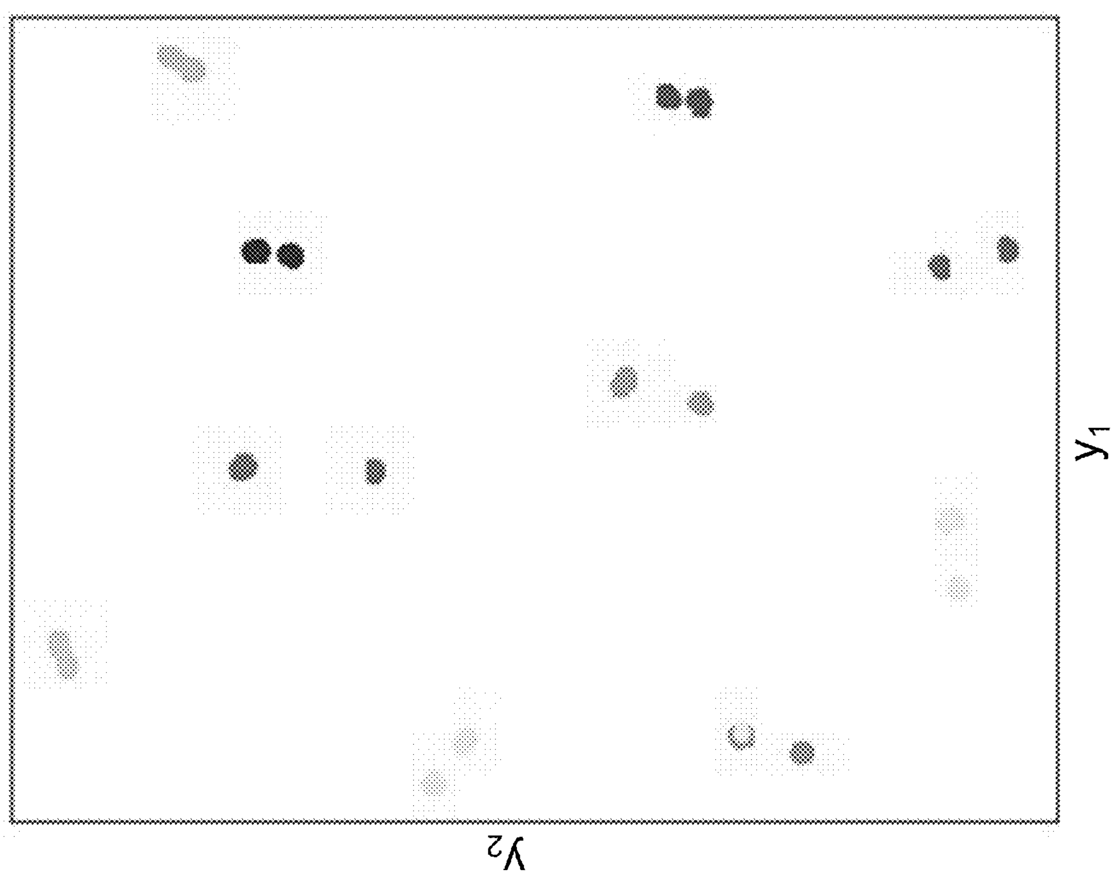

FIG. 3A

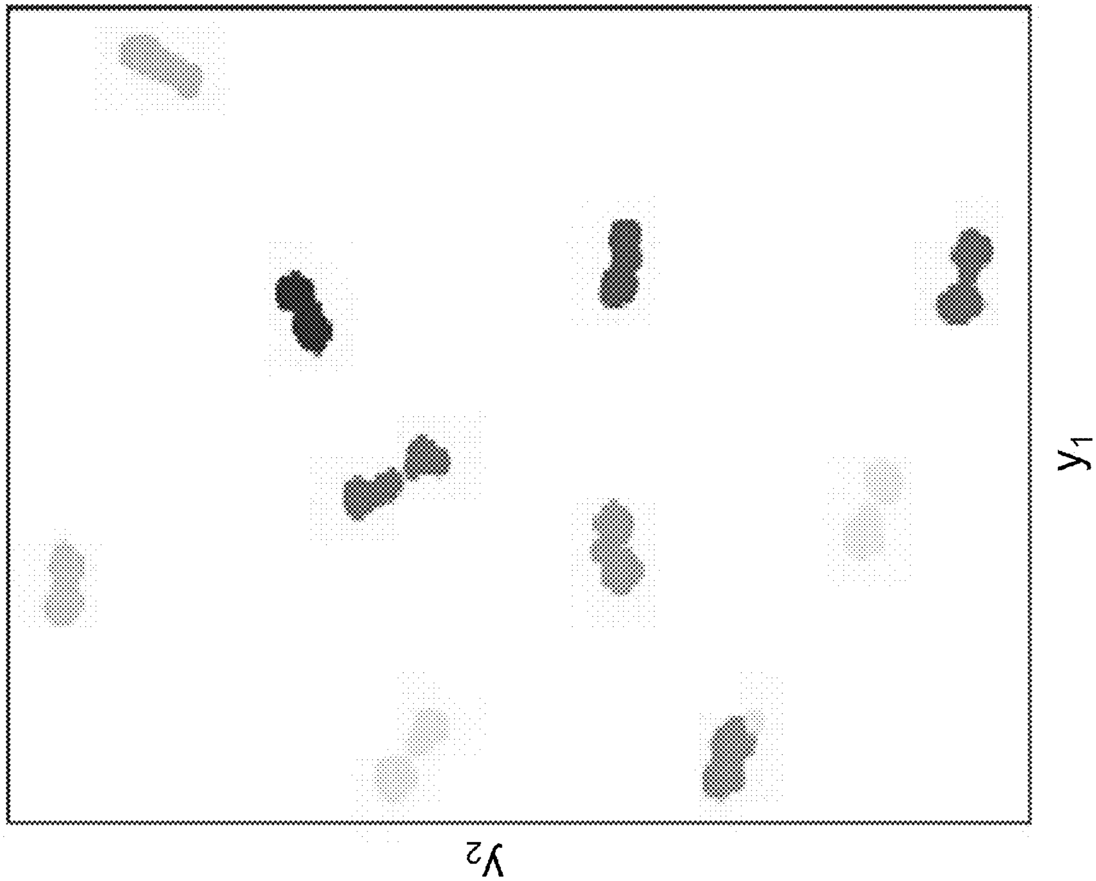

FIG. 3D

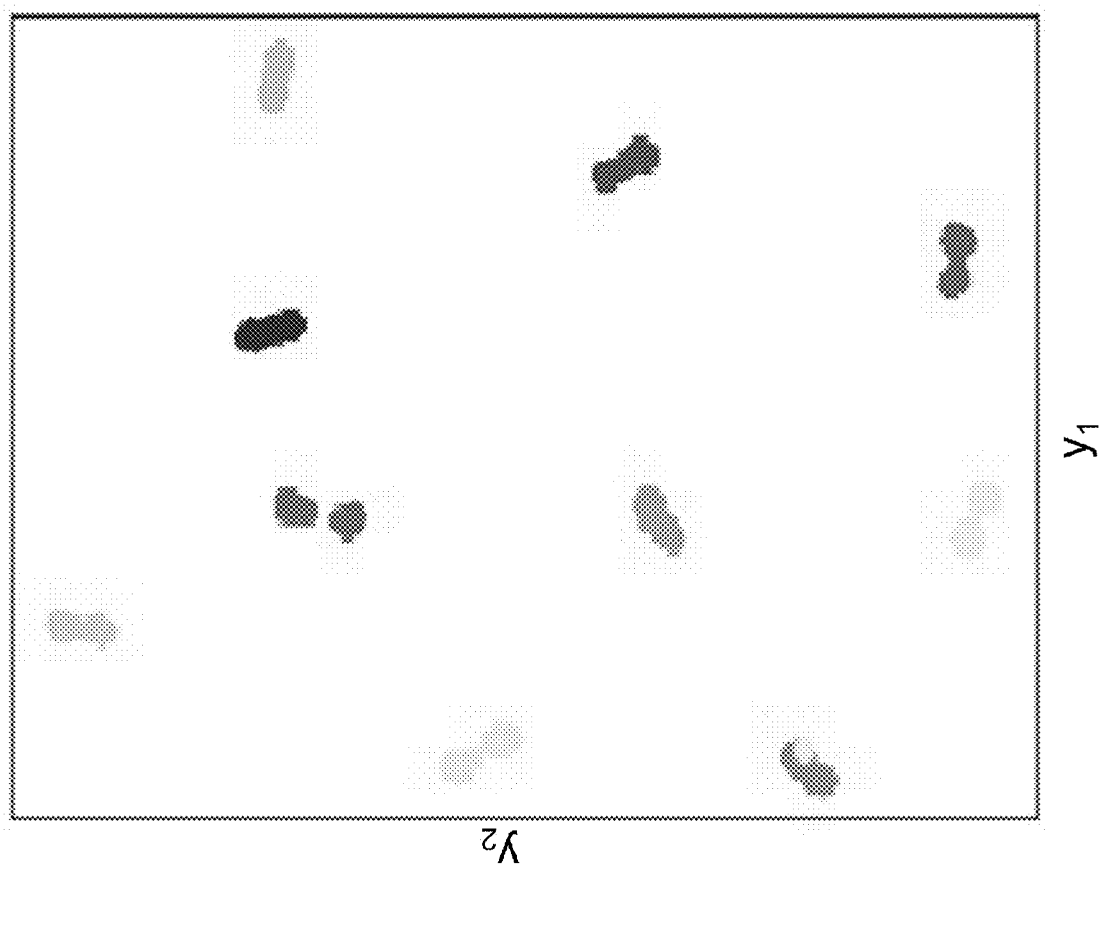

FIG. 3C

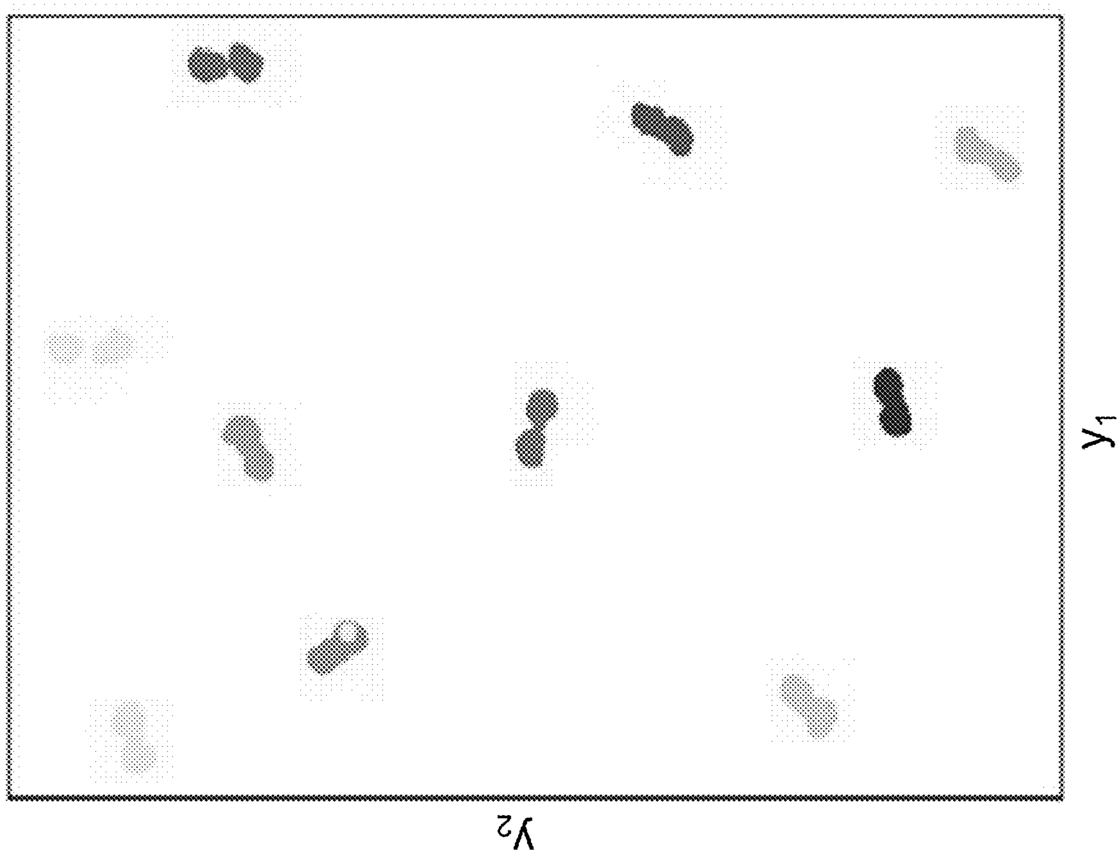

FIG. 4B

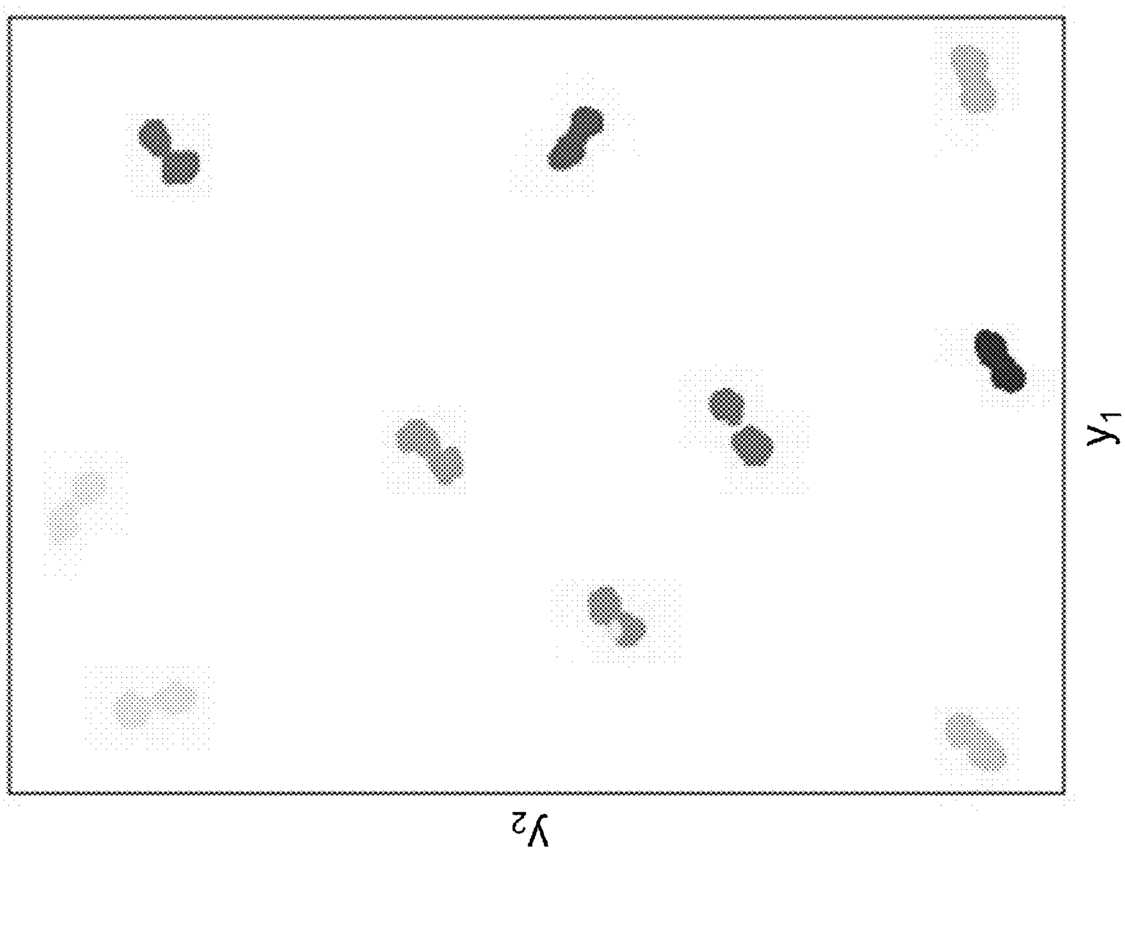

FIG. 4A

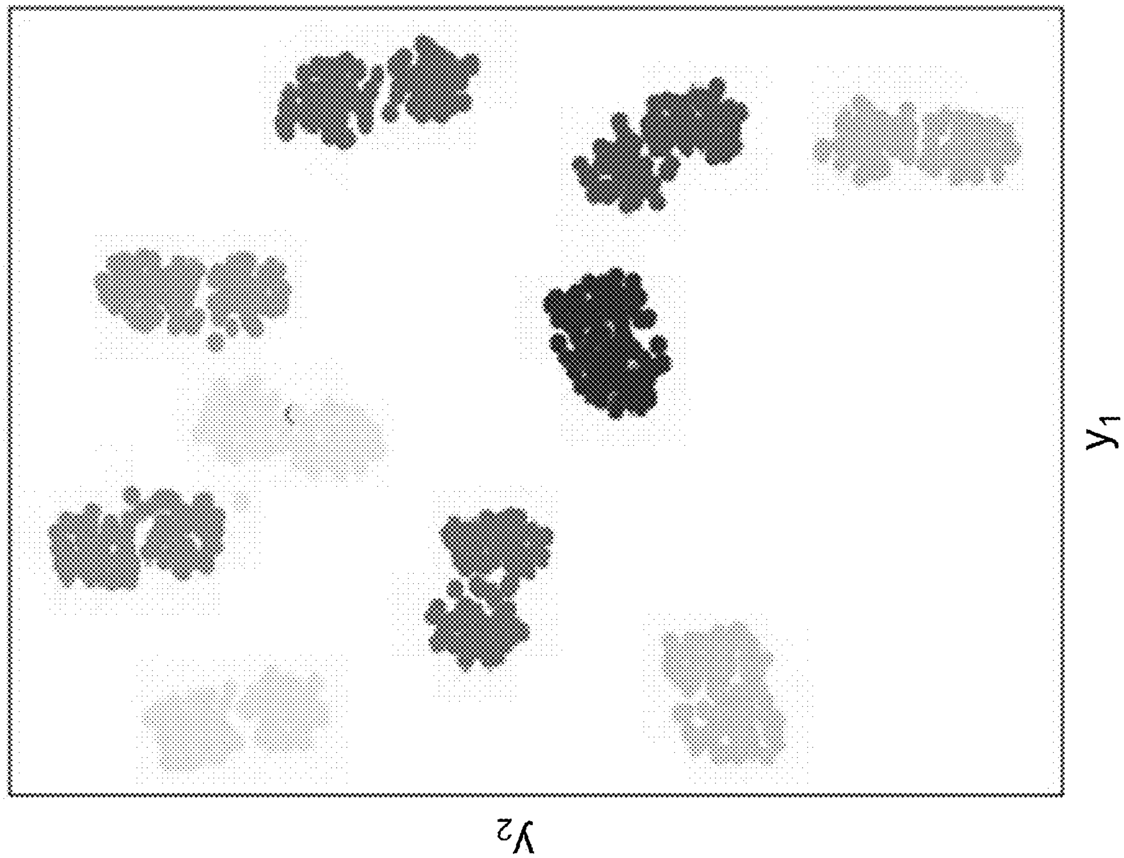

FIG. 4D

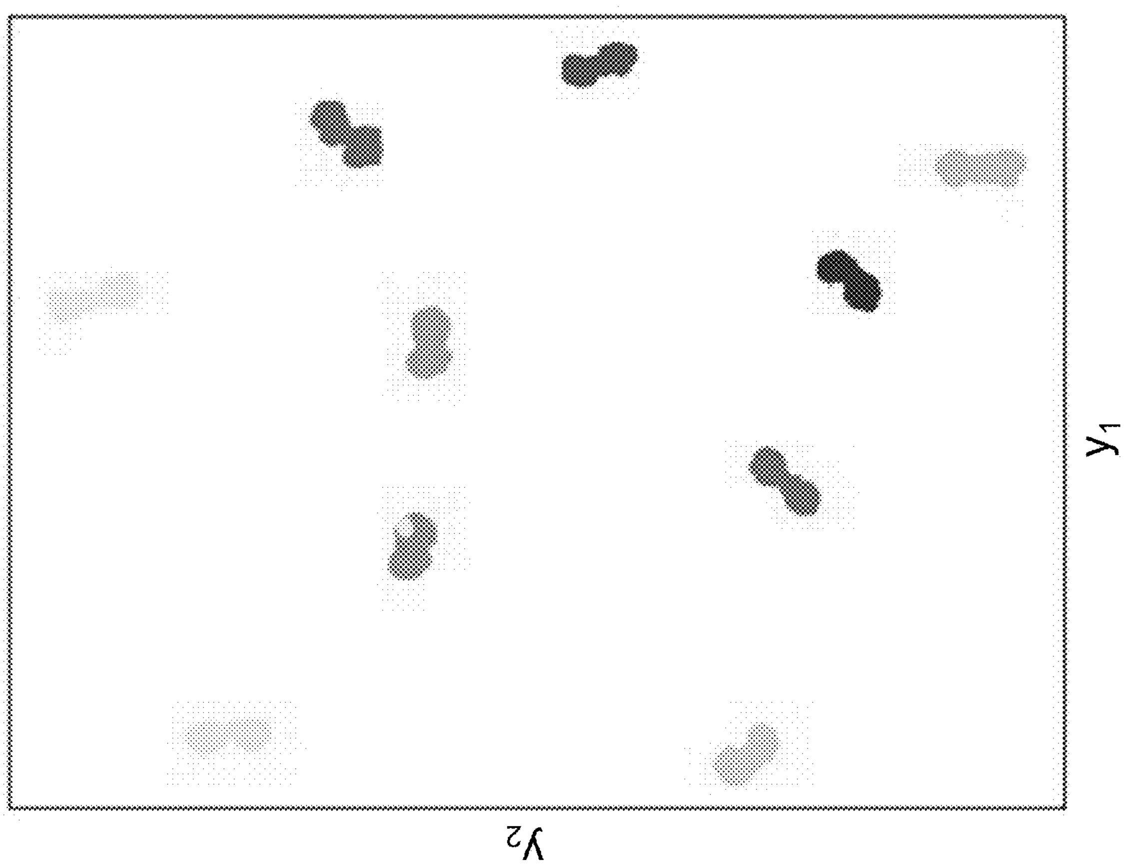

FIG. 4C

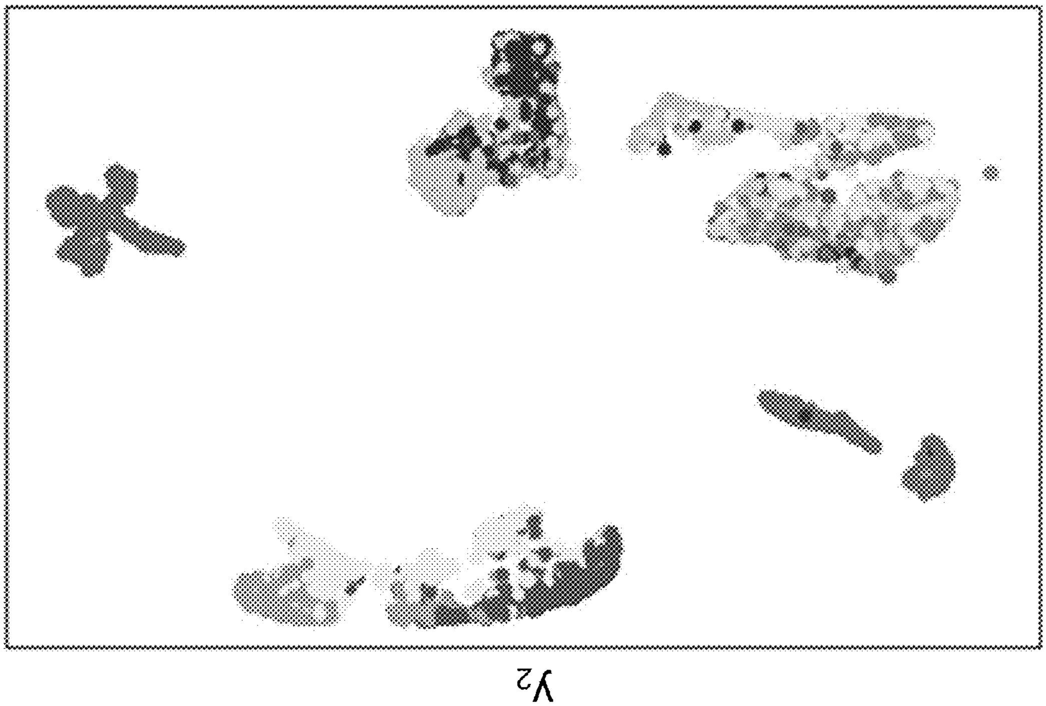

FIG. 5B

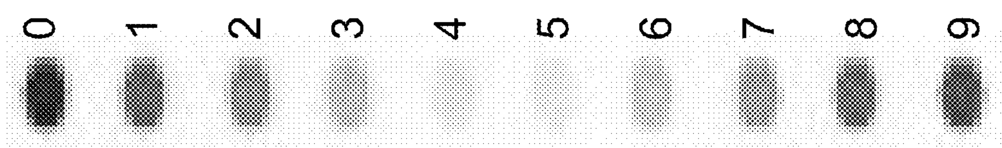

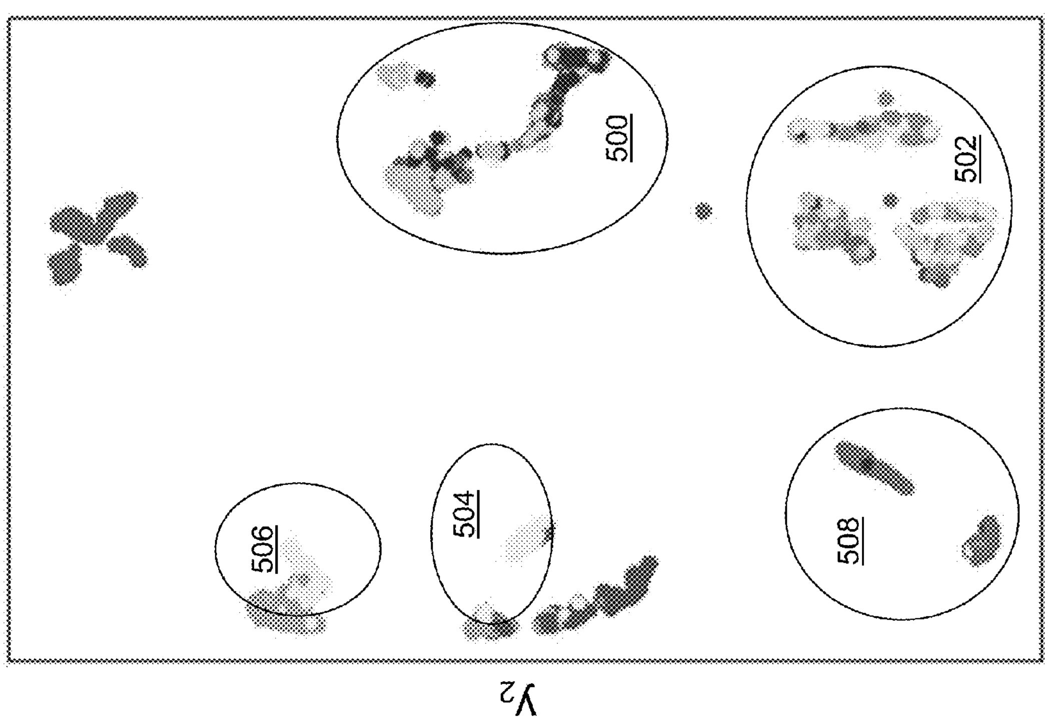

FIG. 5A

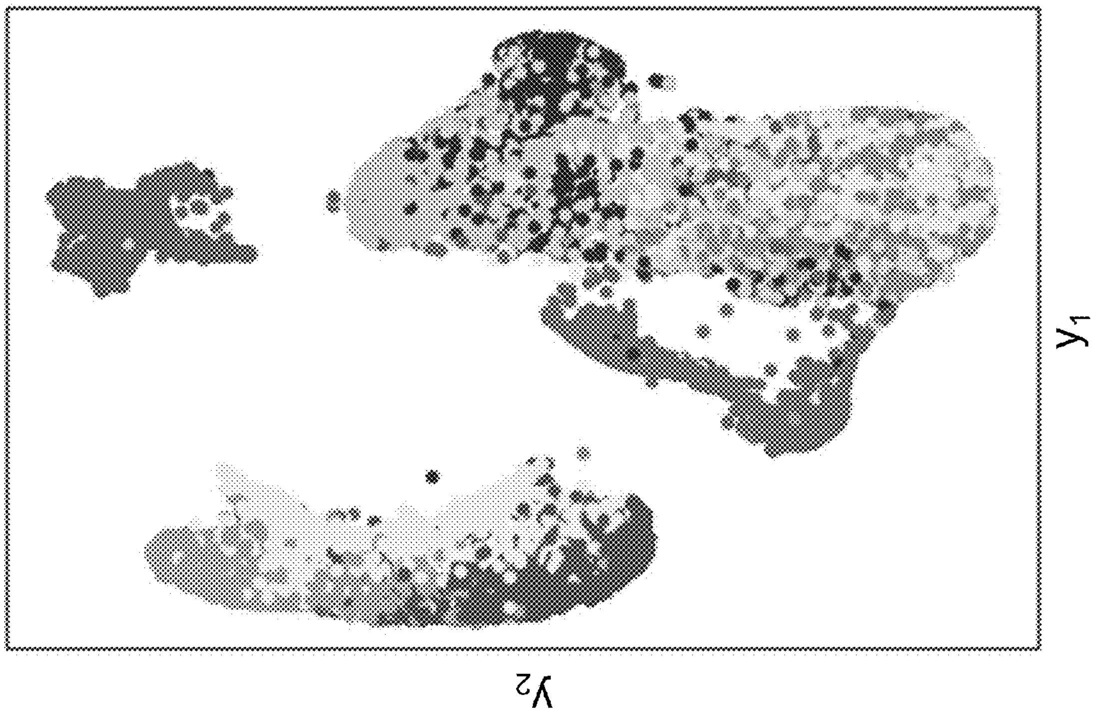

FIG. 5D

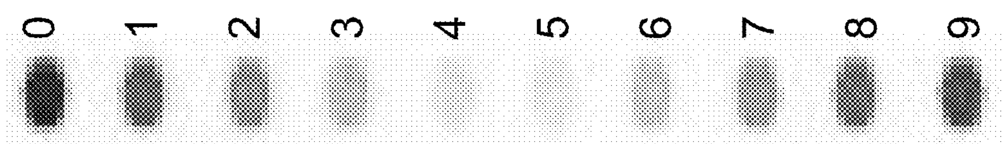

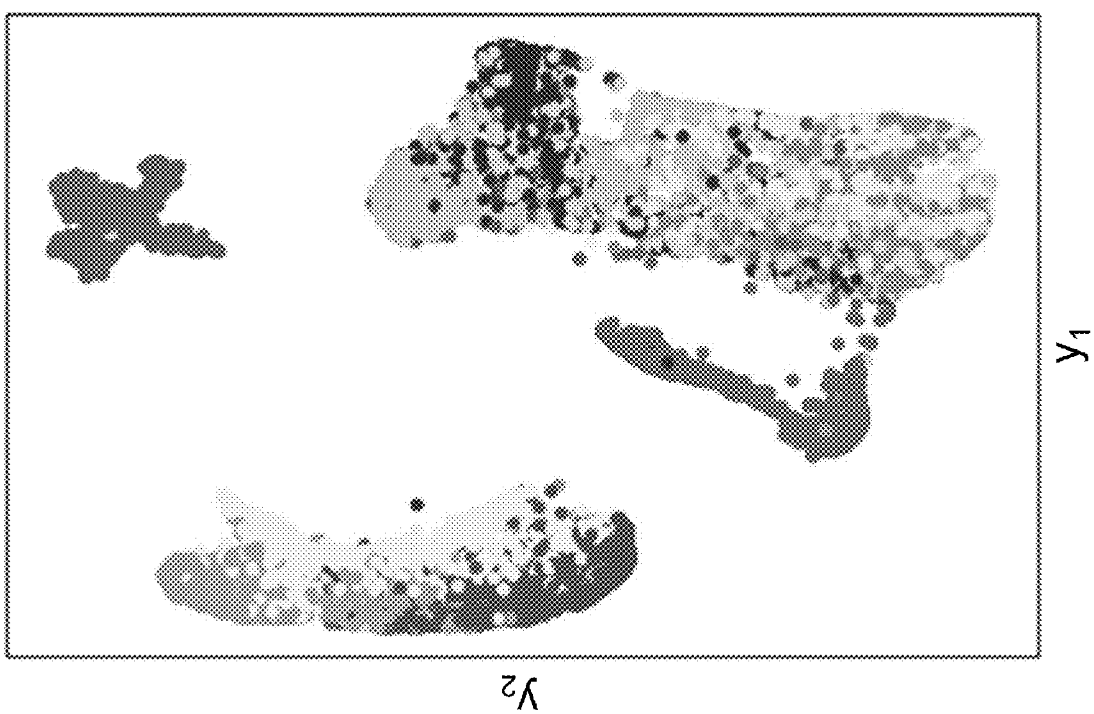

FIG. 5C

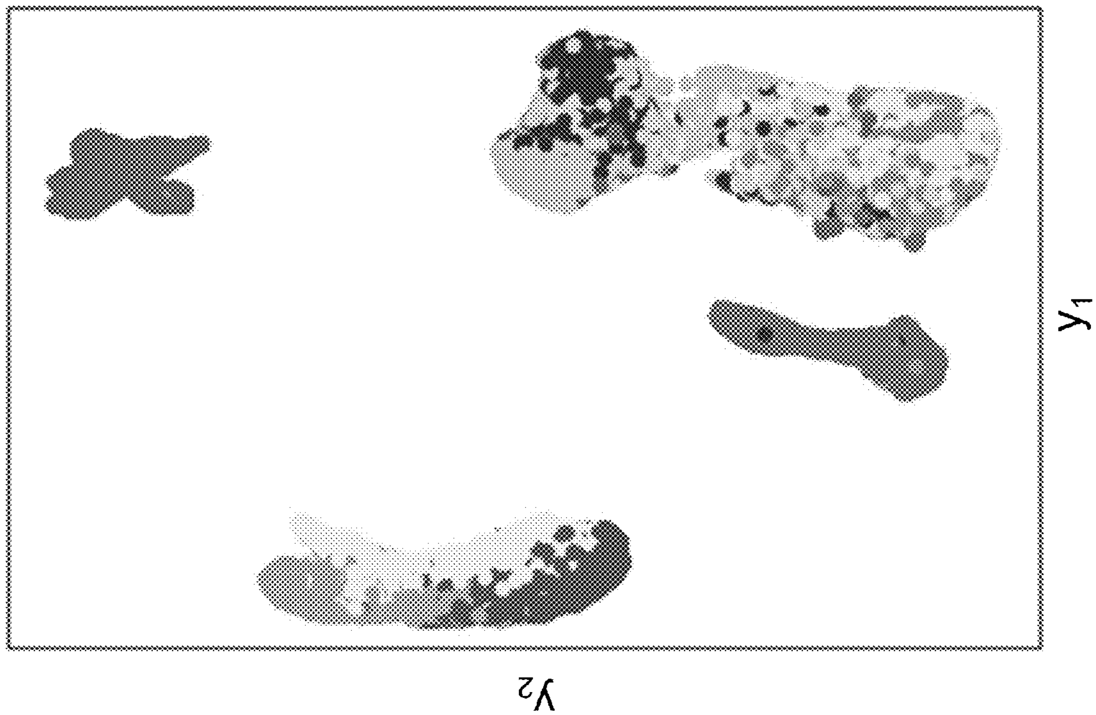

FIG. 6B

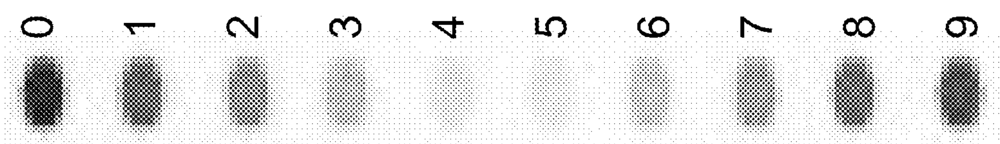

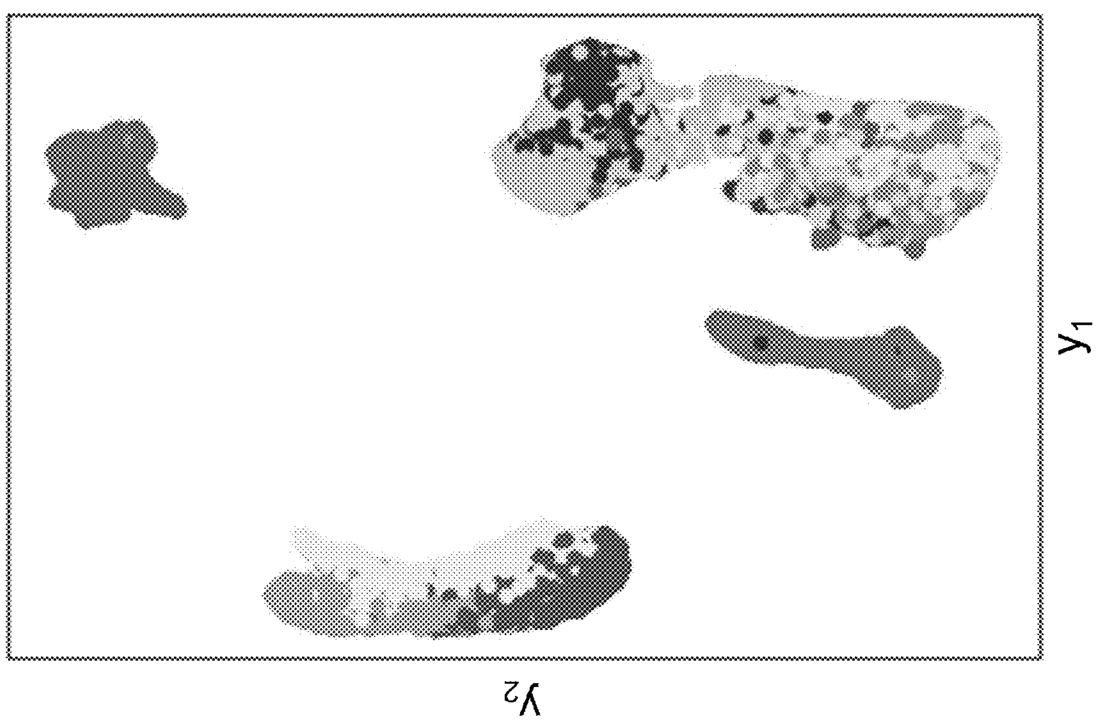

FIG. 6A

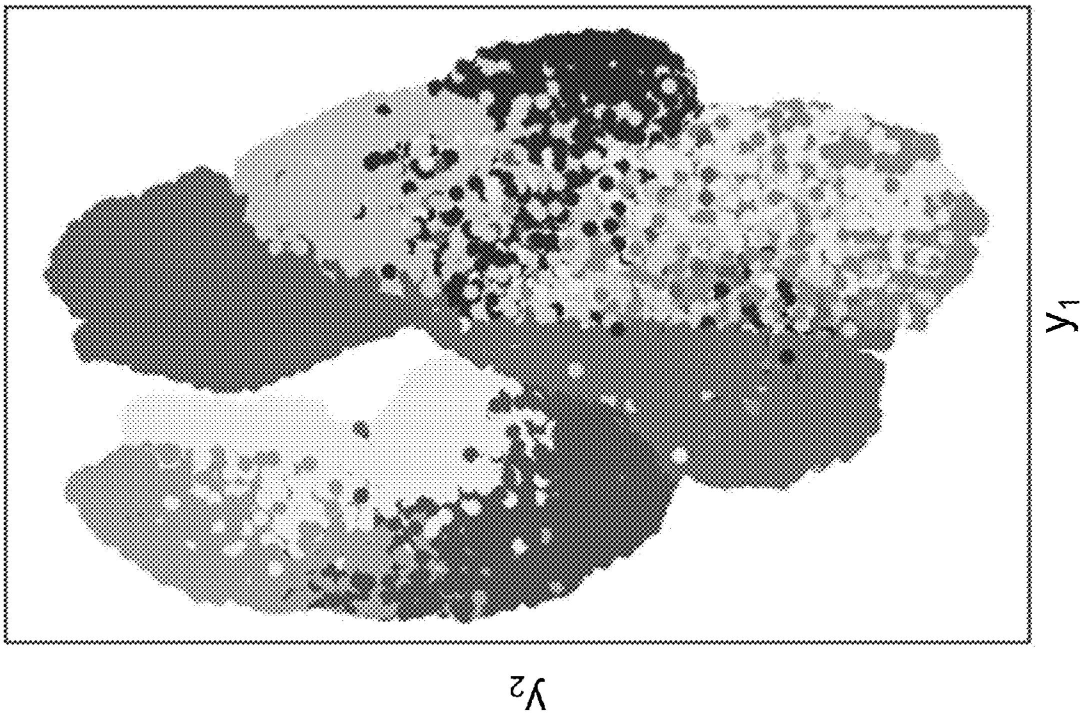

FIG. 6D

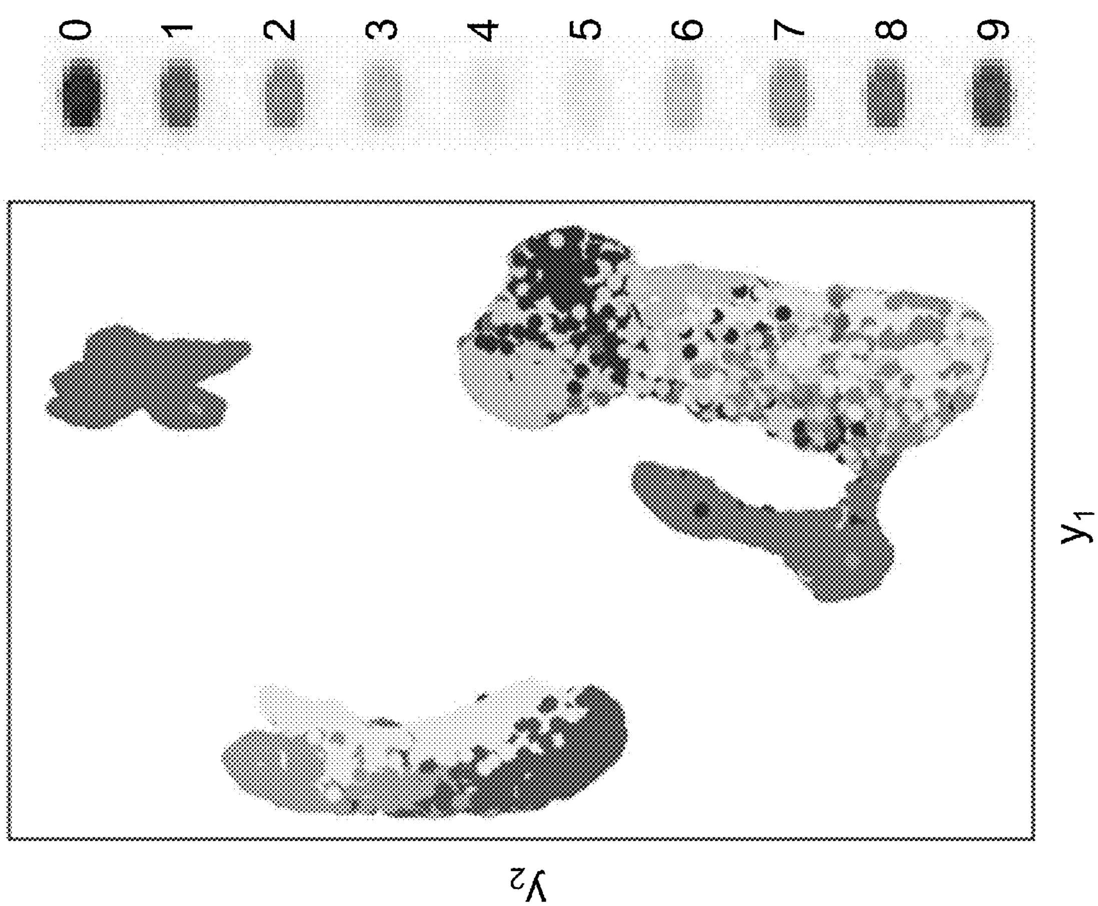

FIG. 6C

FIG. 7A

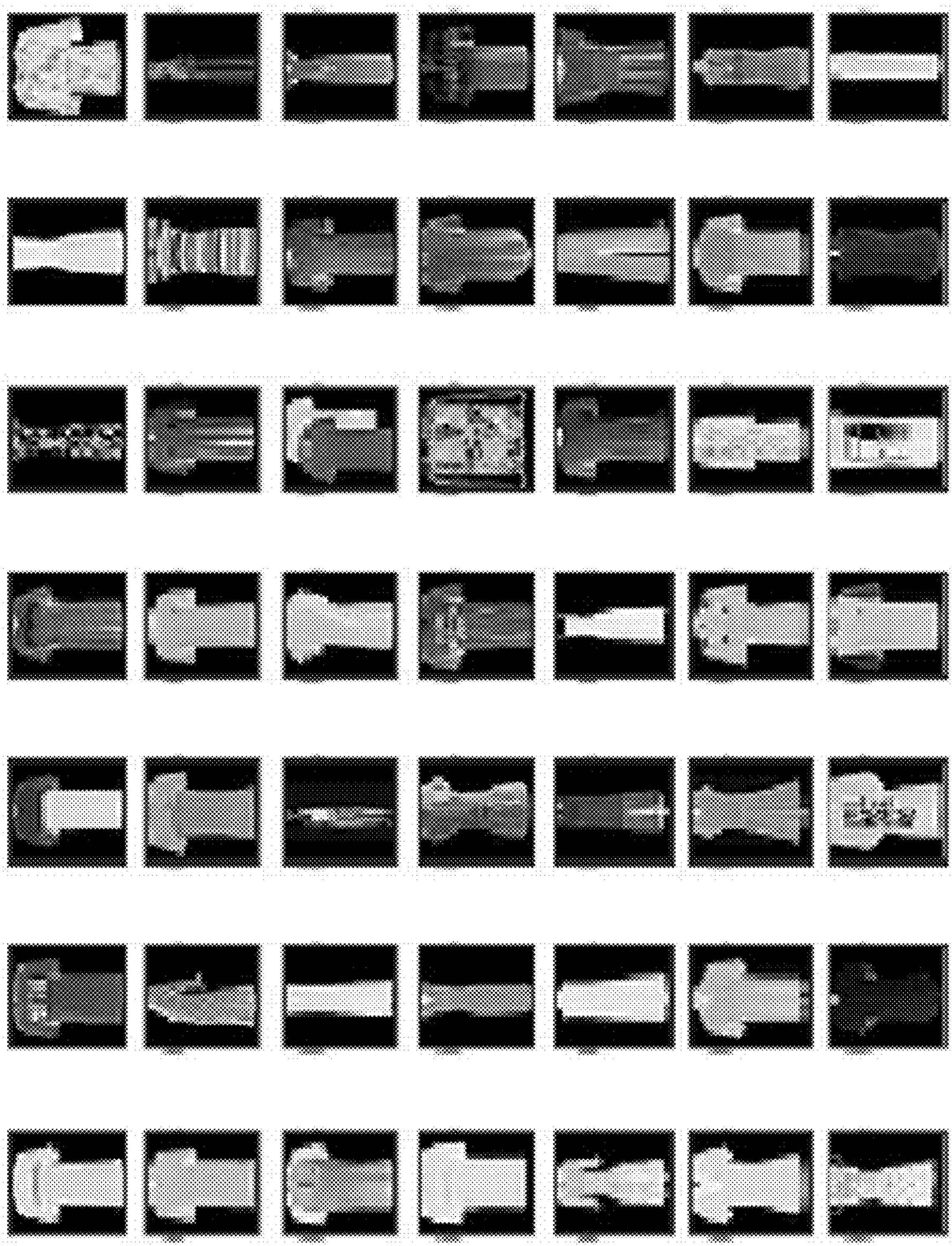

FIG. 7B

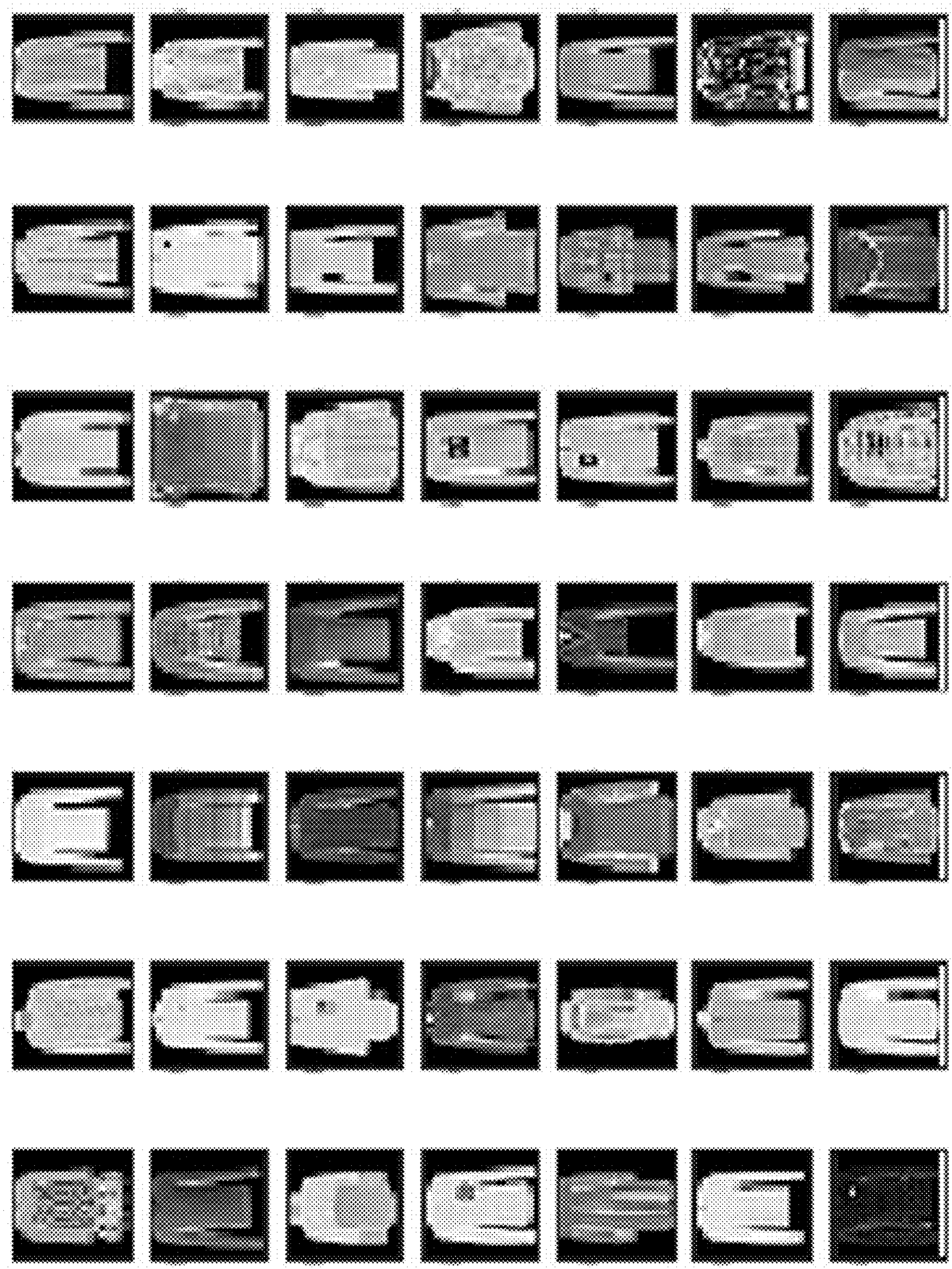

FIG. 7C

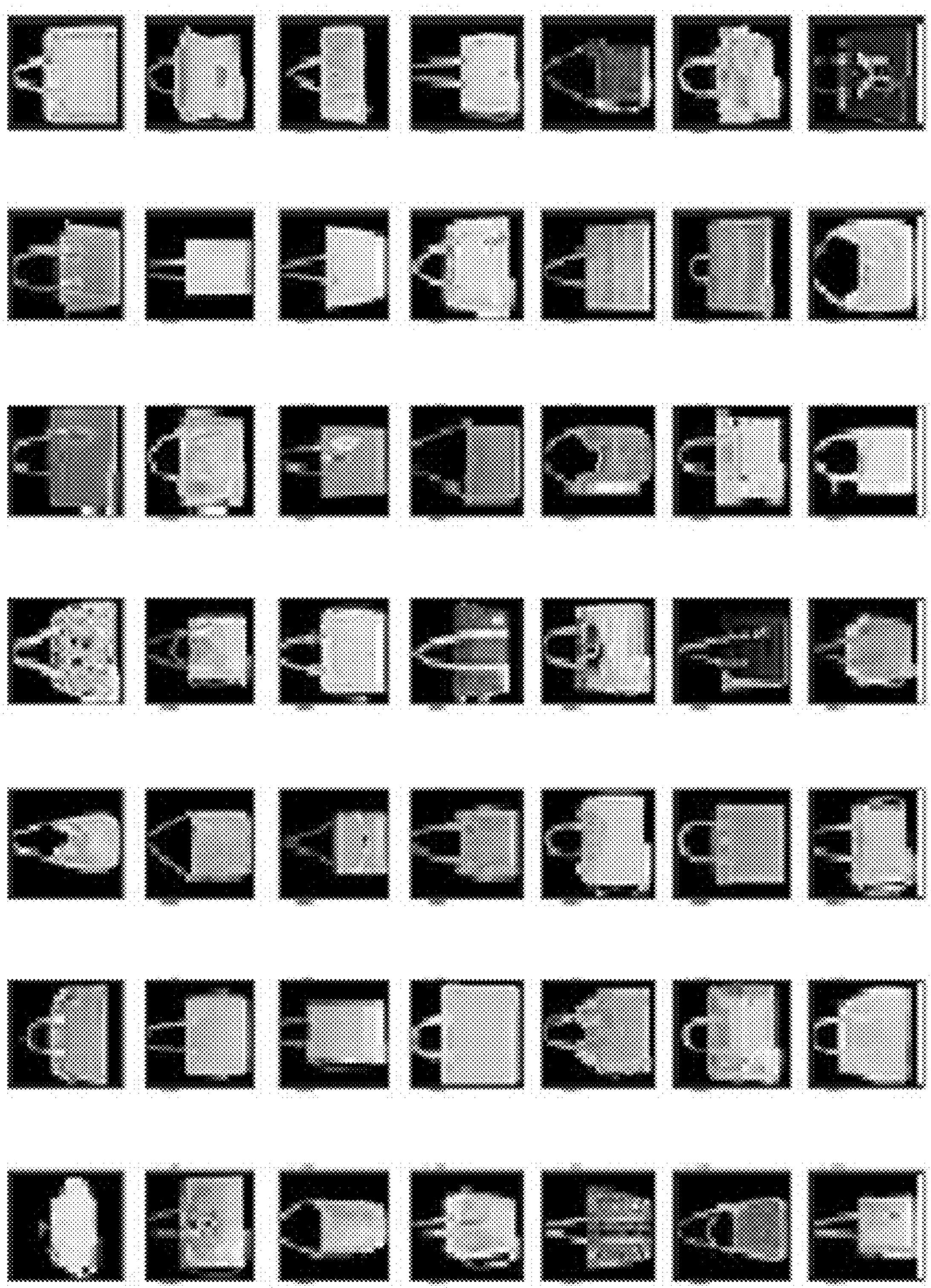

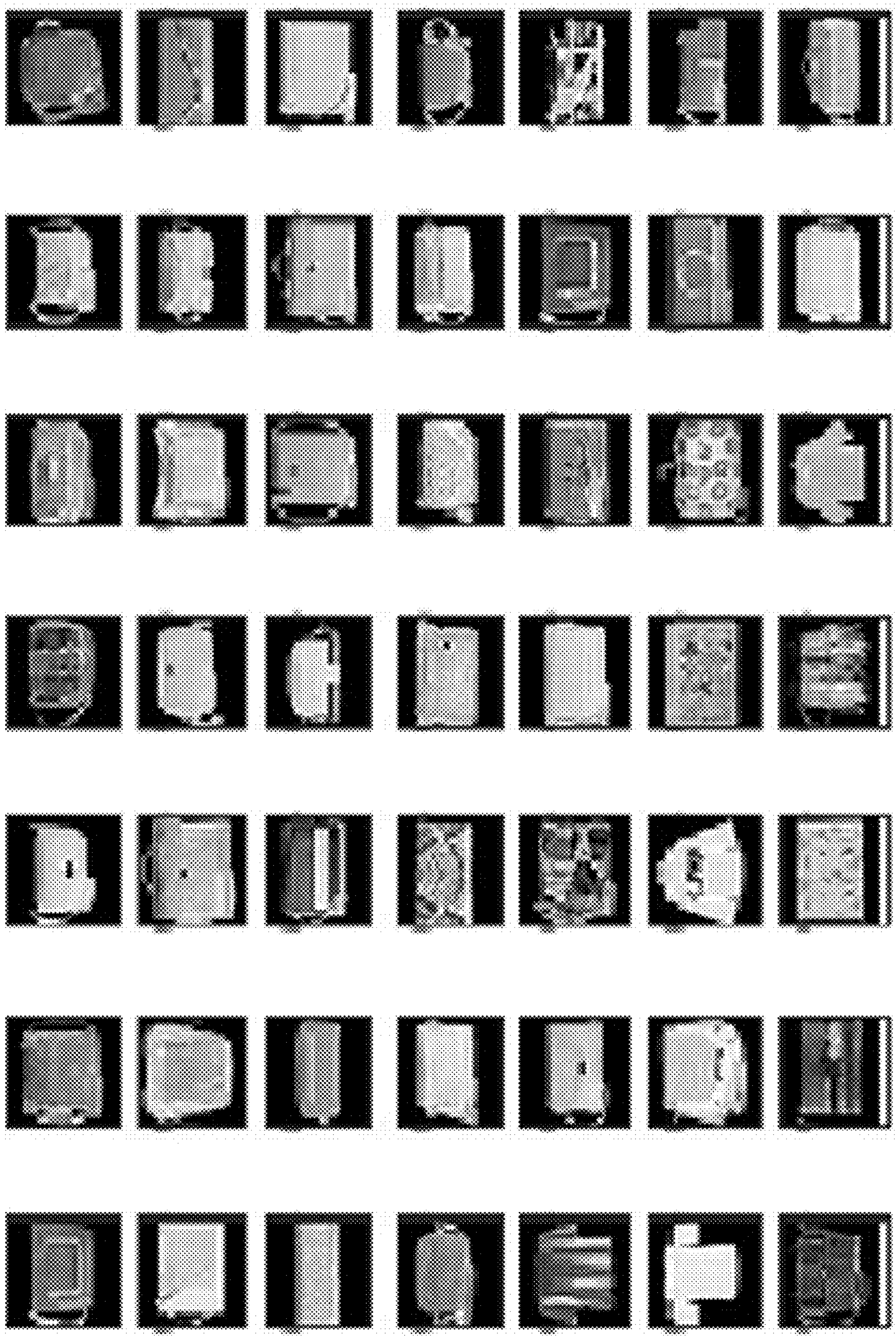

FIG. 7D

FIG. 7E

FIG. 7F

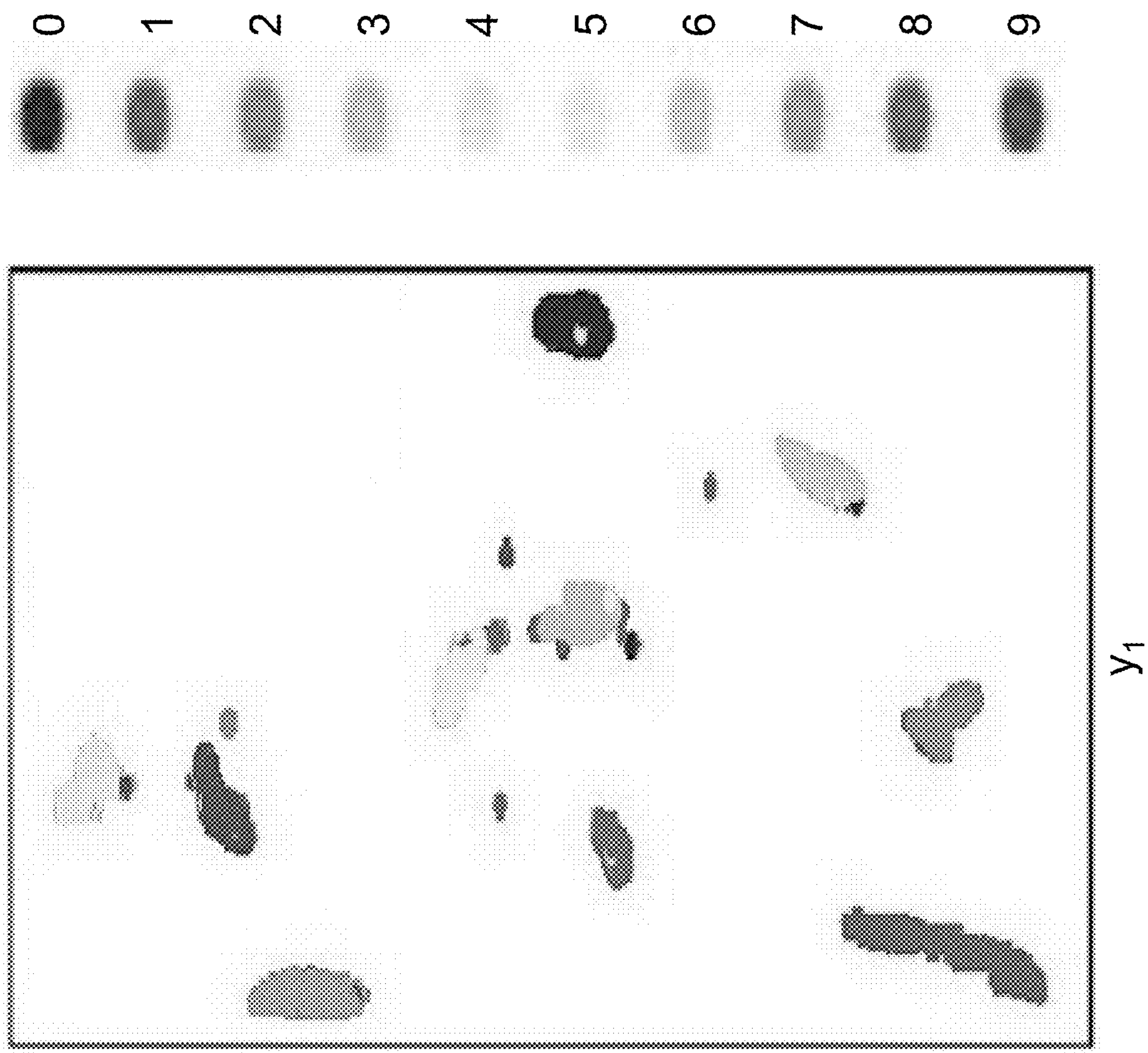

FIG. 8A

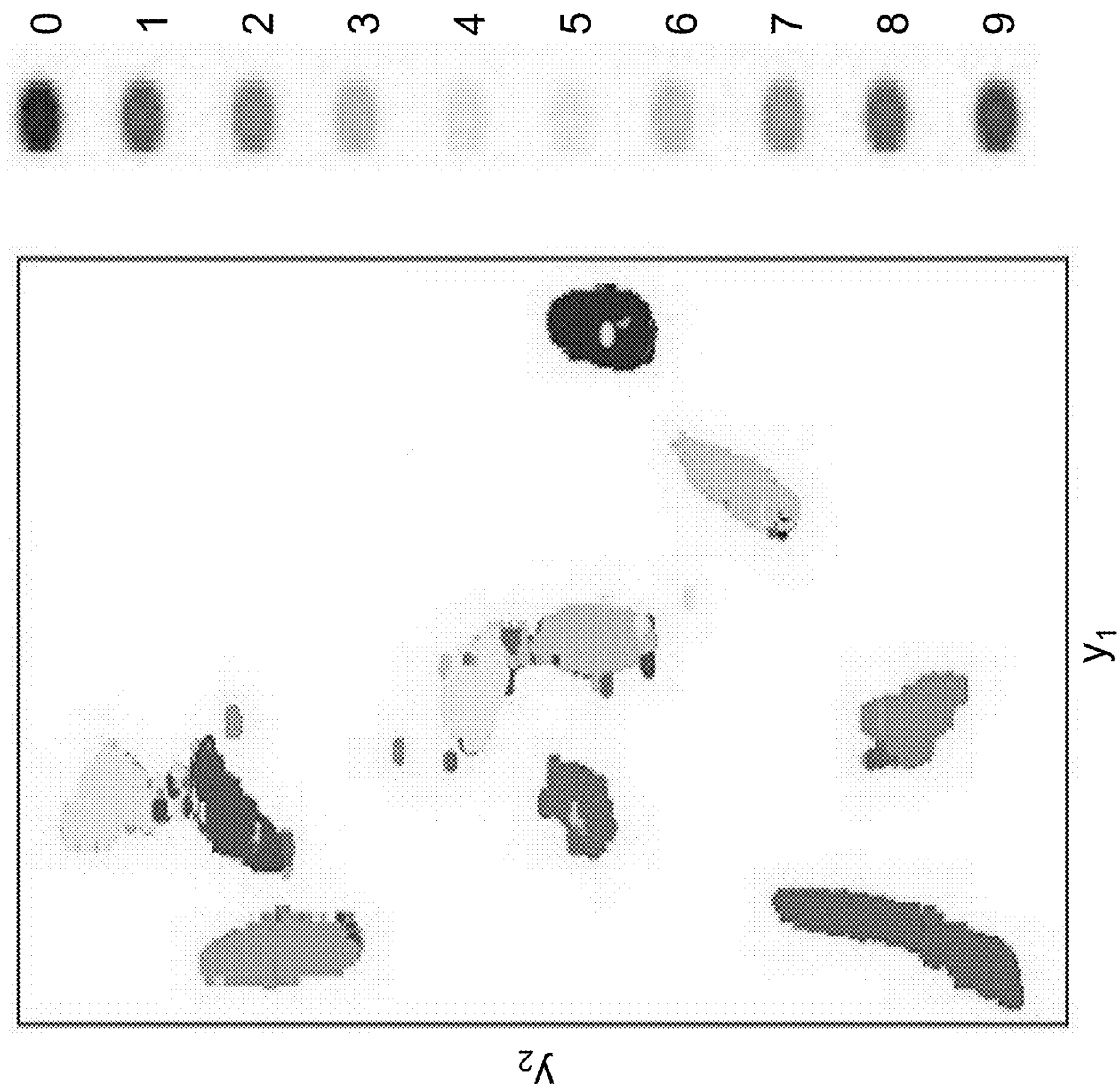

FIG. 8B

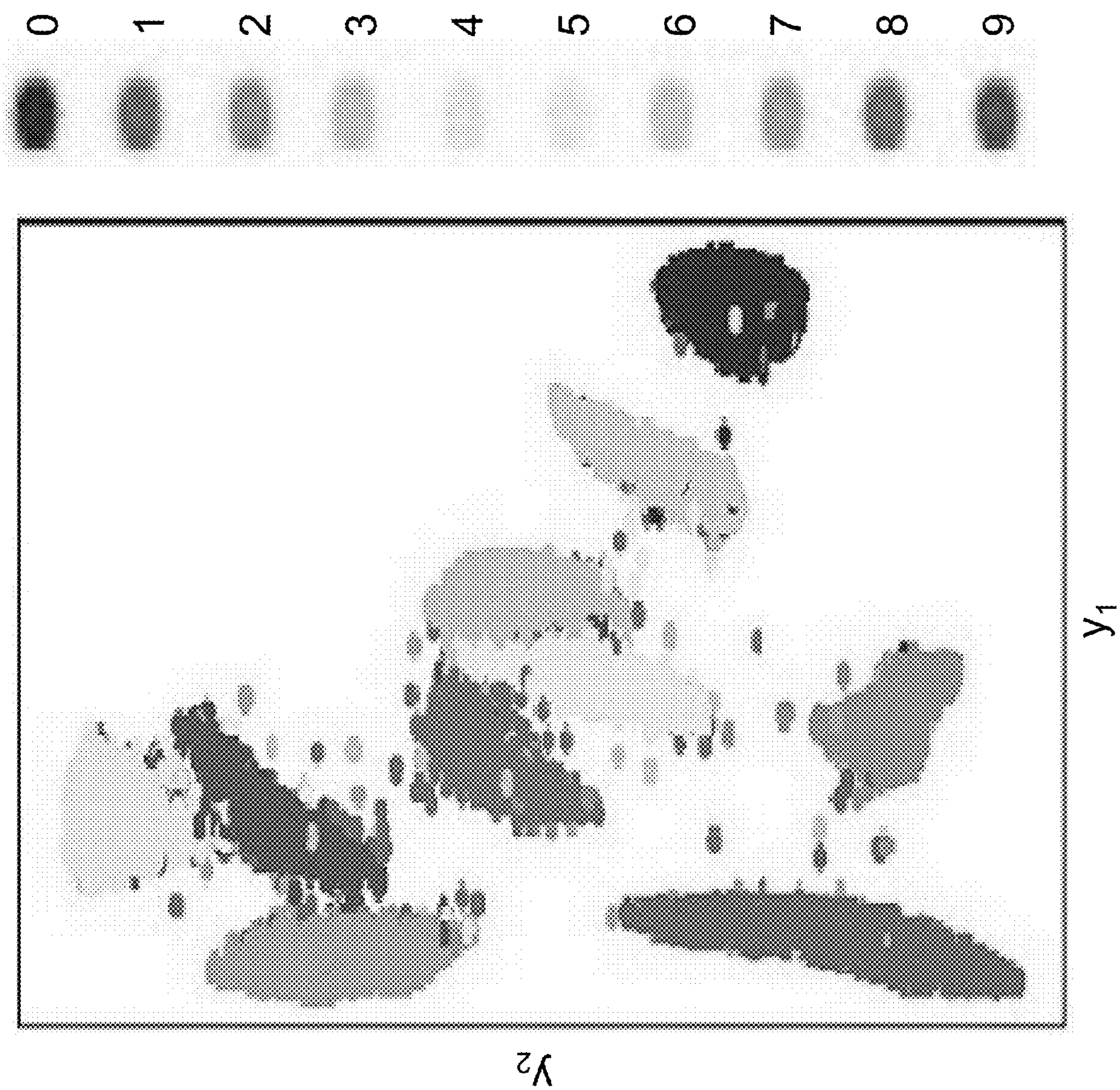

FIG. 8C

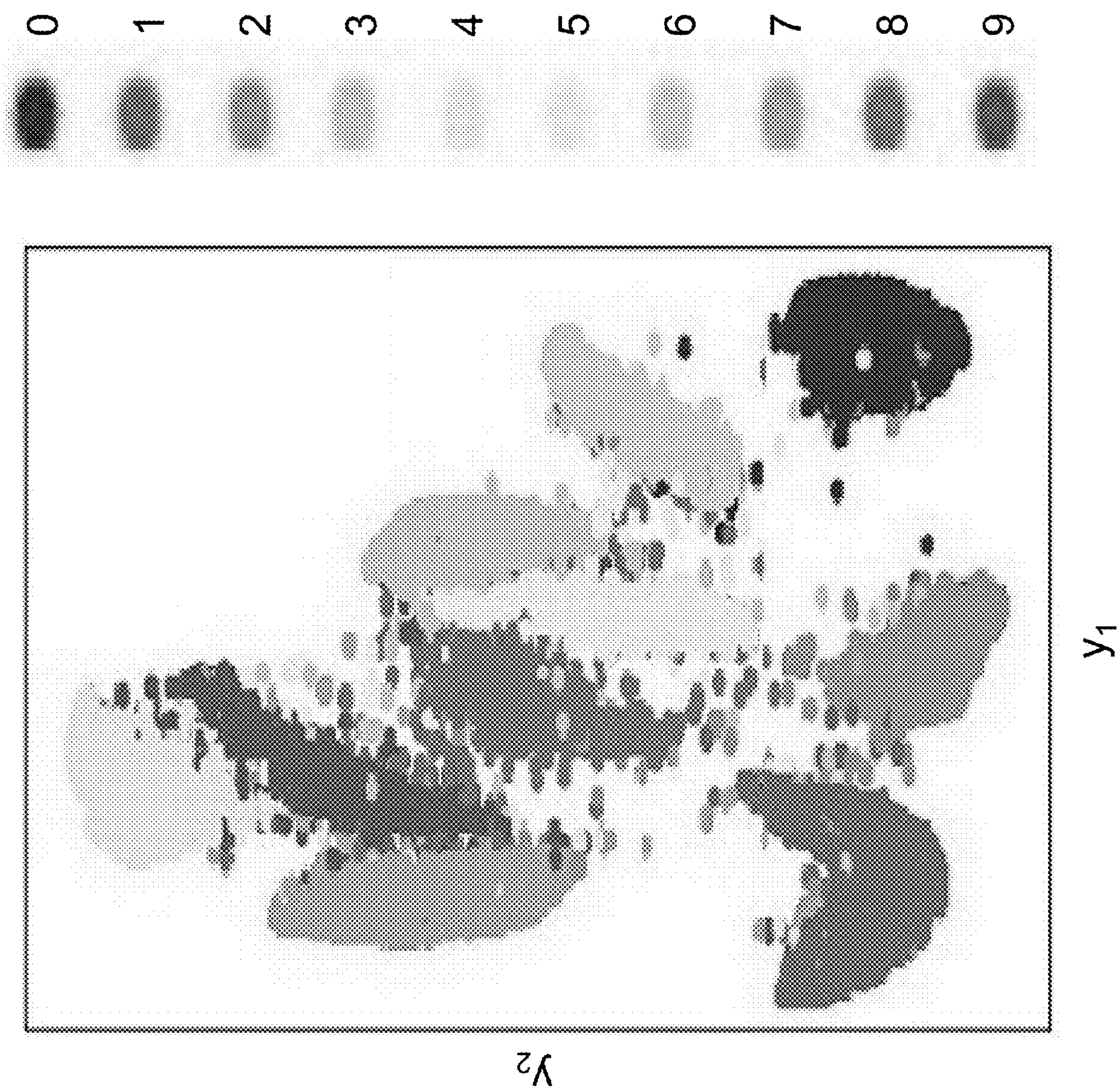

FIG. 8D

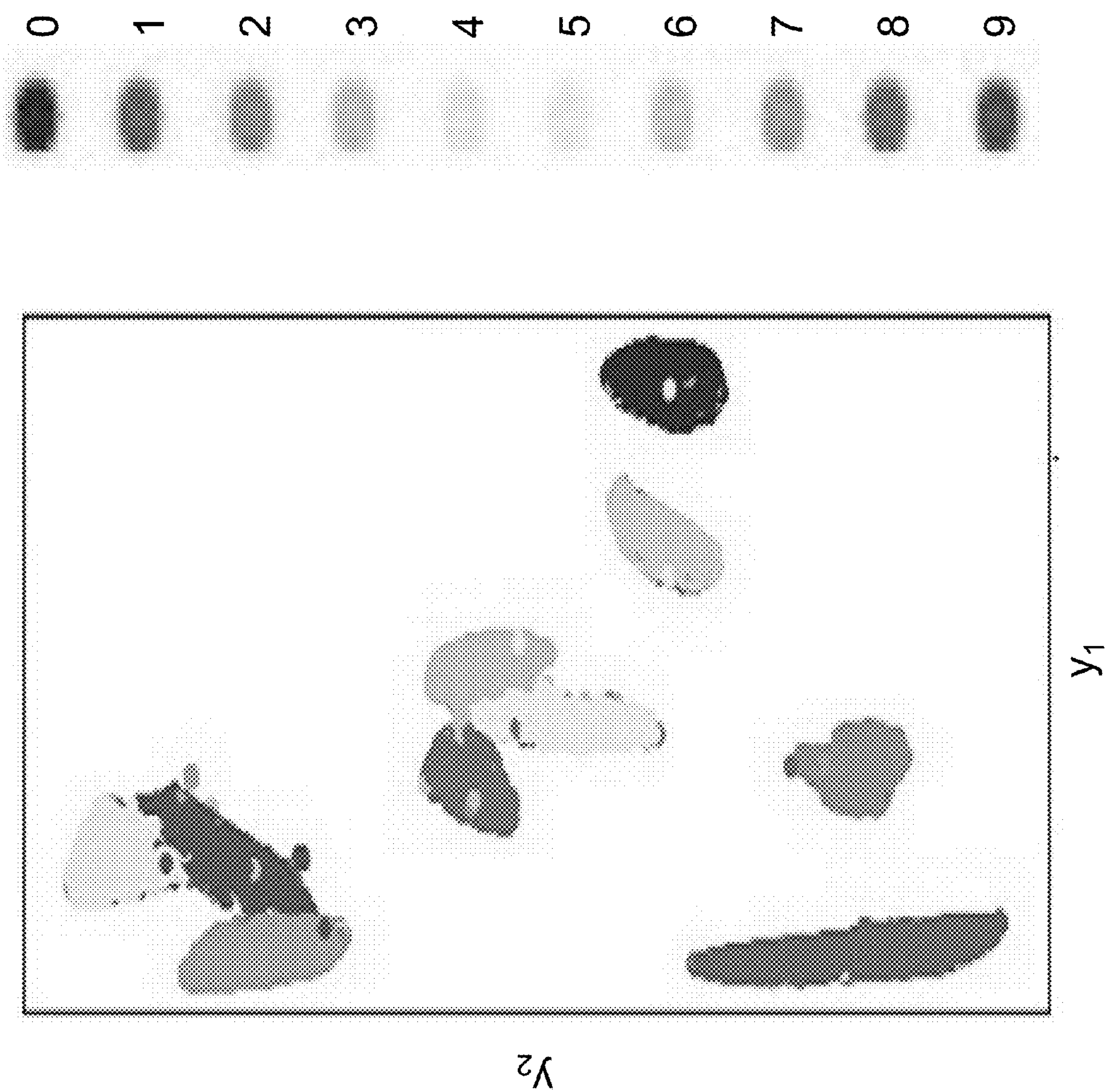

FIG. 9A

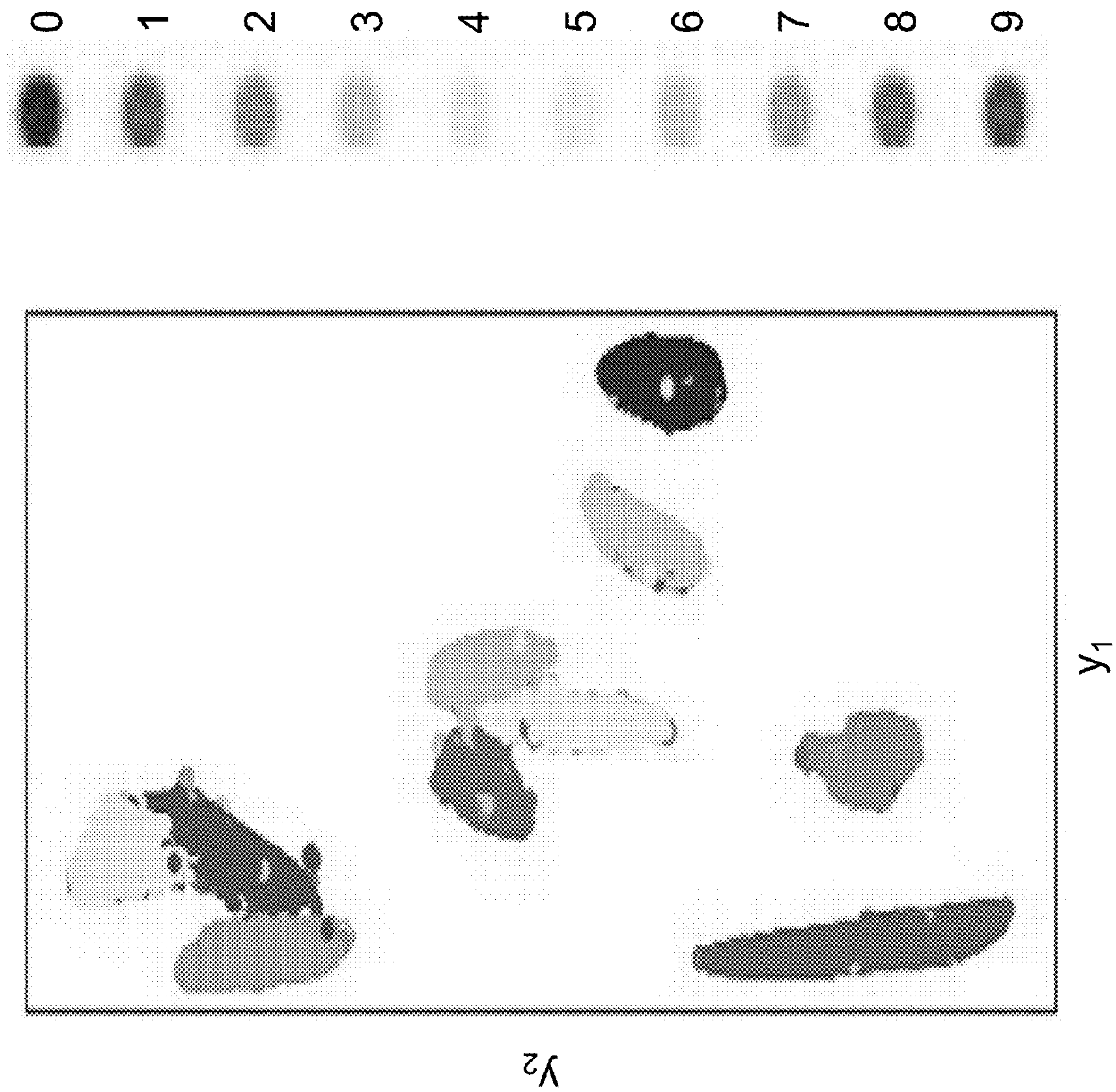

FIG. 9B

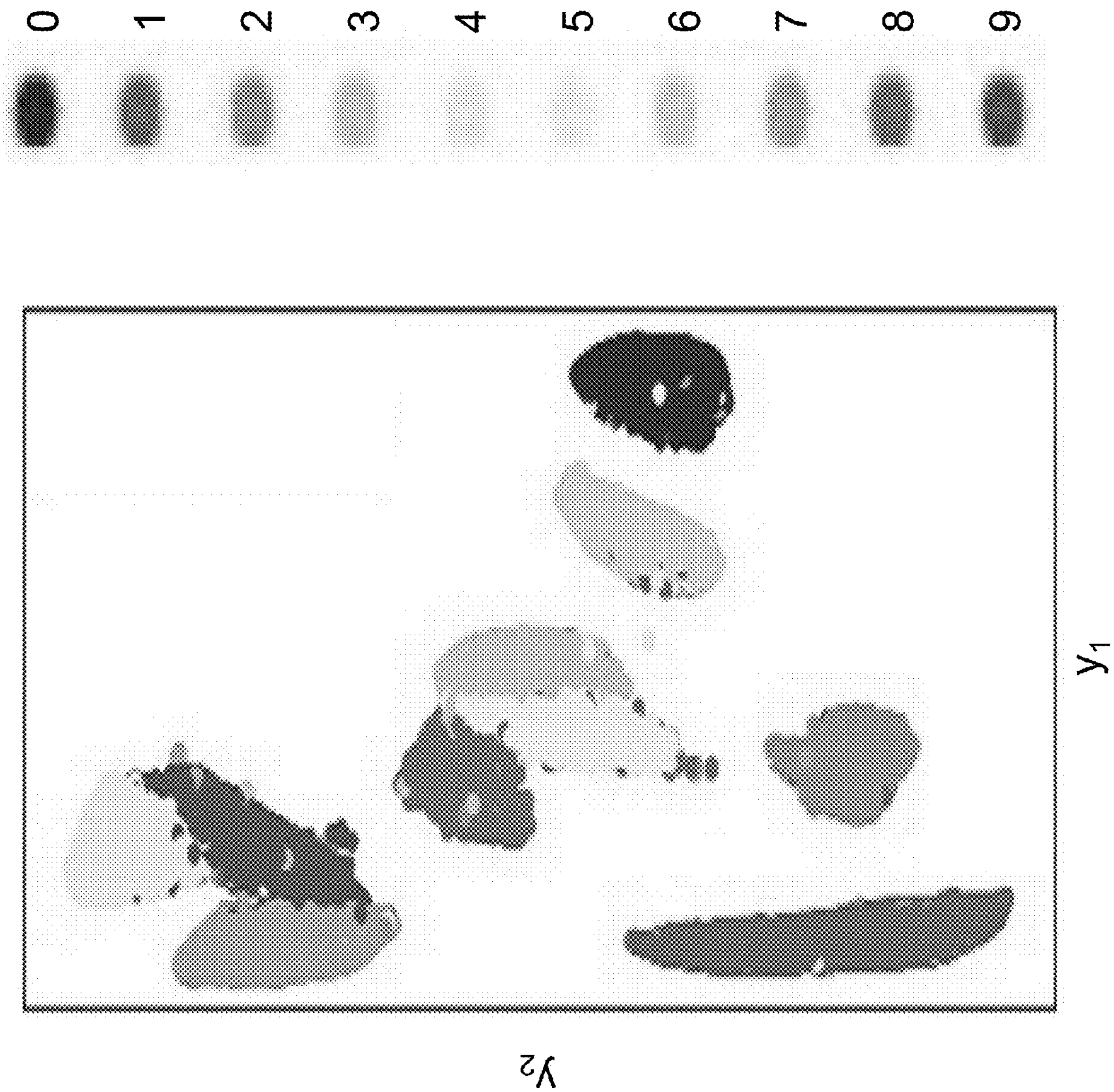

FIG. 9C

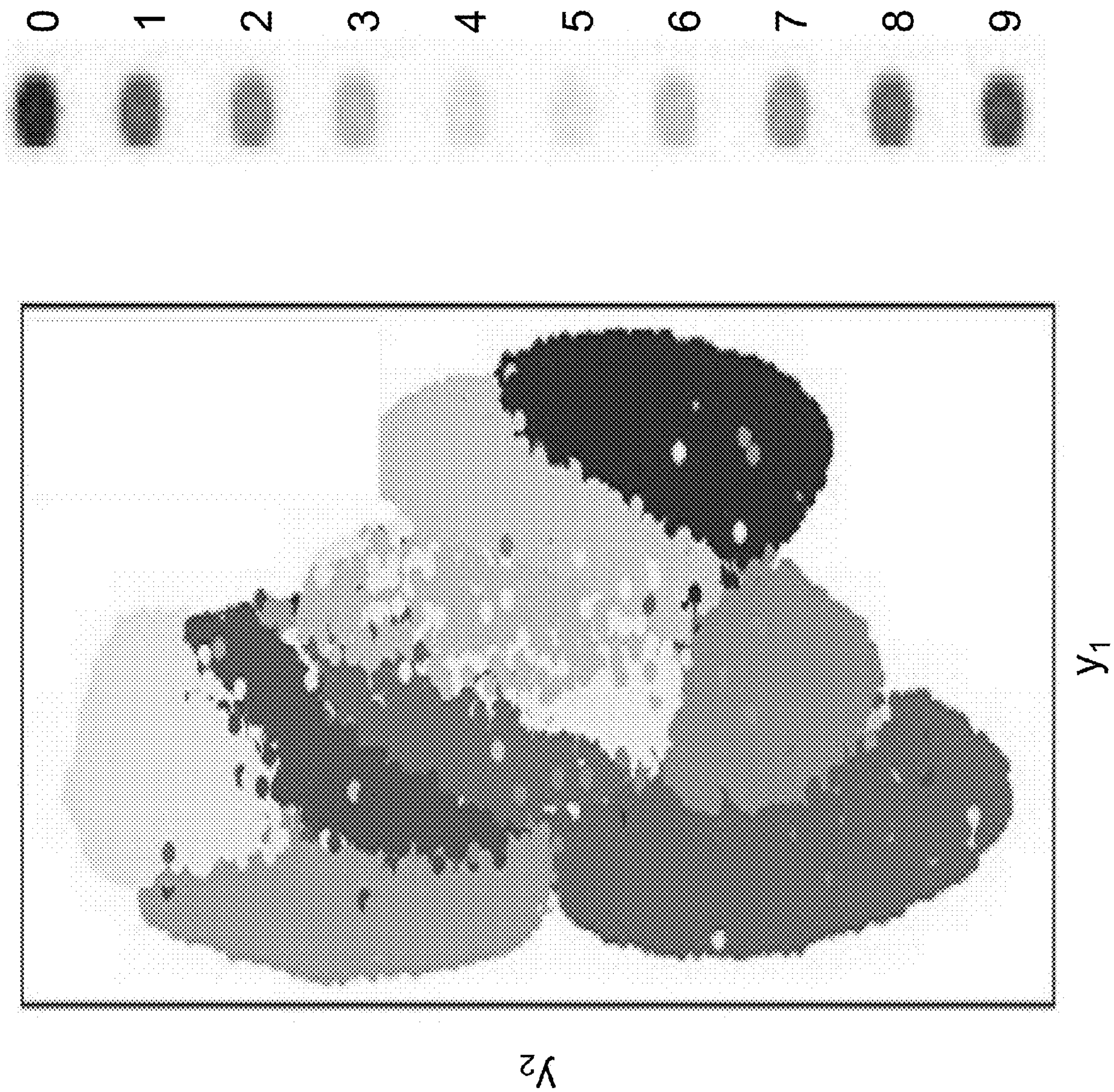

FIG. 9D

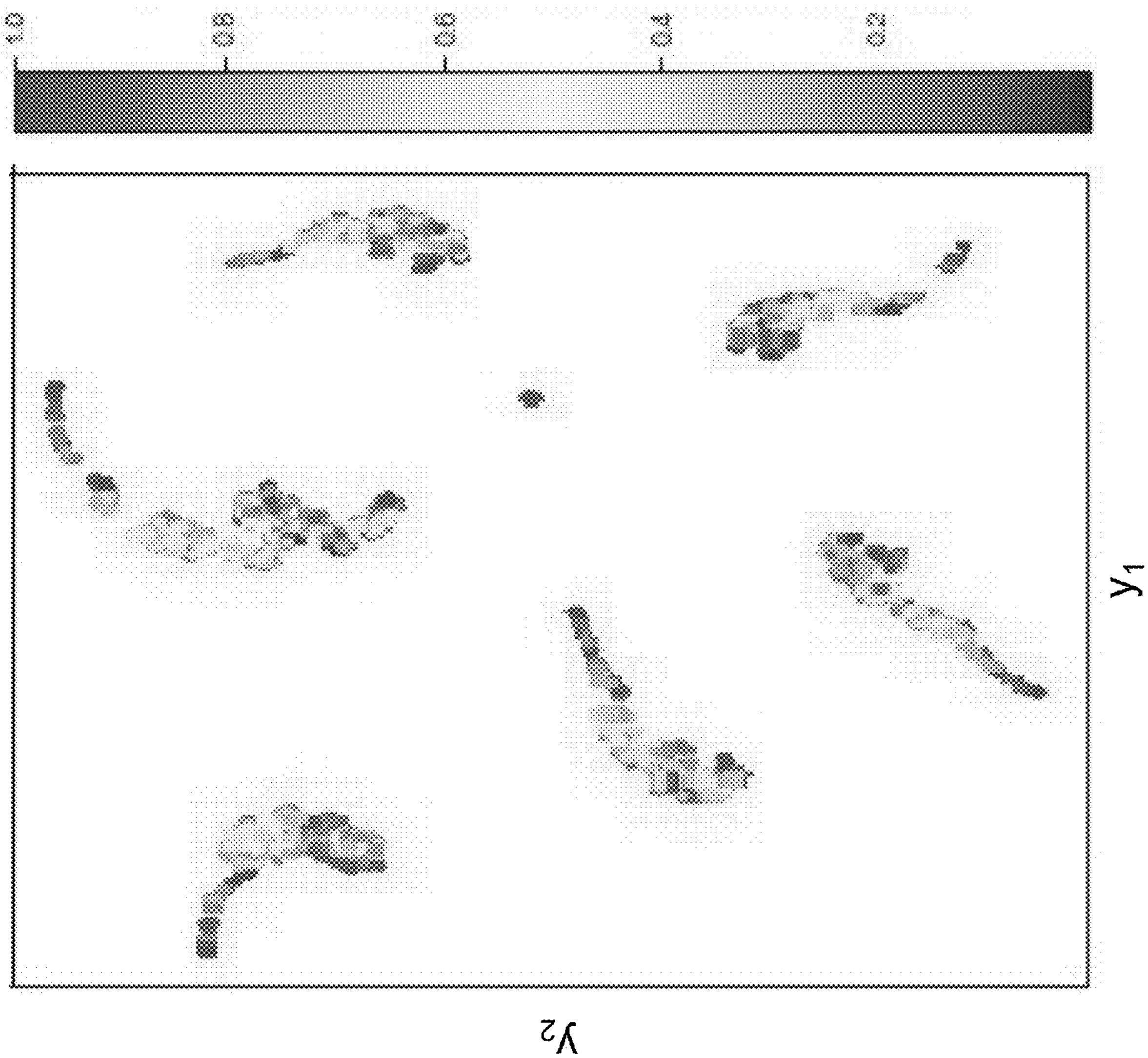

FIG. 10A

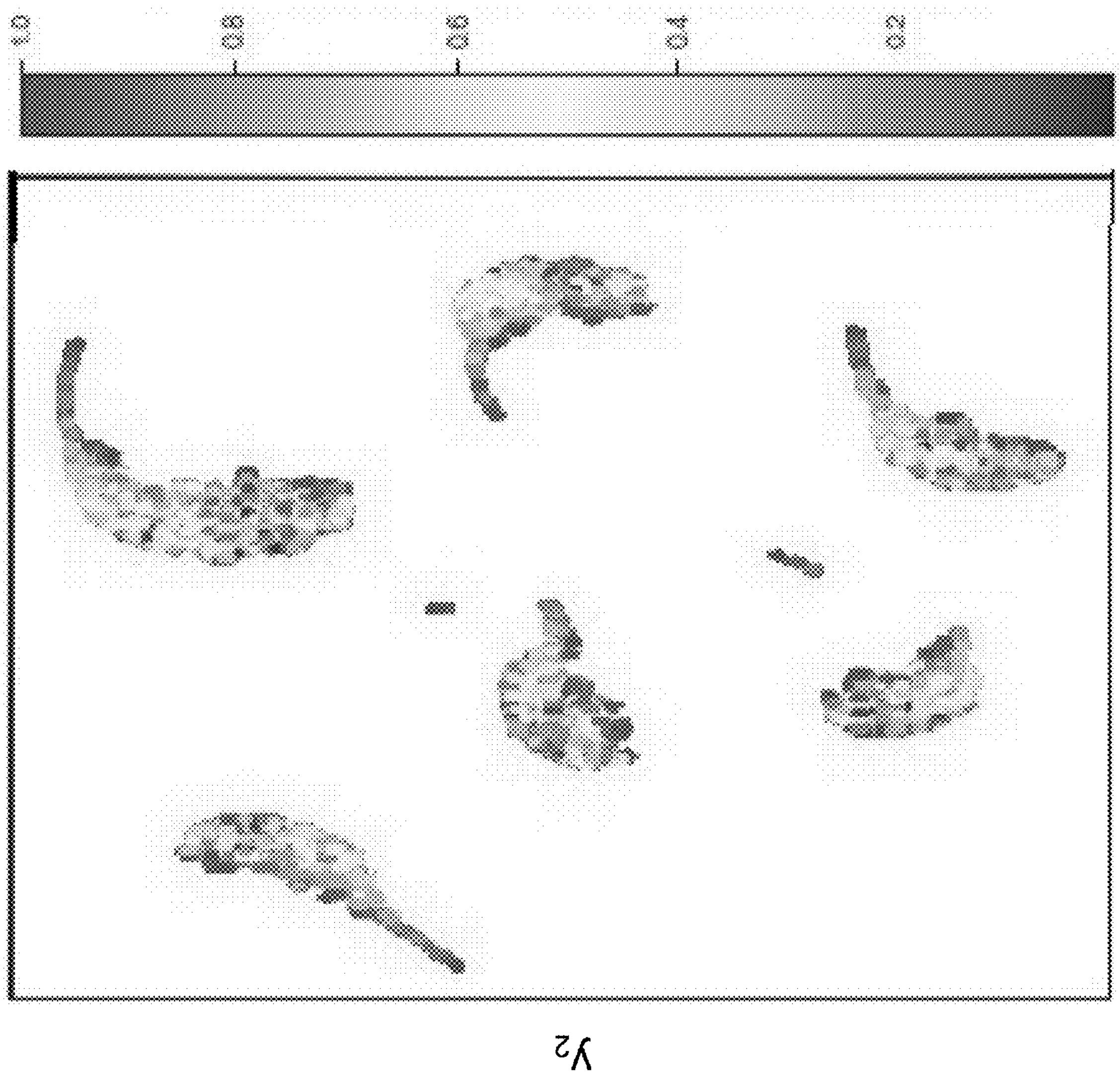

FIG. 10B

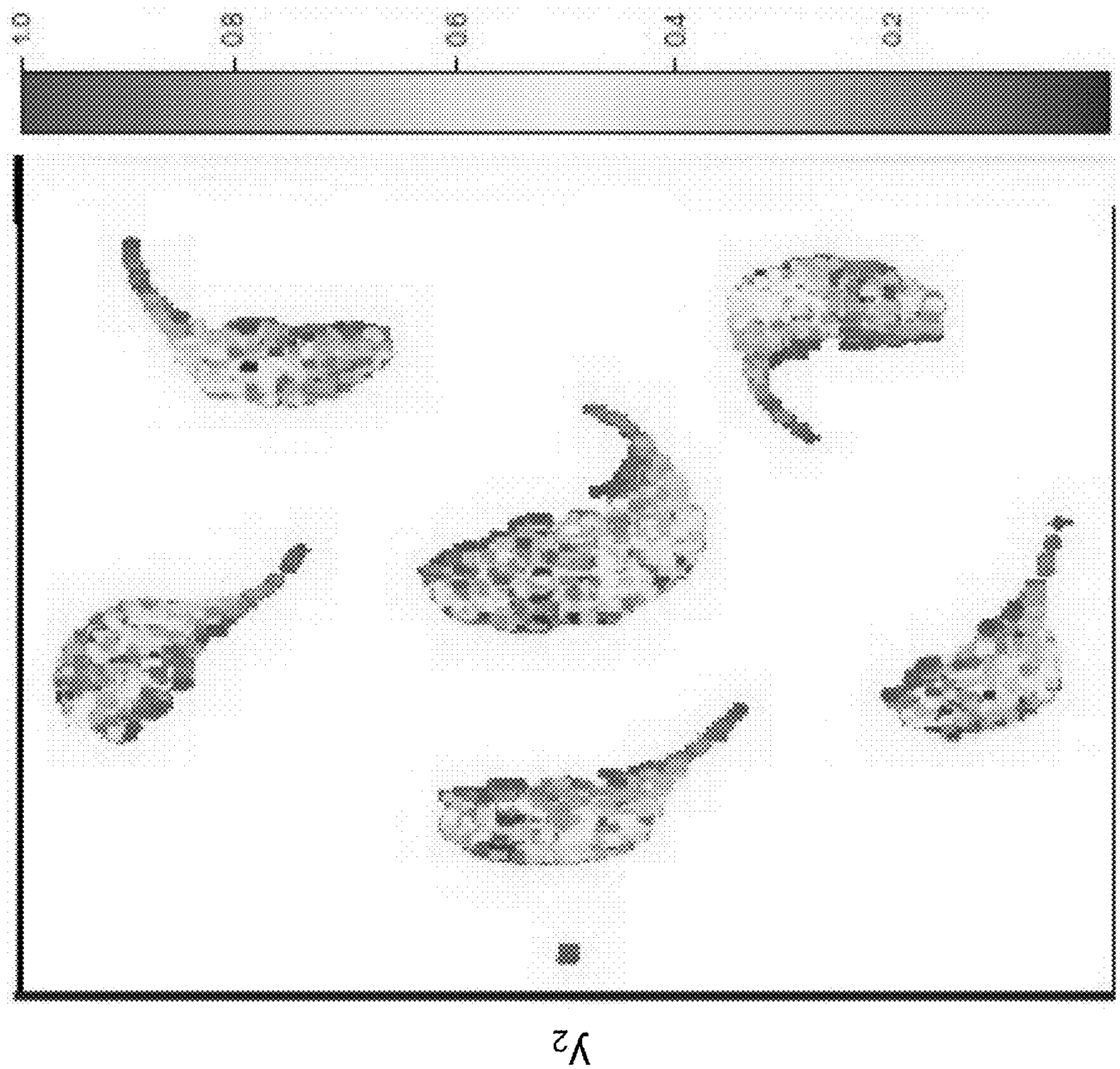

FIG. 10C

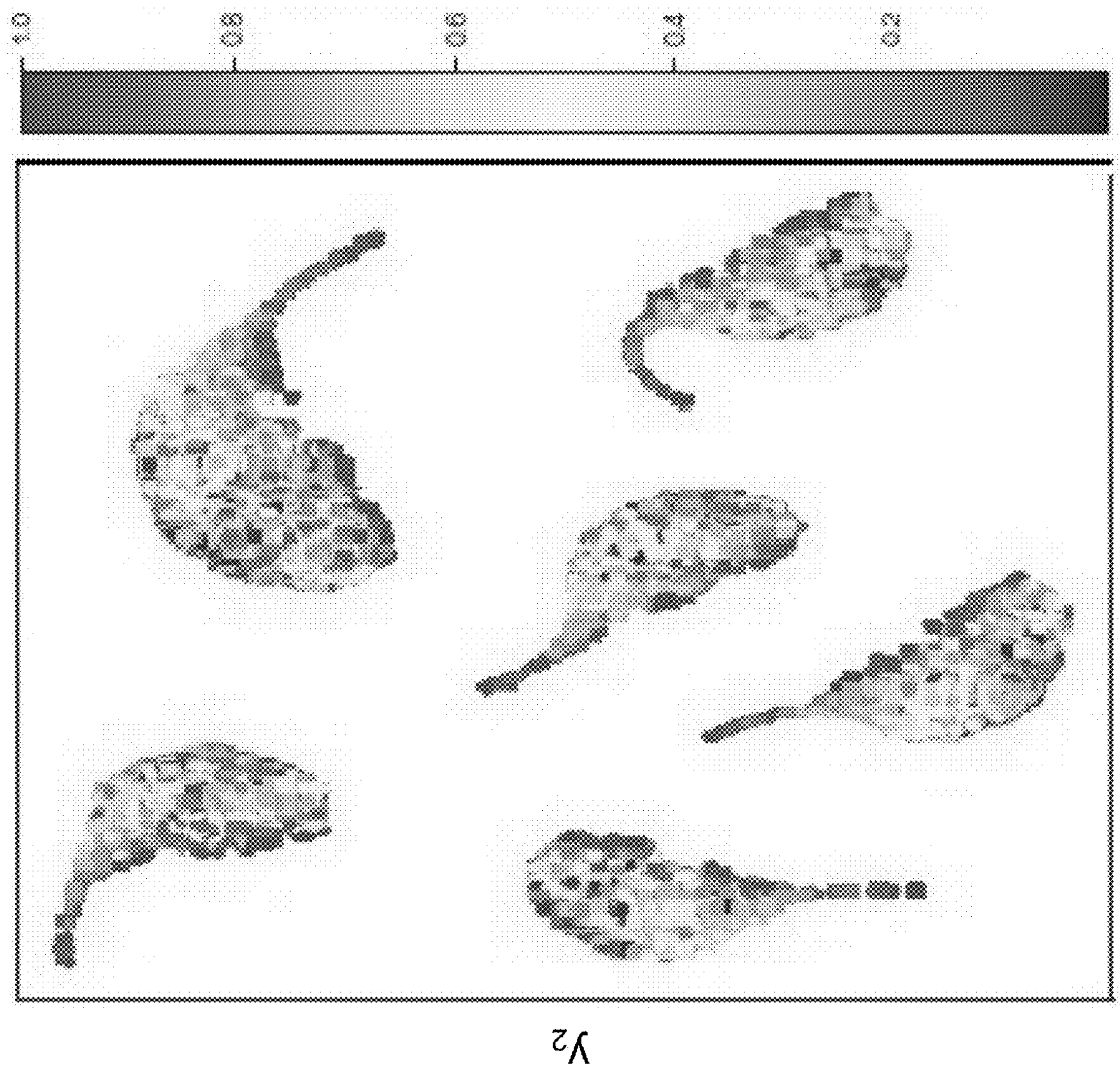

FIG. 10D

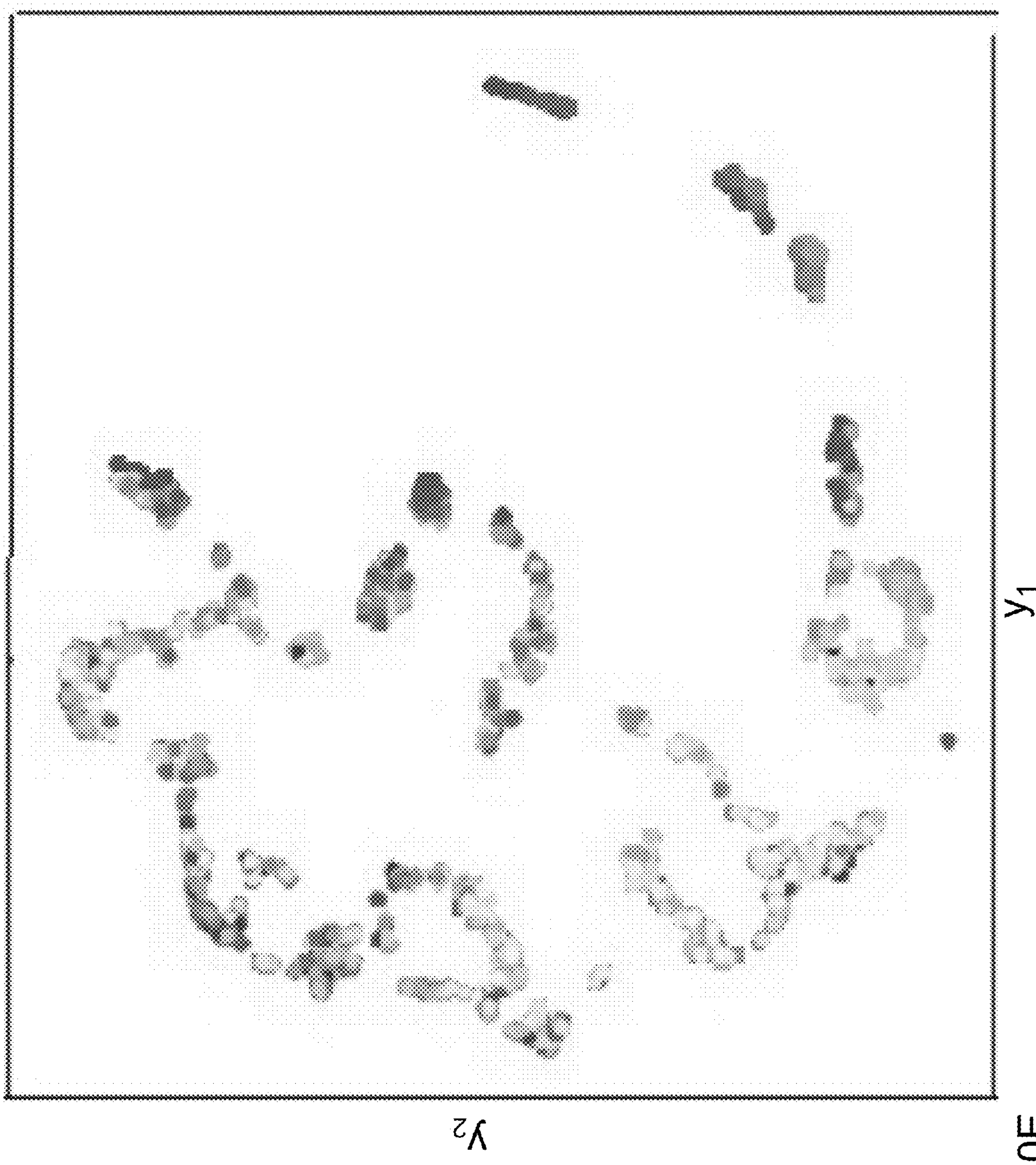

FIG. 10E

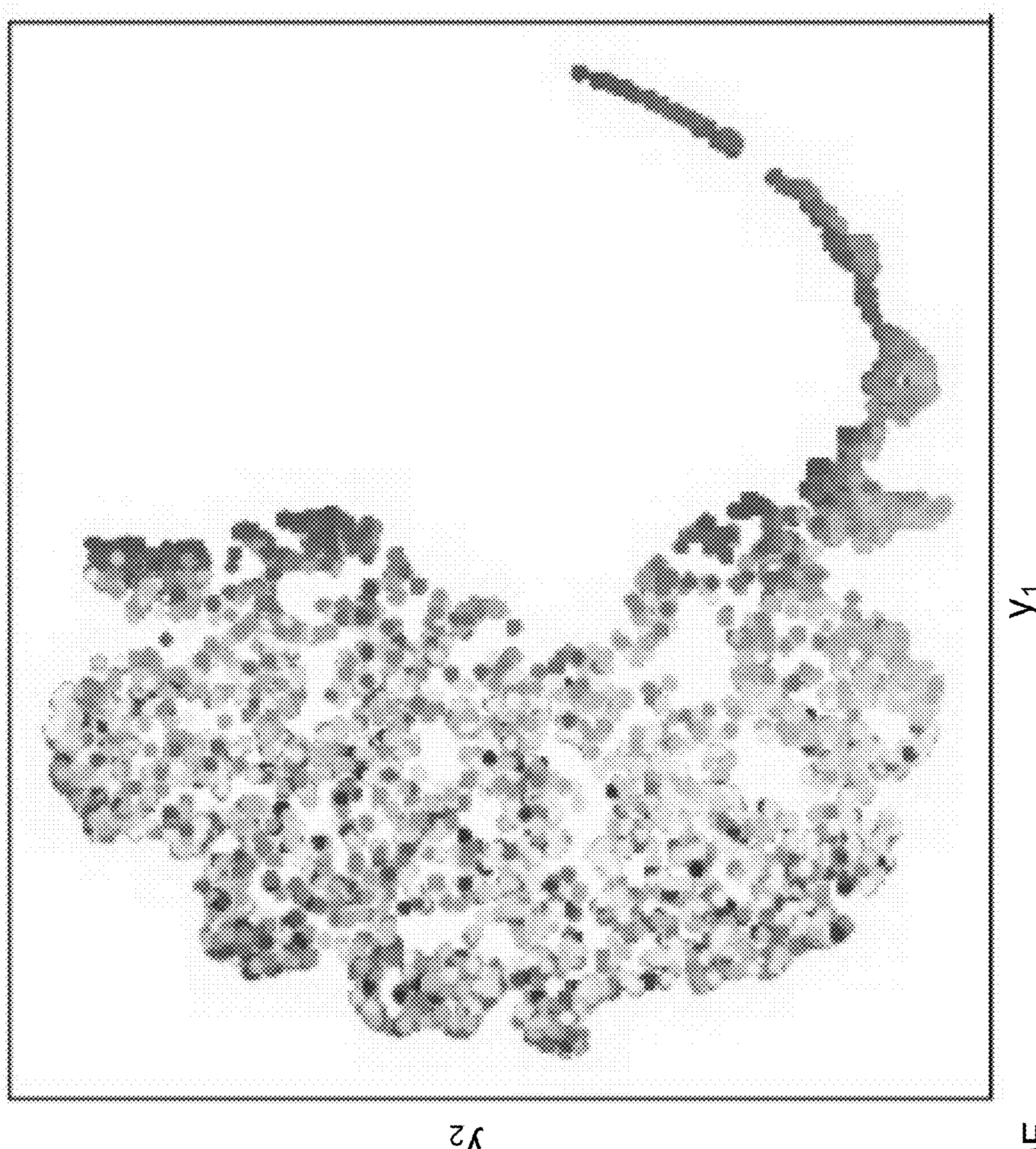

FIG. 10F

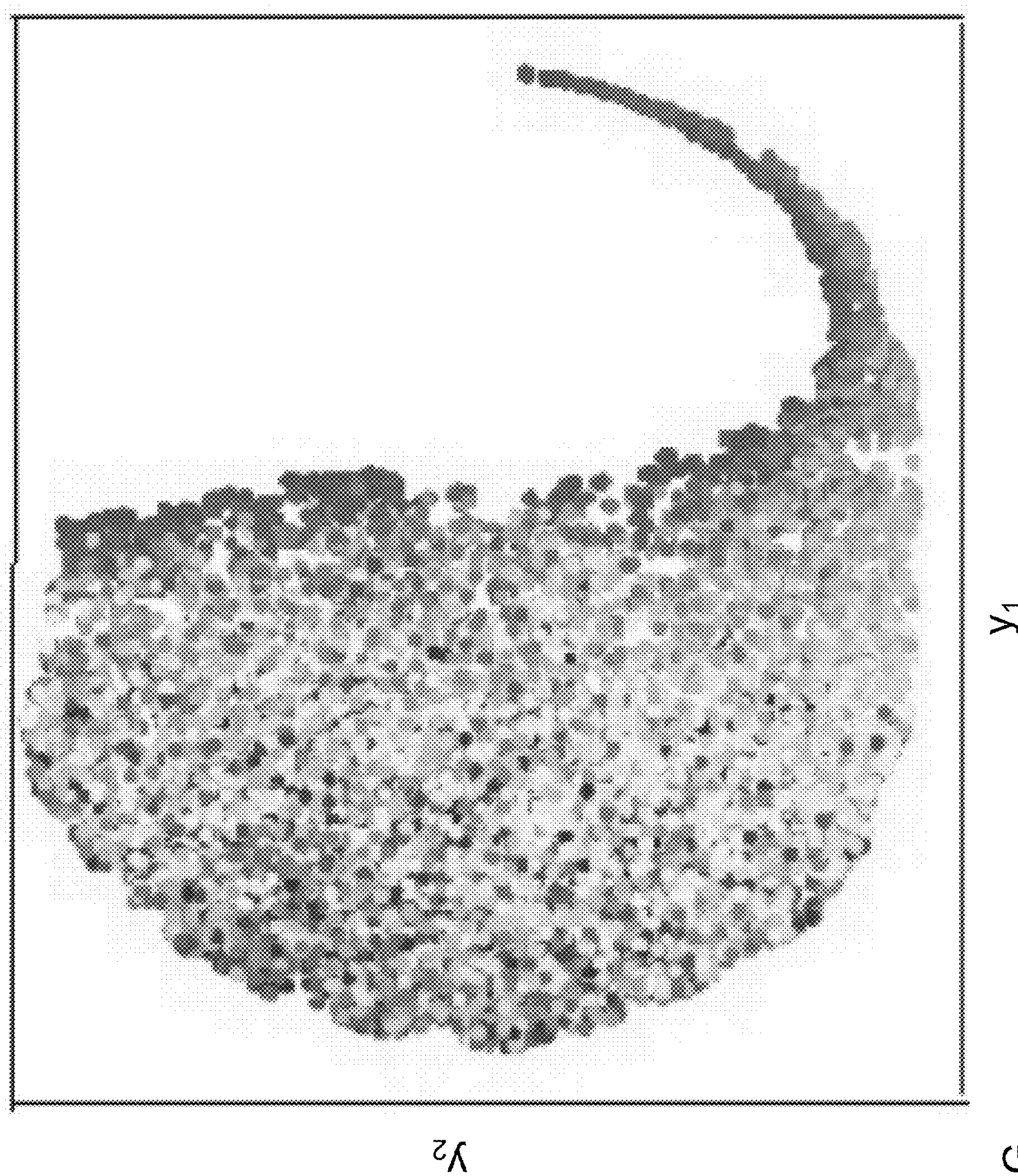

FIG. 10G

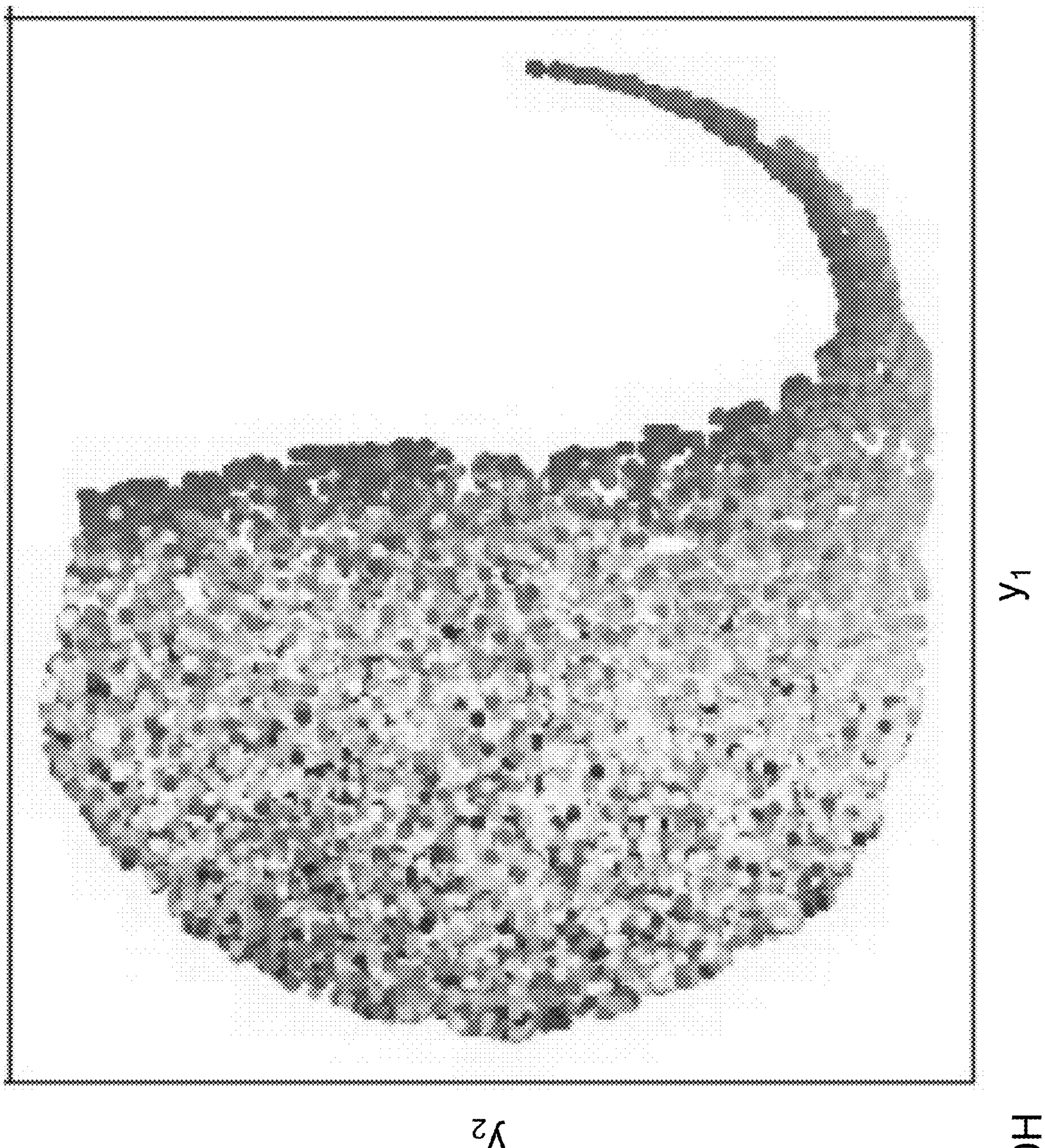

FIG. 10H

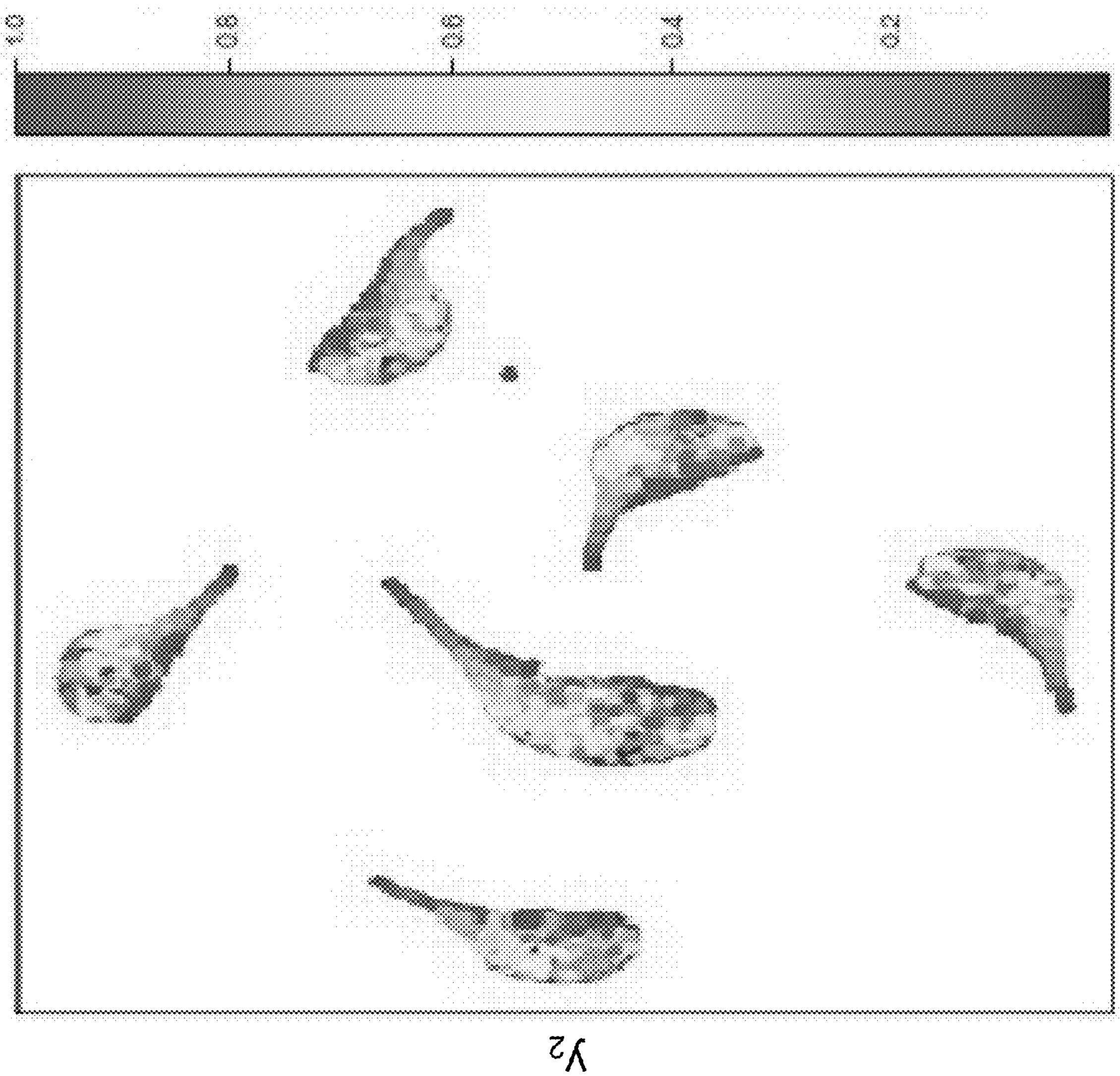

FIG. 11A

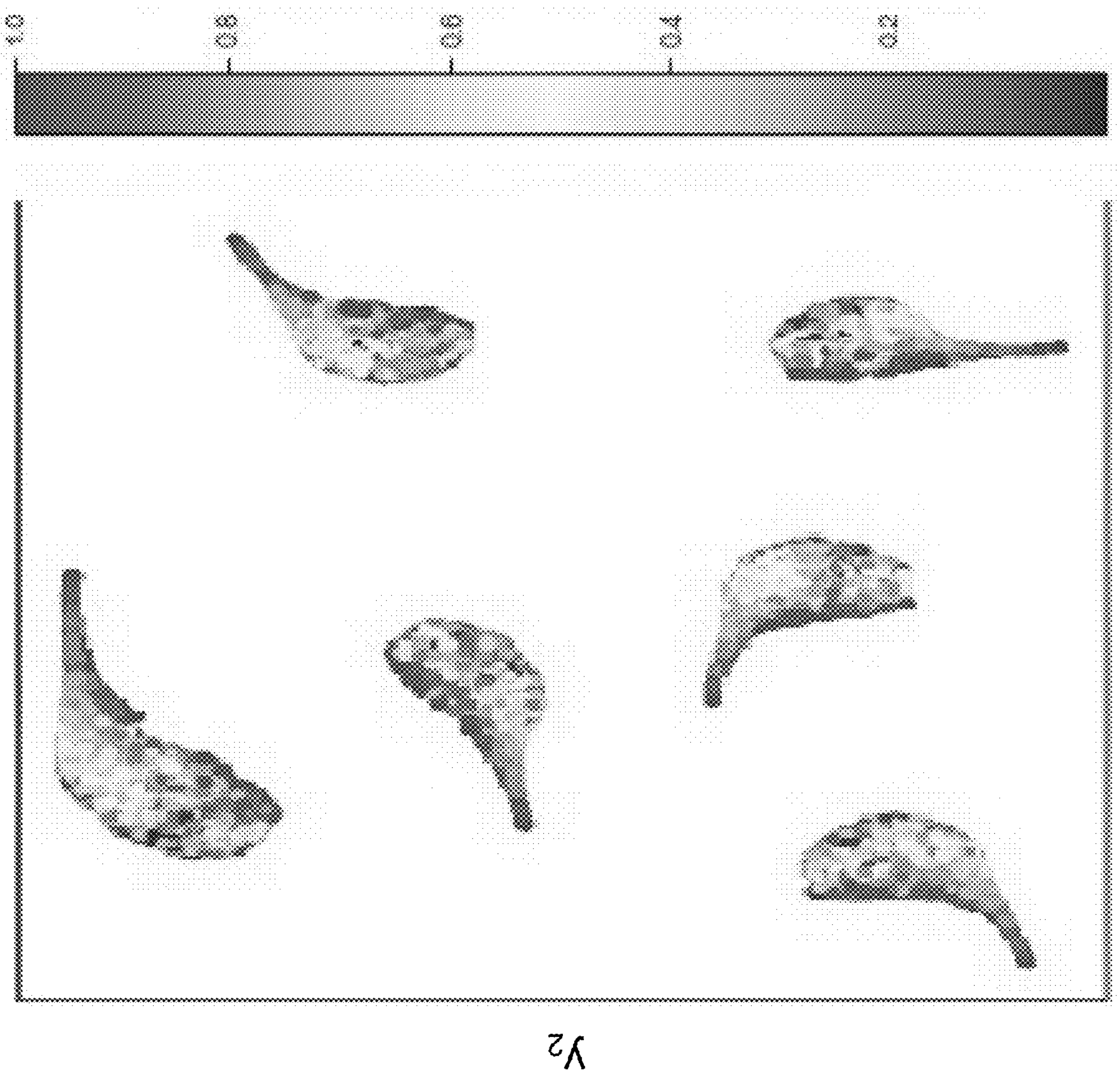

FIG. 11B

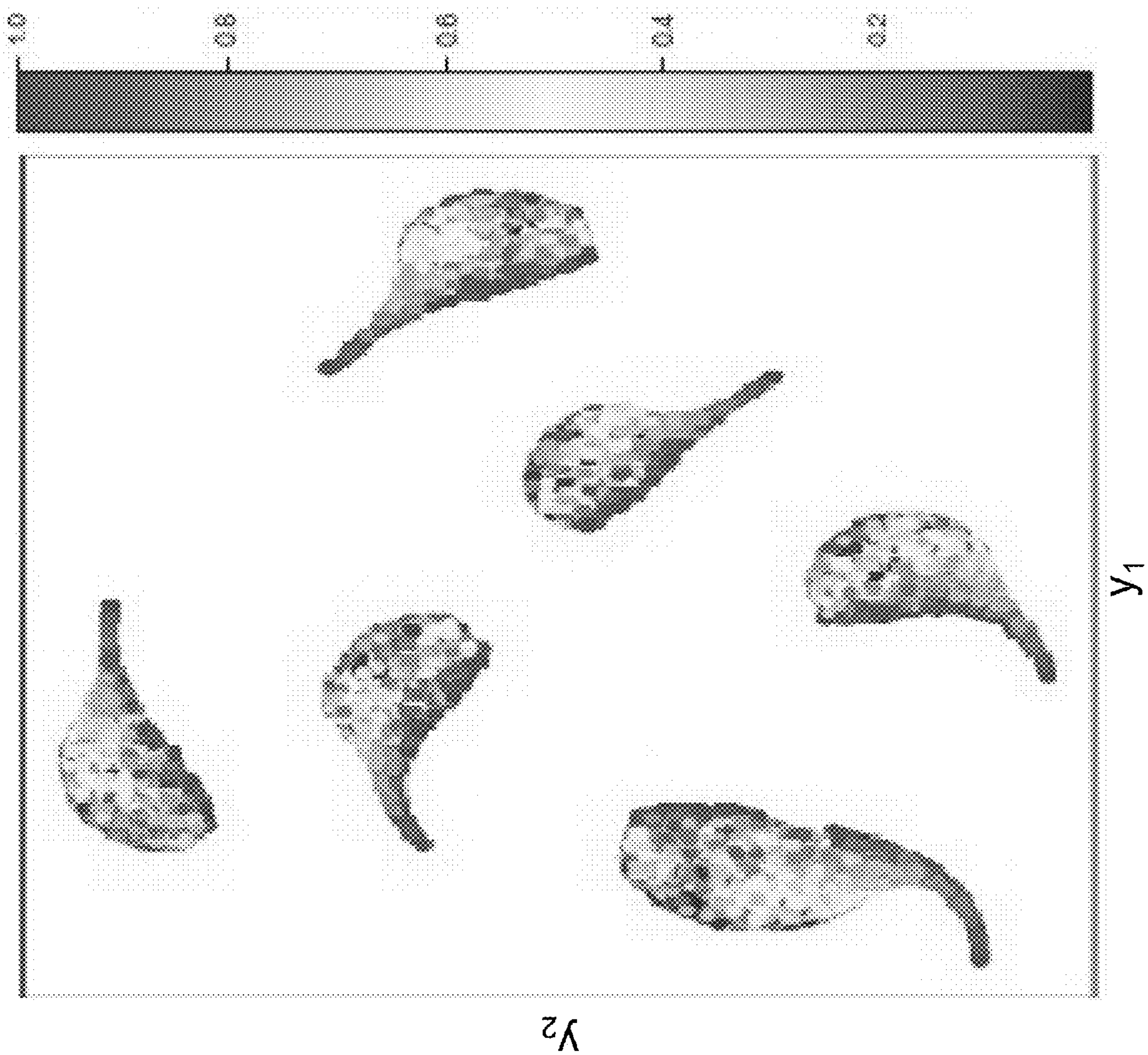

FIG. 11C

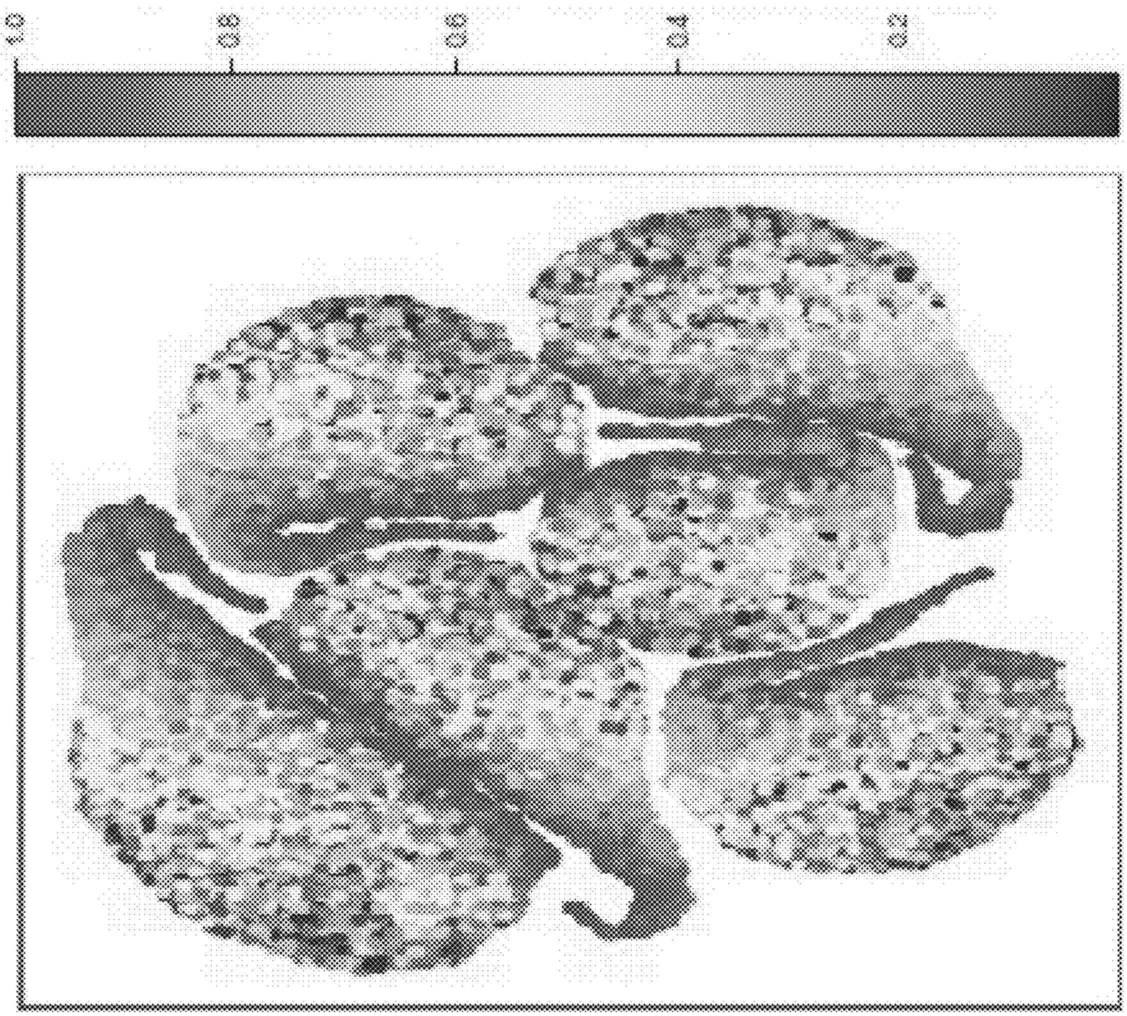

FIG. 11D

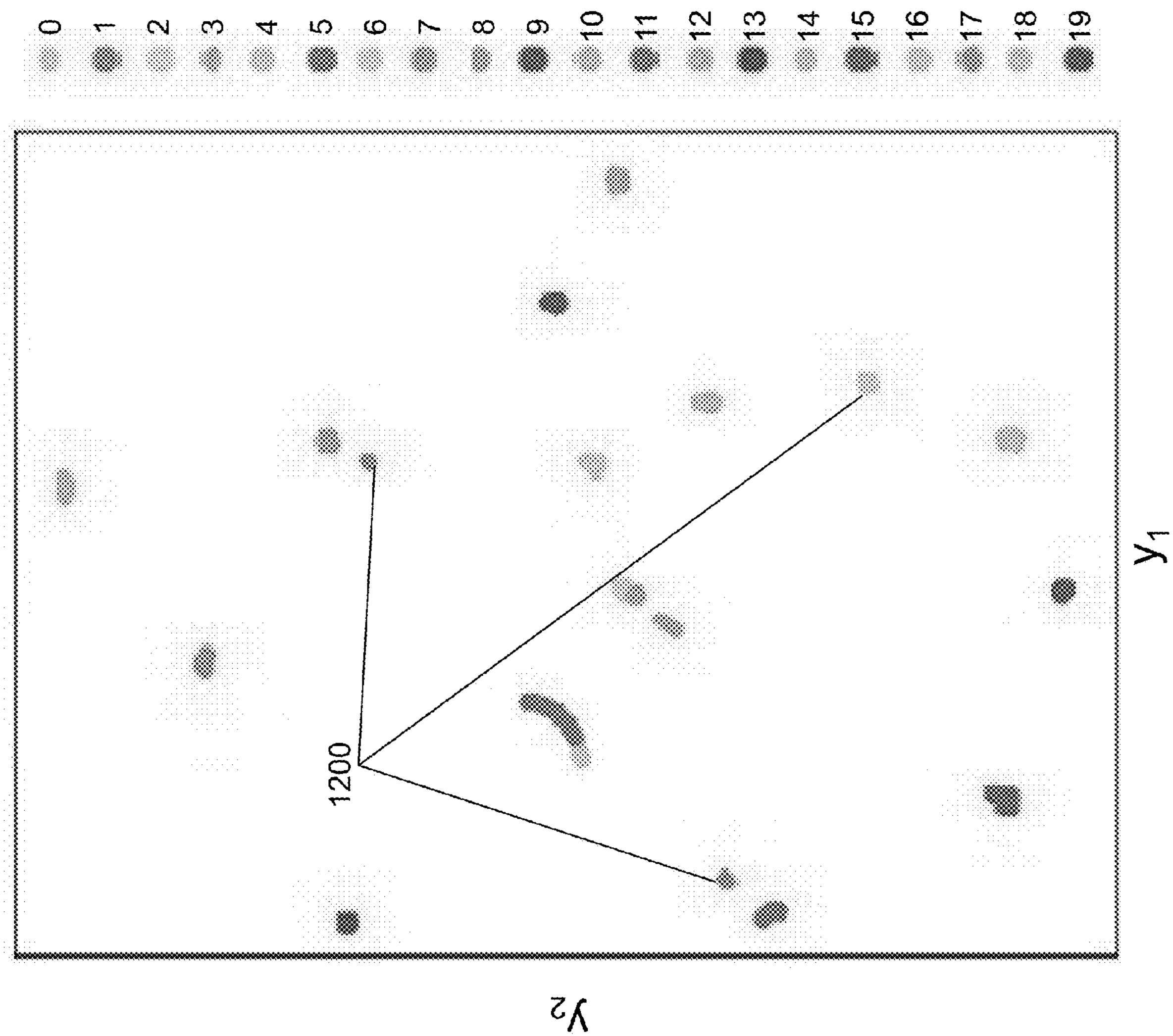

FIG. 12A

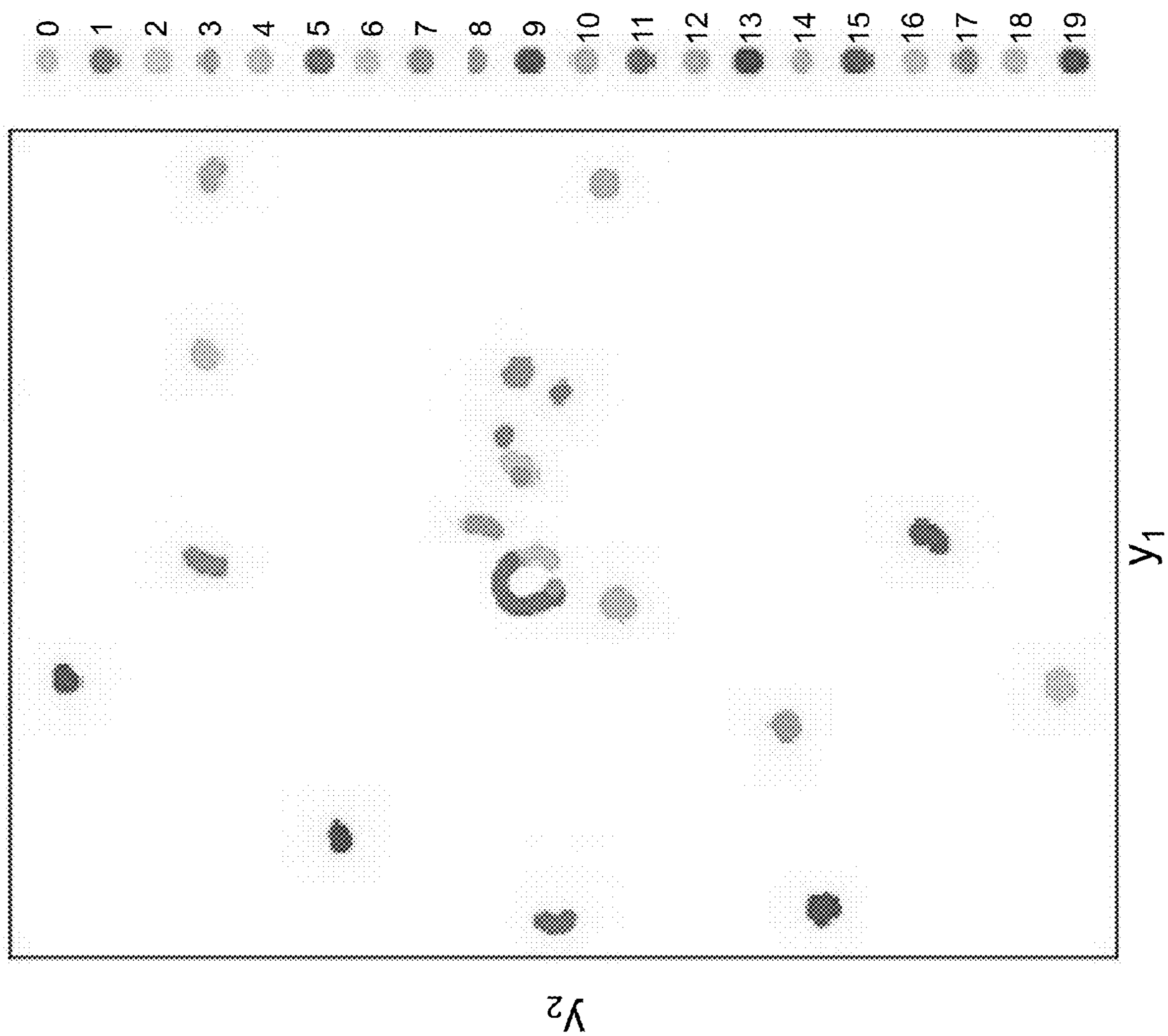

FIG. 12B

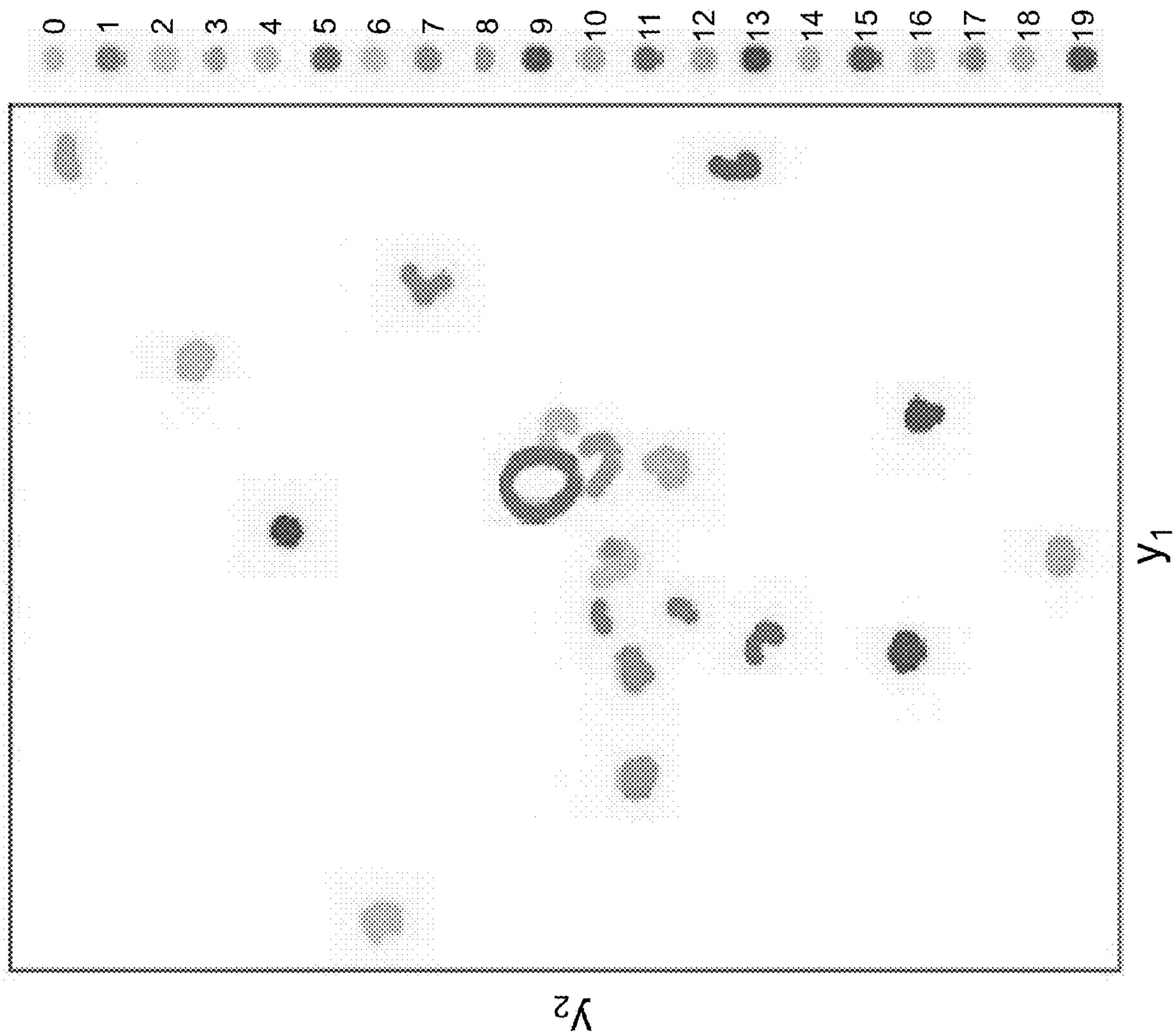

FIG. 12C

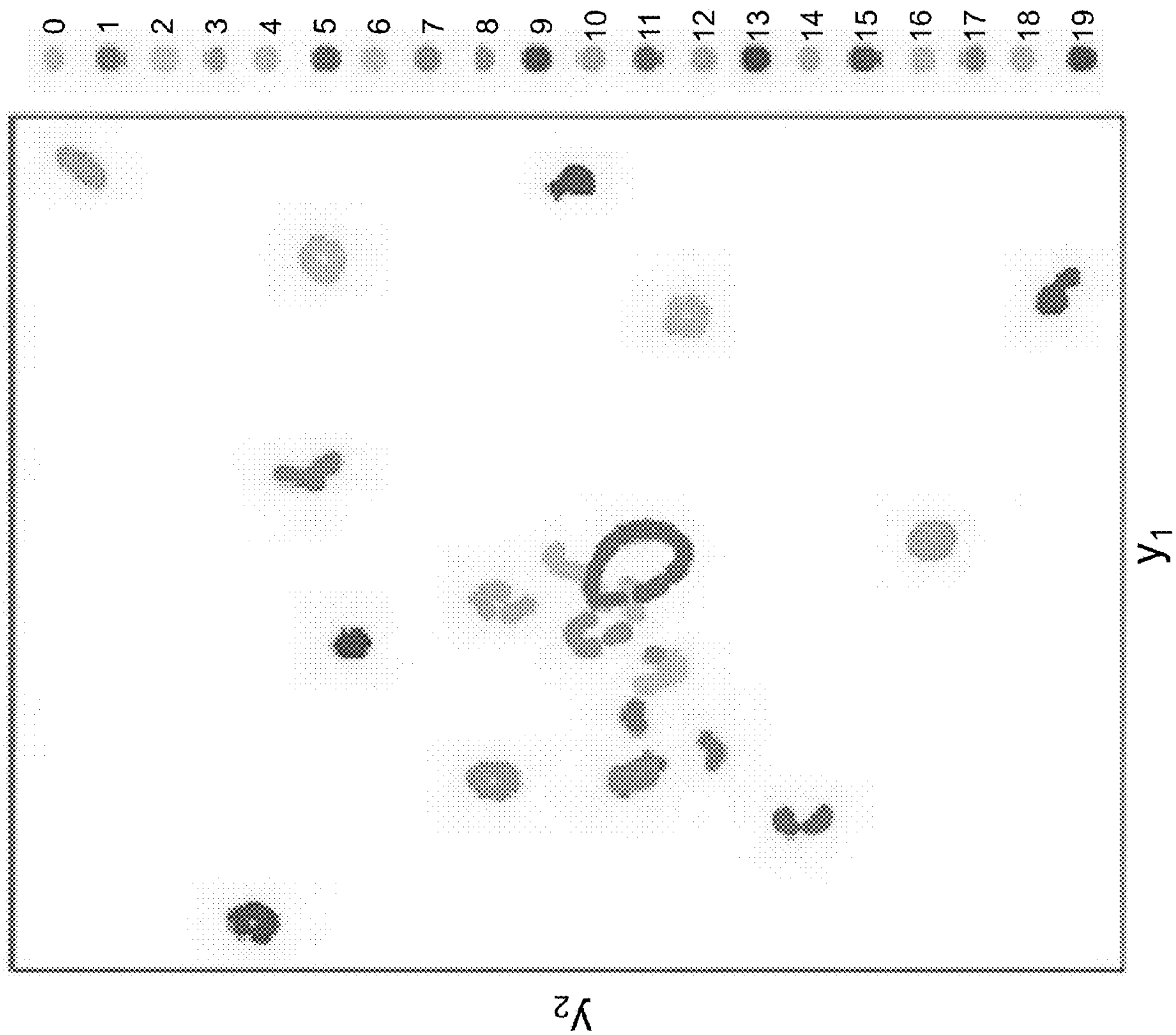

FIG. 12D

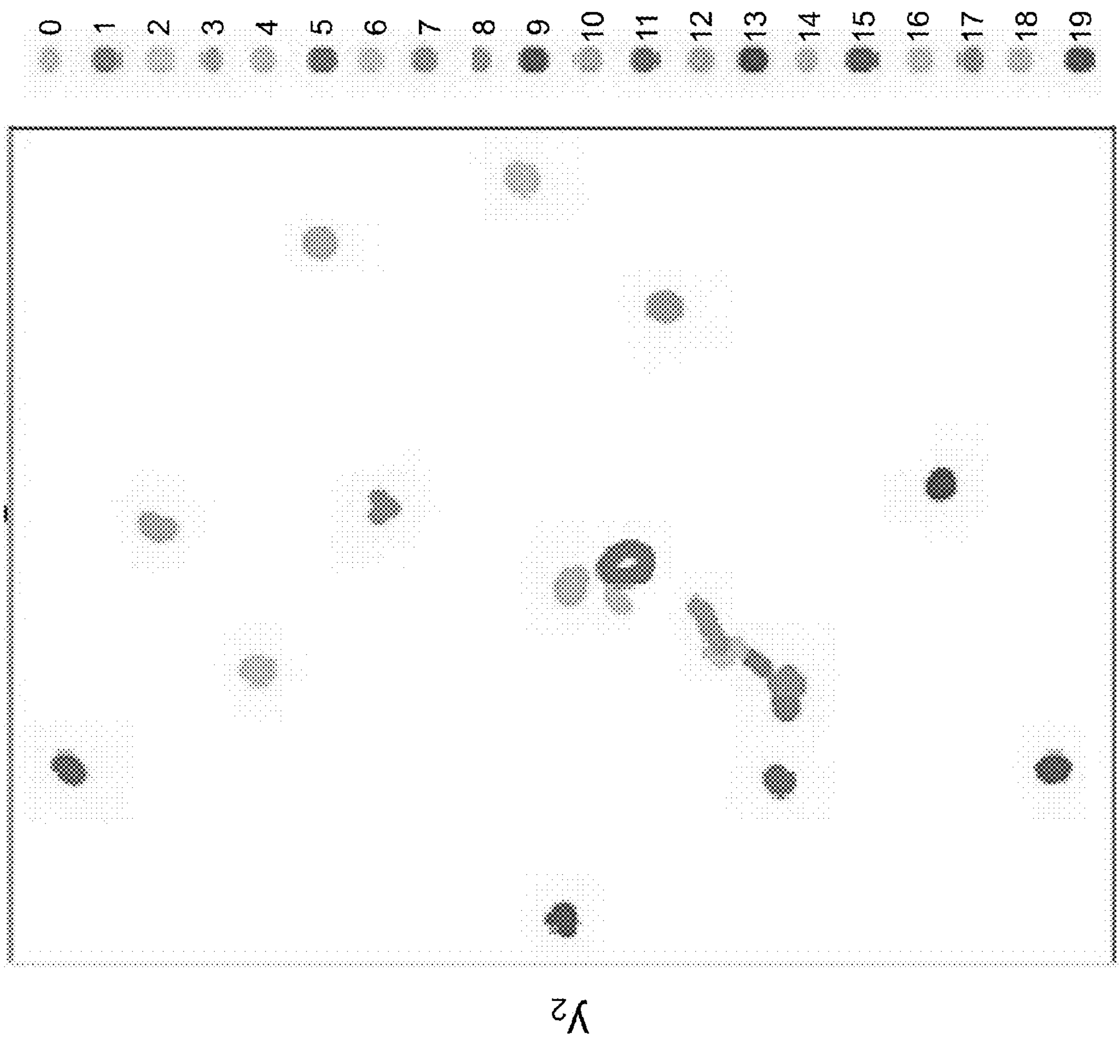

FIG. 13A

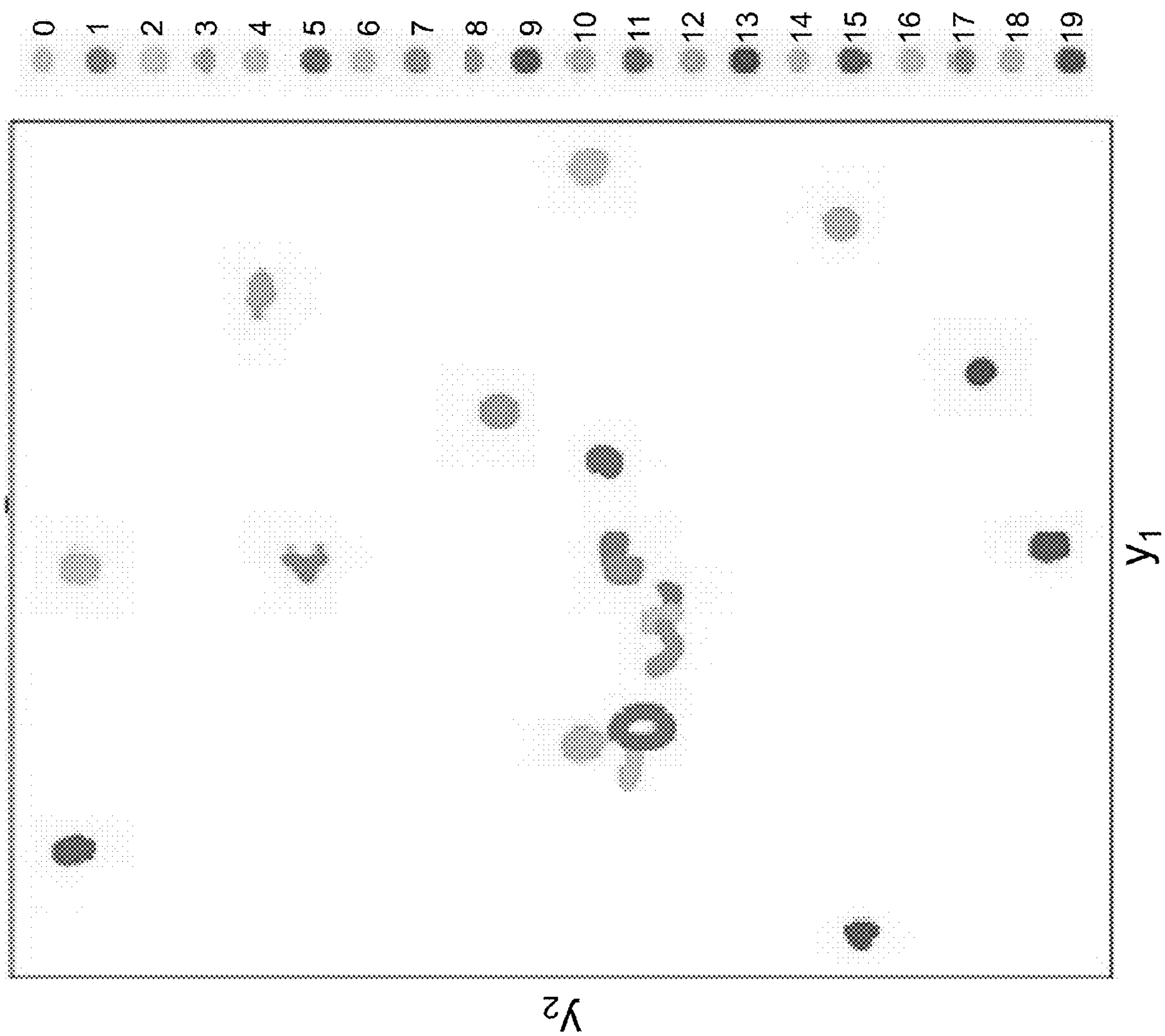

FIG. 13B

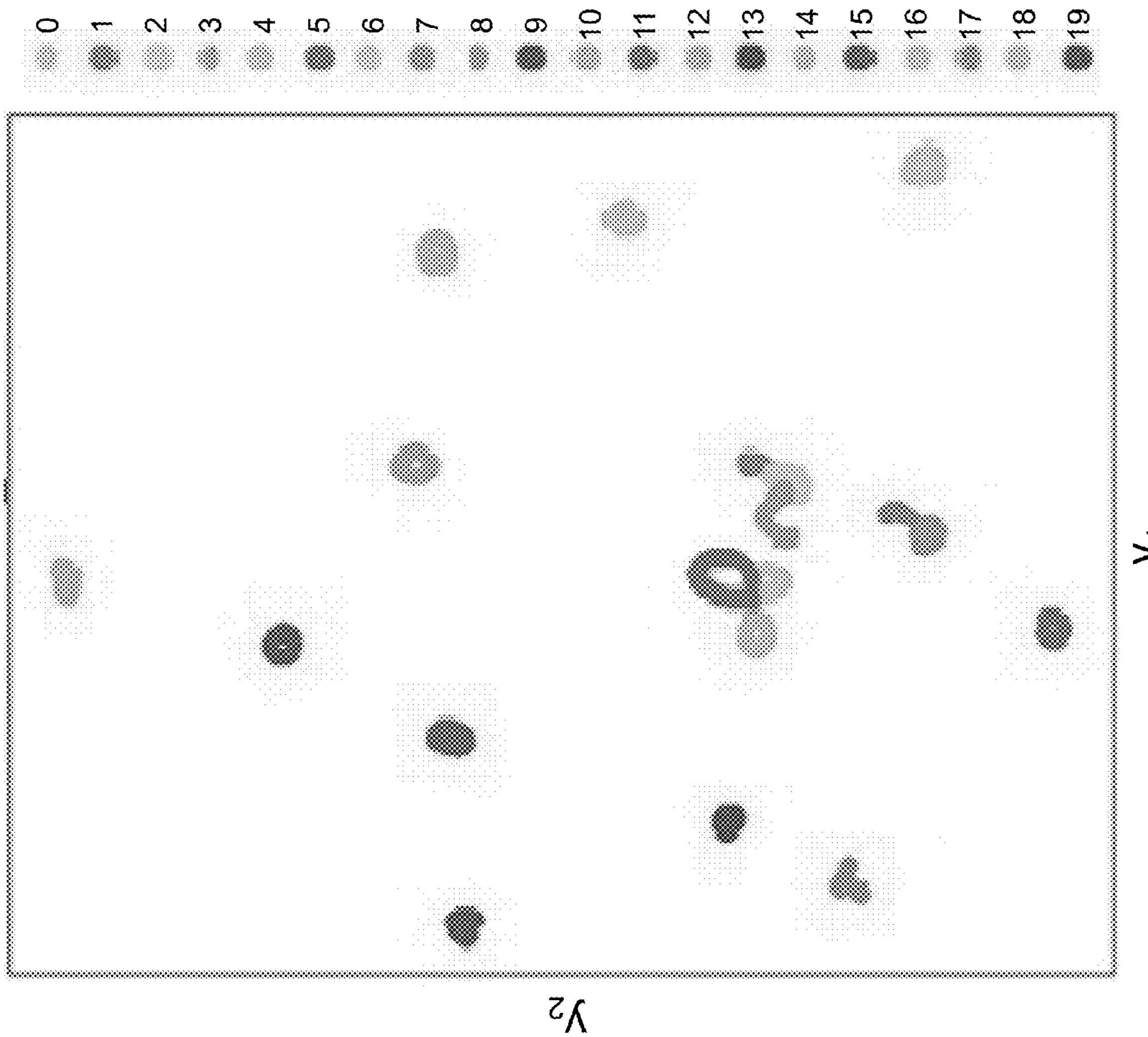

FIG. 13C

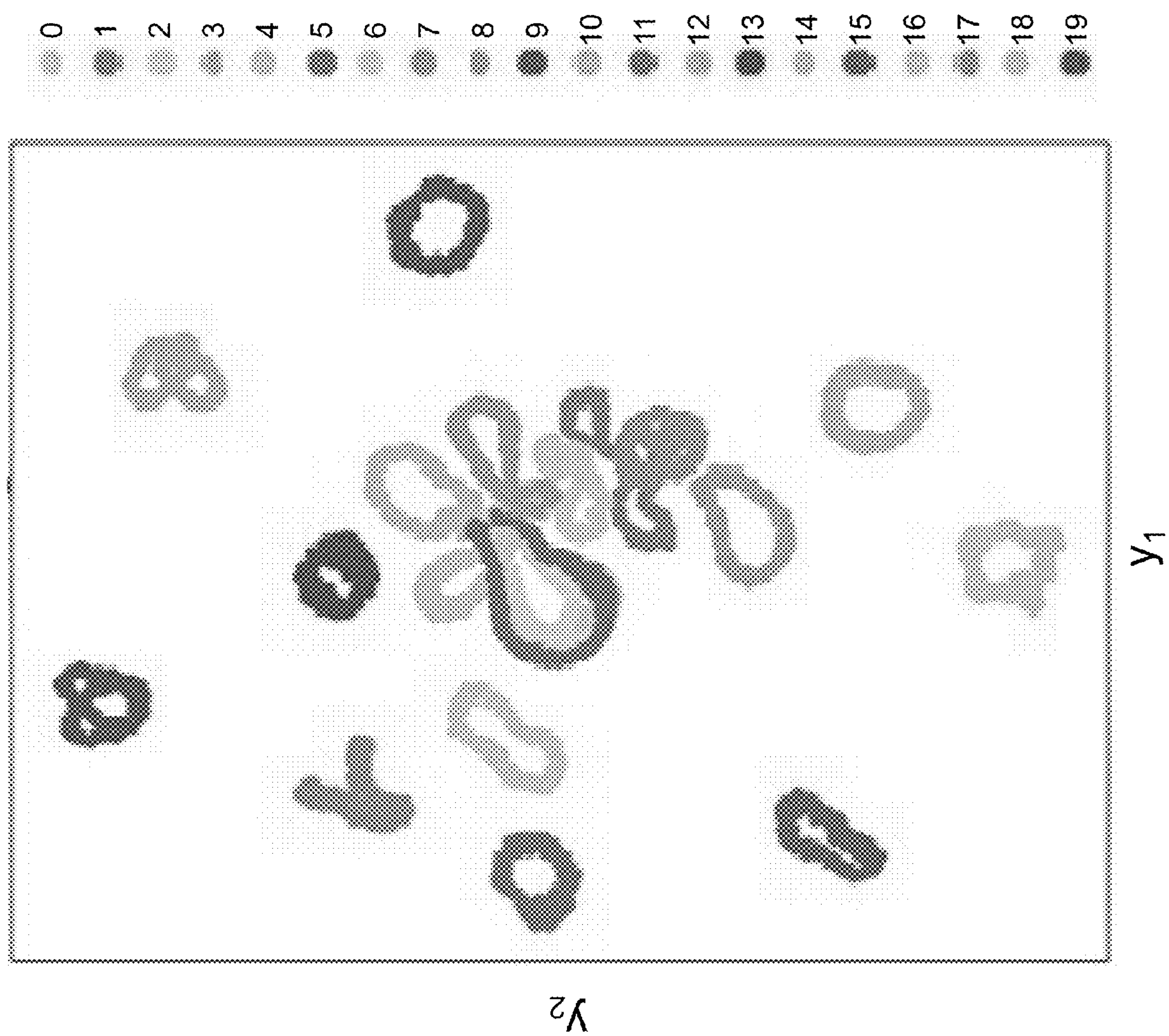

FIG. 13D

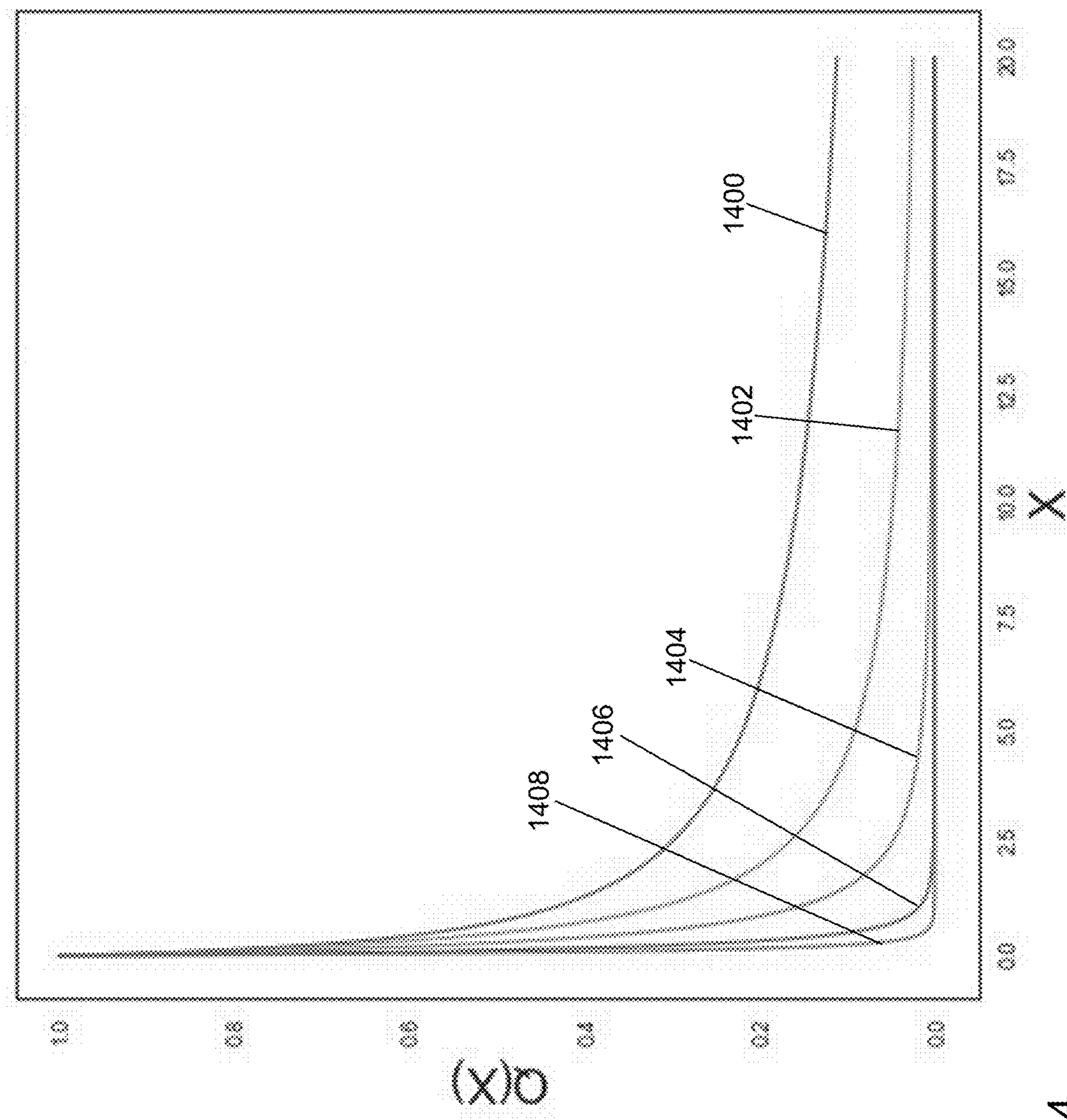

FIG. 14

HIGH DIMENSIONAL TO LOW DIMENSIONAL DATA TRANSFORMATION AND VISUALIZATION SYSTEM

CROSS-REFERENCE TO RELATED APPLICATIONS

The present application claims the benefit of and priority under 35 U.S.C. § 119(e) to U.S. Provisional Patent Application No. 63/057,141 filed Jul. 27, 2020, the entire contents of which are hereby incorporated by reference. The present application also claims the benefit of and priority under 35 U.S.C. § 119(e) to U.S. Provisional Patent Application No. 63/047,111 filed Jul. 1, 2020, the entire contents of which are hereby incorporated by reference.

BACKGROUND

Dimension reduction and visualization of high-dimensional data have become important research topics in many scientific fields because of the rapid growth of data sets with large sample size and/or number of dimensions. Currently, there are linear methods that primarily focus on preserving the most significant structure or maximum variance in data, nonlinear methods that primarily focus on preserving the long or short distances in the high-dimensional space, and manifold learning methods that primarily focus on preserving the intrinsic structure of the high-dimensional data. Linear and non-linear methods generally perform well in preserving the global structure of data, but can fail to preserve the local structure. Many of the manifold learning methods suffer from the "crowding problem" while preserving a local distance of high-dimensional data in low-dimensional space. This means that to describe small distances in high-dimensional space faithfully, the points with moderate or large distances between them in high-dimensional space are placed too far away from each other in low-dimensional space. Therefore, in the visualization, the points with small or moderate distances between them crash together.

SUMMARY

In an example embodiment, a computer-readable medium is provided having stored thereon computer-readable instructions that when executed by a computing device, cause the computing device to transform high-dimensional data into low-dimensional data. (A) An observation vector is selected from a plurality of observation vectors. Each observation vector of the plurality of observation vectors includes a value for each variable of a plurality of variables. The plurality of variables define a high-dimensional space. (B) A distance is computed between the selected observation vector and each observation vector of the plurality of observation vectors. (C) A plurality of nearest neighbors to the selected observation vector are selected using the computed distances. A number of the plurality of nearest neighbors is a predefined number. Each nearest neighbor of the plurality of nearest neighbors is one of the plurality of observation vectors that are closest to the selected observation vector. (D) A first sigmoid function is applied to compute a distance similarity value between the selected observation vector and each of the selected plurality of nearest neighbors based on the value of each variable of the plurality of variables of the selected observation vector and on the value of each variable of the plurality of variables of each of the plurality of nearest neighbors. (A) through (D) are repeated with each observation vector of the plurality of observation vectors selected as the observation vector in (A). Each of the computed distance similarity values computed in (D) are added to a first matrix. An initial matrix is computed from the plurality of observation vectors. The initial matrix represents a transformation of each observation vector of the plurality of observation vectors into a low-dimensional space defined to include a predefined number of dimensions. The predefined number of dimensions is less than a number of the plurality of variables. An optimization method is executed with the computed initial matrix, the first matrix, and a gradient of a second sigmoid function that computes a second distance similarity value between the selected observation vector and each of the plurality of nearest neighbors in the low-dimensional space. The optimization method determines an optimized matrix that represents a transformation of each observation vector of the plurality of observation vectors into the low-dimensional space. The optimized matrix is output.

In another example embodiment, a computing device is provided. The computing device includes, but is not limited to, a processor and a computer-readable medium operably coupled to the processor. The computer-readable medium has instructions stored thereon that, when executed by the processor, cause the computing device to transform high-dimensional data into low-dimensional data.

In yet another example embodiment, a method of transforming high-dimensional data into low-dimensional data is provided.

Other principal features of the disclosed subject matter will become apparent to those skilled in the art upon review of the following drawings, the detailed description, and the appended claims.

BRIEF DESCRIPTION OF THE DRAWINGS

The patent or application file contains at least one drawing executed in color. Copies of this patent or patent application publication with color drawing(s) will be provided by the Office upon request and payment of the necessary fee.

Illustrative embodiments of the disclosed subject matter will hereafter be described referring to the accompanying drawings, wherein like numerals denote like elements.

FIG. **1** depicts a block diagram of a transformation device in accordance with an illustrative embodiment.

FIGS. **2**A through **2**C depict a flow diagram illustrating examples of operations performed by a transformation application of the transformation device of FIG. **1** in accordance with an illustrative embodiment.

FIGS. **3**A through **3**D provide comparative clustering results using the transformation application with different values of a hyperparameter b value for a first dataset in accordance with an illustrative embodiment.

FIGS. **4**A through **4**D provide comparative clustering results using an existing clustering application with different values of a minimum distance hyperparameter value for the first dataset in accordance with an illustrative embodiment.

FIGS. **5**A through **5**D provide comparative clustering results using the transformation application with different values of the hyperparameter b value for a second dataset in accordance with an illustrative embodiment.

FIGS. **6**A through **6**D provide comparative clustering results using an existing clustering application with different values of the minimum distance hyperparameter value for the second dataset in accordance with an illustrative embodiment.

FIGS. **7**A through **7**F provide illustrative observations included in different clusters depicted in FIG. **5**A in accordance with an illustrative embodiment.

FIGS. **8**A through **8**D provide comparative clustering results using the transformation application with different values of the hyperparameter b value for a third dataset in accordance with an illustrative embodiment.

FIGS. **9**A through **9**D provide comparative clustering results using an existing clustering application with different values of the minimum distance hyperparameter value for the third dataset in accordance with an illustrative embodiment.

FIGS. **10**A through **10**D provide comparative clustering results using the transformation application with different values of the hyperparameter b value for a fourth dataset in accordance with an illustrative embodiment.

FIGS. **10**E through **10**H provide comparative clustering results using the transformation application with different values of the hyperparameter b value for a modified fourth dataset in accordance with an illustrative embodiment.

FIGS. **11**A through **11**D provide comparative clustering results using an existing clustering application with different values of the minimum distance hyperparameter value for the fourth dataset in accordance with an illustrative embodiment.

FIGS. **12**A through **12**D provide comparative clustering results using the transformation application with different values of the hyperparameter b value for a fifth dataset in accordance with an illustrative embodiment.

FIGS. **13**A through **13**D provide comparative clustering results using an existing clustering application with different values of the minimum distance hyperparameter value for the fifth dataset in accordance with an illustrative embodiment.

FIG. **14** presents a graph illustrating an effect of various values of a hyperparameter on a distance similarity in low-dimensional in accordance with an illustrative embodiment.

DETAILED DESCRIPTION

Referring to FIG. **1**, a block diagram of a transformation device **100** is shown in accordance with an illustrative embodiment. Transformation device **100** may include an input interface **102**, an output interface **104**, a communication interface **106**, a non-transitory computer-readable medium **108**, a processor **110**, a transformation application **122**, input dataset **124**, and a transformed dataset **126**. Fewer, different, and/or additional components may be incorporated into transformation device **100**. Transformation application **122** uses a hyperparameter b value that can be adjusted to reveal a finer cluster structure of data stored in input dataset **124** or to assist in visualizing the data stored in input dataset **124** by increasing a continuity of neighbors. As a result, transformation application **122** provides improved visibility of the intrinsic structure of the data that may not be visible using existing dimension reduction and high-dimensional data visualization techniques.

Input interface **102** provides an interface for receiving information from the user or another device for entry into transformation device **100** as understood by those skilled in the art. Input interface **102** may interface with various input technologies including, but not limited to, a keyboard **112**, a microphone **113**, a mouse **114**, a display **116**, a track ball, a keypad, one or more buttons, etc. to allow the user to enter information into transformation device **100** or to make selections presented in a user interface displayed on display **116**.

The same interface may support both input interface **102** and output interface **104**. For example, display **116** comprising a touch screen provides a mechanism for user input and for presentation of output to the user. Transformation device **100** may have one or more input interfaces that use the same or a different input interface technology. The input interface technology further may be accessible by transformation device **100** through communication interface **106**.

Output interface **104** provides an interface for outputting information for review by a user of transformation device **100** and/or for use by another application or device. For example, output interface **104** may interface with various output technologies including, but not limited to, display **116**, a speaker **118**, a printer **120**, etc. Transformation device **100** may have one or more output interfaces that use the same or a different output interface technology. The output interface technology further may be accessible by transformation device **100** through communication interface **106**.

Communication interface **106** provides an interface for receiving and transmitting data between devices using various protocols, transmission technologies, and media as understood by those skilled in the art. Communication interface **106** may support communication using various transmission media that may be wired and/or wireless. Transformation device **100** may have one or more communication interfaces that use the same or a different communication interface technology. For example, transformation device **100** may support communication using an Ethernet port, a Bluetooth antenna, a telephone jack, a USB port, etc. Data and/or messages may be transferred between transformation device **100** and another computing device of a distributed computing system **130** using communication interface **106**.

Computer-readable medium **108** is a non-transitory electronic holding place or storage for information so the information can be accessed by processor **110** as understood by those skilled in the art. Computer-readable medium **108** can include, but is not limited to, any type of random access memory (RAM), any type of read only memory (ROM), any type of flash memory, etc. such as magnetic storage devices (e.g., hard disk, floppy disk, magnetic strips, . . .), optical disks (e.g., compact disc (CD), digital versatile disc (DVD), . . .), smart cards, flash memory devices, etc. Transformation device **100** may have one or more computer-readable media that use the same or a different memory media technology. For example, computer-readable medium **108** may include different types of computer-readable media that may be organized hierarchically to provide efficient access to the data stored therein as understood by a person of skill in the art. As an example, a cache may be implemented in a smaller, faster memory that stores copies of data from the most frequently/recently accessed main memory locations to reduce an access latency. Transformation device **100** also may have one or more drives that support the loading of a memory media such as a CD, DVD, an external hard drive, etc. One or more external hard drives further may be connected to transformation device **100** using communication interface **106**.

Processor **110** executes instructions as understood by those skilled in the art. The instructions may be carried out by a special purpose computer, logic circuits, or hardware circuits. Processor **110** may be implemented in hardware and/or firmware. Processor **110** executes an instruction, meaning it performs/controls the operations called for by that instruction. The term "execution" is the process of running an application or the carrying out of the operation called for by an instruction. The instructions may be written using one or more programming language, scripting language, assembly language, etc. Processor **110** operably couples with input interface **102**, with output interface **104**, with communication interface **106**, and with computer-readable medium **108** to receive, to send, and to process information. Processor **110** may retrieve a set of instructions from a permanent memory device and copy the instructions in an executable form to a temporary memory device that is generally some form of RAM. Transformation device **100** may include a plurality of processors that use the same or a different processing technology.

Some machine-learning approaches may be more efficiently and speedily executed and processed with machine-learning specific processors (e.g., not a generic central processing unit (CPU)). Such processors may also provide additional energy savings when compared to generic CPUs. For example, some of these processors can include a graphical processing unit (GPU), an application-specific integrated circuit, a field-programmable gate array, an artificial intelligence accelerator, a purpose-built chip architecture for machine learning, and/or some other machine-learning specific processor that implements a machine learning approach using semiconductor (e.g., silicon, gallium arsenide) devices. These processors may also be employed in heterogeneous computing architectures with a number of and a variety of different types of cores, engines, nodes, and/or layers to achieve additional various energy efficiencies, processing speed improvements, data communication speed improvements, and/or data efficiency targets and improvements throughout various parts of the system.

Transformation application **122** performs operations associated with defining transformed dataset **126** from data stored in input dataset **124**. Transformed dataset **126** includes a low-dimensional representation of observation vectors included in input dataset **124**. For example, the low dimensional representation may be a transformation of the observation vectors included in input dataset **124** from high-dimensional data to two or three dimensions that can be graphically presented to understand how the observations included in input dataset **124** may be related. Such a visualization is not possible when directly using the observation vectors included in input dataset **124**. The transformed observation vectors stored in transformed dataset **126** further may be clustered to present a visualization of the groupings of observation vectors included in input dataset **124** that may be used to classify or otherwise label the observation vectors included in input dataset **124**. The classification or label may define a characteristic value associated with each observation vector included in input dataset **124**. Some or all of the operations described herein may be embodied in transformation application **122**. The operations may be implemented using hardware, firmware, software, or any combination of these methods.

Referring to the example embodiment of FIG. **1**, transformation application **122** is implemented in software (comprised of computer-readable and/or computer-executable instructions) stored in computer-readable medium **108** and accessible by processor **110** for execution of the instructions that embody the operations of transformation application **122**. Transformation application **122** may be written using one or more programming languages, assembly languages, scripting languages, etc. Transformation application **122** may be integrated with other analytic tools. As an example, transformation application **122** may be part of an integrated data analytics software application and/or software architecture such as that offered by SAS Institute Inc. of Cary, N.C., USA. Merely for illustration, transformation application **122** may be implemented using or integrated with one or more SAS software tools such as JMP®, Base SAS, SAS® Enterprise Miner™, SAS® Event Stream Processing, SAS/STAT®, SAS® High Performance Analytics Server, SAS® Visual Data Mining and Machine Learning, SAS® LASR™, SAS® In-Database Products, SAS® Scalable Performance Data Engine, SAS® Cloud Analytic Services (CAS), SAS/OR®, SAS/ETS®, SAS® Visual Analytics, SAS® Viya™, SAS In-Memory Statistics for Hadoop®, etc. all of which are developed and provided by SAS Institute Inc. of Cary, N.C., USA. Data mining, statistical analytics, and response prediction are practically applied in a wide variety of industries to solve technical problems.

Transformation application **122** may be implemented as a Web application. For example, transformation application **122** may be configured to receive hypertext transport protocol (HTTP) responses and to send HTTP requests. The HTTP responses may include web pages such as hypertext markup language (HTML) documents and linked objects generated in response to the HTTP requests. Each web page may be identified by a uniform resource locator (URL) that includes the location or address of the computing device that contains the resource to be accessed in addition to the location of the resource on that computing device. The type of file or resource depends on the Internet application protocol such as the file transfer protocol, HTTP, H.323, etc. The file accessed may be a simple text file, an image file, an audio file, a video file, an executable, a common gateway interface application, a Java applet, an extensible markup language (XML) file, or any other type of file supported by HTTP.

Input dataset **124** may include, for example, a plurality of rows and a plurality of columns. The plurality of rows may be referred to as observation vectors or records (observations), and the columns may be referred to as variables. In an alternative embodiment, input dataset **124** may be transposed. The plurality of variables defines a vector x_i for each observation vector $i=1, 2, \ldots, N$, where N is a number of the observation vectors included in input dataset **124**. Each vector $x_i=\{x_1, x_2, \ldots, x_{N_V}\}$ includes a variable value for each variable, where N_V is a number of the plurality of variables. Input dataset **124** may include additional variables that are not included in the plurality of variables. One or more variables of the plurality of variables may describe a characteristic of a physical object. For example, if input dataset **124** includes data related to operation of a vehicle, the variables may include a type of vehicle, an oil pressure, a speed, a gear indicator, a gas tank level, a tire pressure for each tire, an engine temperature, a radiator level, etc.

In data science, engineering, and statistical applications, data often consists of multiple measurements (across sensors, characteristics, responses, etc.) collected across multiple time instances (patients, test subjects, etc.). These measurements may be collected in input dataset **124** for analysis and processing or streamed to transformation device **100** as it is generated. Input dataset **124** may include data captured as a function of time for one or more physical objects. The data stored in input dataset **124** may be captured at different time points periodically, intermittently, when an event occurs, etc. Input dataset **124** may include data captured at a high data rate such as 200 or more observation vectors per second for one or more physical objects. One or more columns of input dataset **124** may include a time and/or date value. Input dataset **124** may include data captured under normal and/or abnormal operating conditions of the physical object.

The data stored in input dataset **124** may be received directly or indirectly from the source and may or may not be pre-processed in some manner. For example, the data may be pre-processed using an event stream processor such as the SAS® Event Stream Processing Engine (ESPE), developed and provided by SAS Institute Inc. of Cary, N.C., USA. For example, data stored in input dataset **124** may be generated as part of the Internet of Things (IoT), where things (e.g., machines, devices, phones, sensors) can be connected to networks and the data from these things collected and processed within the things and/or external to the things before being stored in input dataset **124**. For example, the IoT can include sensors in many different devices and types of devices, and high value analytics can be applied to identify hidden relationships and drive increased efficiencies. This can apply to both big data analytics and real-time analytics. Some of these devices may be referred to as edge devices, and may involve edge computing circuitry. These devices may provide a variety of stored or generated data, such as network data or data specific to the network devices themselves. Again, some data may be processed with an ESPE, which may reside in the cloud or in an edge device before being stored in input dataset **124**.

The data stored in input dataset **124** may include any type of content represented in any computer-readable format such as binary, alphanumeric, numeric, string, markup language, etc. The content may include textual information, graphical information, image information, audio information, numeric information, etc. that further may be encoded using various encoding techniques as understood by a person of skill in the art.

Input dataset **124** may be stored on computer-readable medium **108** or on one or more computer-readable media of distributed computing system **130** and accessed by transformation device **100** using communication interface **106**, input interface **102**, and/or output interface **104**. Input dataset **124** may be stored in various compressed formats such as a coordinate format, a compressed sparse column format, a compressed sparse row format, etc. The data may be organized using delimited fields, such as comma or space separated fields, fixed width fields, using a SAS® dataset, etc. The SAS dataset may be a SAS® file stored in a SAS® library that a SAS® software tool creates and processes. The SAS dataset contains data values that are organized as a table of observation vectors (rows) and variables (columns) that can be processed by one or more SAS software tools.

Input dataset **124** may be stored using various data structures as known to those skilled in the art including one or more files of a file system, a relational database, one or more tables of a system of tables, a structured query language database, etc. on transformation device **100** or on distributed computing system **130**. Transformation device **100** may coordinate access to input dataset **124** that is distributed across distributed computing system **130** that may include one or more computing devices. For example, input dataset **124** may be stored in a cube distributed across a grid of computers as understood by a person of skill in the art. As another example, input dataset **124** may be stored in a multi-node Hadoop® cluster. For instance, Apache™ Hadoop® is an open-source software framework for distributed computing supported by the Apache Software Foundation. As another example, input dataset **124** may be stored in a cloud of computers and accessed using cloud computing technologies, as understood by a person of skill in the art. The SAS® LASR™ Analytic Server may be used as an analytic platform to enable multiple users to concurrently access data stored in input dataset **124**. The SAS Viya open, cloud-ready, in-memory architecture also may be used as an analytic platform to enable multiple users to concurrently access data stored in input dataset **124**. SAS CAS may be used as an analytic server with associated cloud services in SAS Viya. Some systems may use SAS In-Memory Statistics for Hadoop® to read big data once and analyze it several times by persisting it in-memory for the entire session. Some systems may be of other types and configurations.

Referring to FIGS. **2**A to **2**C, example operations associated with transformation application **122** are described. Additional, fewer, or different operations may be performed depending on the embodiment of transformation application **122**. The order of presentation of the operations of FIGS. **2**A to **2**C is not intended to be limiting. Some of the operations may not be performed in some embodiments. Although some of the operational flows are presented in sequence, the various operations may be performed in various repetitions and/or in other orders than those that are illustrated. For example, a user may execute transformation application **122**, which causes presentation of a first user interface window, which may include a plurality of menus and selectors such as drop-down menus, buttons, text boxes, hyperlinks, etc. associated with transformation application **122** as understood by a person of skill in the art. The plurality of menus and selectors may be accessed in various orders. An indicator may indicate one or more user selections from a user interface, one or more data entries into a data field of the user interface, one or more data items read from computer-readable medium **108** or otherwise defined with one or more default values, etc. that are received as an input by transformation application **122**. The operations of transformation application **122** further may be performed in parallel using a plurality of threads and/or a plurality of worker computing devices.

Referring to FIG. **2**A, in an operation **200**, a first indicator may be received that indicates input dataset **124**. For example, the first indicator indicates a location and a name of input dataset **124**. As an example, the first indicator may be received by transformation application **122** after selection from a user interface window or after entry by a user into a user interface window. In an alternative embodiment, input dataset **124** may not be selectable. For example, a most recently created dataset may be used automatically.

In an operation **202**, a second indicator may be received that indicates the plurality of variables or features to include when transforming the observation vectors included in input dataset **124**. For example, the second indicator may indicate a plurality of column numbers or a plurality of column names. As another option, all of the columns may be used by default. Each observation vector x_i, i= . . . , N_V read from input dataset **124** may include a value for each variable of the plurality of variables to define N_V dimensions or features. Input dataset **124** includes a set of observation vectors $X=[x_{j,i}]$, i=1, 2, . . . , N_V, j=1, 2, . . . , N. When a value for a variable of the plurality of variables is missing, the observation vector may not be included in the number of observation vectors N, a value may be computed for the missing variable.

In an operation **204**, a third indicator of a distance function may be received. For example, the third indicator indicates a name of a distance function. The third indicator may be received by transformation application **122** after selection from a user interface window or after entry by a user into a user interface window. A default value for the distance function may further be stored, for example, in computer-readable medium **108**. As an example, a distance function may be selected from “Euclidean”, “Kullback-Leibler”, “Manhattan”, “Minkowski”, “Cosine”, “Chebyshev”, “Hamming”, etc. As an example, a default distance function may be “Euclidean”. Of course, the distance function may be labeled or selected in a variety of different manners by the user as understood by a person of skill in the art. In an alternative embodiment, the distance function may not be selectable, and a single distance function is implemented by transformation application **122**.

In an operation **206**, a fourth indicator of a nearest neighbor search function may be received. For example, the fourth indicator indicates a name of a nearest neighbor search function. The fourth indicator may be received by transformation application **122** after selection from a user interface window or after entry by a user into a user interface window. A default value for the nearest neighbor search function may further be stored, for example, in computer-readable medium **108**. As an example, a nearest neighbor search function may be selected from “K Nearest Neighbor”, K-D Tree”, “Nearest Neighbor Descent”, etc. As an example, a default nearest neighbor search function may be “K Nearest Neighbor”. Of course, the nearest neighbor search function may be labeled or selected in a variety of different manners by the user as understood by a person of skill in the art. In an alternative embodiment, the nearest neighbor search function may not be selectable, and a single nearest neighbor search function is implemented by transformation application **122**.

In an operation **208**, a fifth indicator of a number of nearest neighbors value k may be received in addition to any other hyperparameters used by the nearest neighbor search function indicated in operation **206**. In an alternative embodiment, the fifth indicator may not be received. For example, a default value(s) may be stored, for example, in computer-readable medium **108** and used automatically. In another alternative embodiment, the number of nearest neighbors value k may not be selectable. Instead, a fixed, predefined value may be used. For illustration, a default value for the number of nearest neighbors value k may be k=10 though other values may be used. The number of nearest neighbors value k indicates a number of observation vectors from input dataset **124** to identify as nearest neighbor relative to each observation vector to define a graph of the observation vectors included in input dataset **124**.

In an operation **210**, a sixth indicator of a number of dimensions value d may be received. In an alternative embodiment, the sixth indicator may not be received. For example, a default value may be stored, for example, in computer-readable medium **108** and used automatically. In another alternative embodiment, the value of the number of dimensions value d may not be selectable. Instead, a fixed, predefined value may be used. For illustration, a default value for the number of dimensions value d may be d=2 though other values may be used. The number of dimensions value d indicates a number of dimensions to include in the low-dimensional transformation of the observation vectors included in input dataset **124**. Typically, the number of dimensions value d may be d=2 or d=3 to allow a graphical presentation of the observation vectors included in input dataset **124** in the low-dimensional space though other values may be used.

In an operation **212**, a seventh indicator of an optimization method used to determine the low-dimensional space may be received. For example, the seventh indicator indicates a name of an optimization method. The seventh indicator may be received by transformation application **122** after selection from a user interface window or after entry by a user into a user interface window. A default value for the optimization method may further be stored, for example, in computer-readable medium **108**. As an example, an optimization method may be selected from “SGD”, “SGD with Negative Sampling”, etc. SGD indicates stochastic gradient descent. SGD with negative sampling, for example, is described in a paper by Tomas Mikolov et al. titled *Distributed Representations of Words and Phrases and their Compositionality* published Oct. 16, 2013 In Advances in neural information processing systems, pp. 3111-3119, 2013. As an example, a default optimization method may be “SGD with Negative Sampling”. Of course, the optimization method may be labeled or selected in a variety of different manners by the user as understood by a person of skill in the art. In an alternative embodiment, the optimization method may not be selectable, and a single optimization method is implemented by transformation application **122**.

In an operation **214**, an eighth indicator of a number of epochs value N_e may be received in addition to any other hyperparameters used by the optimization method indicated in operation **212**. For example, when SGD with negative sampling is selected in operation **212**, a number of negative samples value M may also be received as part of the eighth indicator. As another example, some optimization methods may include a hyperparameter α_k that is a step-size or a learning rate value. In an alternative embodiment, the eighth indicator may not be received. For example, a default value(s) may be stored, for example, in computer-readable medium **108** and used automatically. In another alternative embodiment, the number of epochs value N_e or other hyperparameters used by the optimization method may not be selectable. Instead, a fixed, predefined value(s) may be used. For illustration, a default value for the number of epochs value N_e may be N_e=500 though other values may be used. The number of N_e indicates a number of iterations of the optimization method before processing is stopped. For illustration, a default value for the number of negative samples value M may be M=5 though other values may be used. For illustration, a default value for the step-size α_k may be α_k=1 though other values may be used. The number of negative samples value M and the step-size value α_k may be initial values that can change as the process executes.

In an operation **216**, a ninth indicator of a first hyperparameter α may be received. In an alternative embodiment, the ninth indicator may not be received. For example, a default value may be stored, for example, in computer-readable medium **108** and used automatically. In another alternative embodiment, the value of the first hyperparameter α may not be selectable. Instead, a fixed, predefined value may be used. For illustration, a default value for the first hyperparameter α may be α=1 and a may further be in the range [1,1.5] though other values may be used.

In an operation **218**, a tenth indicator of a second hyperparameter b may be received. In an alternative embodiment, the tenth indicator may not be received. For example, a default value may be stored, for example, in computer-readable medium **108** and used automatically. In another alternative embodiment, the value of the second hyperparameter b may not be selectable. Instead, a fixed, predefined value may be used. For illustration, a default value for the second hyperparameter b may be b=1 though other values may be used.

In an operation **220**, an observation index i is initialized, for example, as i=1.

In an operation **222**, an i^{th} observation vector is selected from input dataset **124**.

In an operation **224**, distances to the k nearest neighbors of the selected i^{th} observation vector are computed using the nearest neighbors search function indicated in operation **208** with the distance function indicated in operation **204**.

In an operation **226**, a closest distance ρ is selected from the computed distances to the k nearest neighbors of the selected i^{th} observation vector.

In an operation **228**, a binary search is used to compute a value for a normalizing factor σ for the selected i^{th} observation vector. For example, the operations of FIG. **2C** may be used to compute the value for normalizing factor σ.

Referring to FIG. **2C**, in an operation **262**, an eleventh indicator of a first bound value τ, a second bound value β, and a tolerance value ε may be received for the binary search. In an alternative embodiment, the eleventh indicator may not be received. For example, a default value(s) may be stored, for example, in computer-readable medium **108** and used automatically. In another alternative embodiment, the value of any of the first bound value τ, the second bound value β, and the tolerance value ε may not be selectable. Instead, a fixed, predefined value(s) may be used. For illustration, a default value for the first bound value τ=0.00001, the second bound value β=1000000, and the tolerance value $\varepsilon=e^{-5}$ though other values may be used.

In an operation **264**, a value for a is computed, for example, using σ=(τ+β)/2.

In an operation **266**, a determination is made concerning whether f(σ)<0, where

$$f(\sigma)=\sum_{j=1}^{k}\frac{1}{1+\frac{\max(0,\,dis_j-\rho)}{\sigma}}-\log_2^k,$$

where dis_j is the distance computed between the j^{th} nearest neighbor and the selected i^{th} observation vector using the distance function indicated in operation **204**. When f(σ)<0, processing continues in an operation **268**. When f(σ)≥0, processing continues in an operation **270**.

In operation **268**, τ=σ, and processing continues in an operation **272**.

In operation **270**, β=σ, and processing continues in operation **272**.

In operation **272**, a determination is made concerning whether |τ−β|<ε. When |τ−β|<ε, processing continues in an operation **274**. When |τ−β|≥ε, processing continues in operation **264**.

In operation **274**, the computation of a is complete and less than the tolerance value E.

Referring again to FIG. **2A**, in an operation **230**, a sigmoid function is applied to compute a distance similarity between each nearest neighbor of the selected i^{th} observation vector as

$$\delta_j=\frac{1}{1+\frac{\max(0,\,dis_j-\rho)}{\sigma}},\ j=1,\ \ldots\ ,k,$$

where δ_j is the distance similarity computed between the j^{th} nearest neighbor and the selected i^{th} observation vector. The computed distance similarity δ_j may be stored in association with the selected i^{th} observation vector. An indicator of the observation vector associated with each nearest neighbor may further be stored. For example, the computed distance similarity δ_j between each nearest neighbor of the selected i^{th} observation vector may be stored as a local fuzzy simplicial set in a manner similar to that described in a paper by Leland McInnes et al. titled UMAP: Uniform Manifold Approximation and Projection for Dimension Reduction published Dec. 6, 2018 at arXiv:1802.03426v2 [stat.ML] (the UMAP paper) though using a generalized sigmoid function

$$\frac{1}{1+\frac{\max(0,\,dis_j-\rho)}{\sigma}}$$

instead of

$$\exp\frac{\max(0,\,dis_j-\rho)}{\sigma},$$

where the fuzzy simplicial set may be defined as

$$fsset(x_i)=\bigcup_{x_j\in KNN(x_i)}\left([x_i,x_j],\ \frac{1}{1+\frac{\max(0,\,dis_j-\rho)}{\sigma}}\right).$$

In an operation **232**, a determination is made concerning whether there is another observation vector included in input dataset **124** to process, for example based on i<N. When i<N, processing continues in an operation **234**. When i≥N, processing continues in an operation **240** shown referring to FIG. **2B**.

In operation **234**, the observation index i is incremented, for example, using i=i+1, and processing continues in operation **222**.

Referring to FIG. **2B**, in operation **240**, a weighted adjacency matrix A is computed. For example, a 1-skeleton of a top-rep is expressed as the weighted adjacency matrix A is used as described in the UMAP paper, where the top-rep is defined as $U_{x\in X}fsset(x_i)$, where X is the set of observation vectors included in input dataset **124**, and

$$A=\begin{bmatrix} w_{11} & \ldots & w_{1N}\\ \vdots & \ddots & \vdots\\ w_{N1} & \ldots & w_{NN}\end{bmatrix}.$$

The weighted adjacency matrix A is a N×N matrix. If x_j is within the KNN of x_i,

$$w_{ij}=\frac{1}{1+\frac{\max(0,\,dis_j-\rho)}{\sigma}},$$

otherwise, $w_{ij}=0$. After calculating the weighted adjacency matrix A, a transformation is applied to matrix A, which may be $B=A+A^T-A^{\circ}A^T$ or $B=A+A^T$, where T indicates a transpose, and indicates a Hadamard product.

In an operation **242**, a degree matrix D is computed from B=

$$\begin{bmatrix} w_{11} & \cdots & w_{1N} \\ \vdots & \ddots & \vdots \\ w_{N1} & \cdots & w_{NN} \end{bmatrix},$$

for example, as described in the UMAP paper using D=

$$\begin{bmatrix} d_1 & & \\ & \ddots & \\ & & d_N \end{bmatrix},$$

where $d_j=\Sigma_{i=1}^{N} w_{ij}$, j=1, 2, . . . , N, if i=j and $d_j=0$ if i≠j.

In an operation **244**, a normalized graph Laplacian matrix L is computed, for example, as described in the UMAP paper as

$$L = D^{-\frac{1}{2}}(D-B)D^{-\frac{1}{2}}.$$

In an operation **246**, a singular value decomposition of the normalized graph Laplacian matrix L is performed to define eigenvectors with associated eigenvalues. For example, the singular value decomposition is defined based on $L=V\Sigma V^T$.

In an operation **248**, d eigenvectors having the smallest eigenvalues are selected from the singular value decomposition V and stored in a matrix Y. Matrix Y includes y_i, i=1, 2, . . . , N, where each y_i is a d-dimensional representation of the i^{th} observation vector included in input dataset **124**. For example, matrix Y is an N×d dimensioned matrix.

In an operation **250**, the optimization method indicated in operation **212** with the hyperparameters indicated in operation **212** and operation **214** is executed with the values of the first hyperparameter α and the second hyperparameter b. For example, using SGD, SGD updates have the form

$$Y_{k+1}=Y_k+\alpha_k g(Y_k)$$

where Y_k denotes a current iterate, a_k the step-size or learning rate value, and $g(Y_k)$ a gradient vector.

The optimization method is computing an optimized solution for matrix Y that includes the d-dimensional transformation of each observation vector included in input dataset **124**. The loss function to be optimized is

$$Loss = -\left(\sum_{(x_i,x_j)\in E} P_{ij}\log Q(i,j) + \sum_{(x_i,x_j)\notin E} \log(1-Q(i,j))\right.$$

where E is a collection of points (x_i, x_1) for which either x_i is one of the k nearest neighbors of x_j or x_j is one of the k nearest neighbors of

$$x_i,\ P_{ij} = P_{j|i} + P_{i|j} - P_{i|j} \odot P_{j|i},$$

$$P_{j|i} = \begin{cases} \delta_j, & \text{if } x_j \text{ is one of the } k \text{ nearest neighbors of } x_i \\ 0, & \text{otherwise} \end{cases},$$

$$P_{i|j} = \begin{cases} \delta_i, & \text{if } x_i \text{ is one of the } k \text{ nearest neighbors of } x_j \\ 0, & \text{otherwise} \end{cases},$$

⊙ indicates component wise multiplication, and

$$Q(i,j) = \frac{1}{\left[1+\left(2^{\frac{1}{b}}-1\right)\|y_i-y_j\|_2^a\right]^b}.$$

The definition of Q(i,j) is based on assuming that a membership strength of y_i and y_i can be modeled using a generalized sigmoid function, which can be expressed as

$$Q(i,j) = \frac{1}{\left[1+\left(2^{\frac{u}{v}}-1\right)\left(\frac{\|y_i-y_j\|_2}{s}\right)^u\right]^{\frac{v}{u}}}$$

Letting α=u and b=v/u,

$$Q(i,j) = \frac{1}{\left[1+\left(2^{\frac{1}{b}}-1\right)\frac{\|y_i-y_j\|_2^a}{s^a}\right]^b}$$

When b=1,

$$Q(i,j) = \frac{1}{1+\frac{\|y_i-y_j\|_2^a}{s^a}}$$

that is equivalent to $\alpha=2b_U$ and $s^{-\alpha}=\alpha_U$, according to the UMAP paper where α_U and b_U are the hyperparameters a and b described in section 3.2 of the UMAP paper.

A simplified version of Q(i,j) can be defined by rescaling by s that results in

$$Q(i,j) = \frac{1}{\left[1+\left(2^{\frac{1}{b}}-1\right)\|y_i-y_j\|_2^a\right]^b}.$$

Using the negative sampling strategy with SGD as described in the UMAP paper, the loss function can be written as

$$\text{Loss} = -\left(\sum_{(x_i x_j)\in E} P_{ij}\log Q(i,j) + \sum_{l=1}^{M}\log(1-Q(i,l))\right.$$

where l indicates an l^{th} negative sample for the i^{th} observation vector. The gradient of the loss function can be computed using

$$\frac{\partial L}{\partial y_i} = -\left(\sum_{(i,j)\in E} P_{ij}\frac{\partial Q(i,j)/\partial y_i}{\partial y_i} - \sum_{l=1}^{M}\frac{\partial Q(i,l)/\partial y_i}{1-Q(i,l)}\right)$$

$$\partial Q(i,j)/\partial y_i = -ab\left(1+(a^{1/b}-1)\|y_i-y_j\|_2^a\right)^{-b-1}\left(2^{\frac{1}{b}}-1\right)\|y_i-y_j\|_2^{a-2}(y_i-y_j)\Big).$$

In an operation **252**, a visualization of the optimized matrix Y is provided, for example, on display **116**. Illustrative graphs that may be presented as part of the visualization are shown in FIGS. **3**A to **3**D, **5**A to **5**D, **8**A to **8**D, **10**A to **10**D, and **12**A to **12**D discussed further below where the data was further clustered.

In operation **254**, a determination is made concerning whether to evaluate another value of b based on the visualization results. When another value of b is to be evaluated, processing continues in an operation **256**. When another value of b is not to be evaluated, processing continues in an operation **258**.

In operation **256**, the tenth indicator of the second hyperparameter b may be received to define a new value for b, and processing continues in operation **250** to compute a new optimized matrix Y.

In operation **258**, the optimized matrix Y is output, for example, to transformed dataset **126**. A cluster assignment may further be output in association with a respective observation vector when clustering is performed of the optimized matrix Y.

The value of the first hyperparameter α is less important than the value of the second hyperparameter b, and setting $\alpha=1$ generally provides satisfactory results. Because the second hyperparameter b controls a rate of the curve approaching 0 and 1, adjusting the value of the second hyperparameter b can affect the embeddings in low-dimensional space and, as a result, the data visualization. Referring to FIG. **14**, a behavior of

$$Q(i,j)=\frac{1}{\left[1+\left(2^{\frac{1}{b}}-1\right)\|y_i-y_j\|_2^{\alpha}\right]^b}$$

with varying values of the second hyperparameter b is shown in accordance with an illustrative embodiment. A first curve **1400** shows a curve shape with b=0.5; a second curve **1402** shows a curve shape with b=1; a third curve **1404** shows a curve shape with b=2; a fourth curve **1406** shows a curve shape with b=5; and a fifth first curve **1408** shows a curve shape with b=10. The smaller the value of the second hyperparameter b, the more heavy-tailed the curve is. The heavy-tail property of the curve can greatly alleviate the crowding problem when embedding high-dimensional data in a low-dimensional space and thus, provides the capability of revealing a finer structure of the data included in input dataset **124**.

A performance of transformation application **122** was evaluated. The performance of transformation application **122** was compared to the UMAP method described in the UMAP paper on an image classification task using a first dataset. The first dataset was randomly generated to include 1,000 observations defined by 20 dimensions. The observations were evenly distributed among 10 clusters with each cluster including 100 observations. Within each cluster, the first 50 observations were randomly sampled from a Gaussian distribution with mean $\mu_i=5e_i+2.3e_{10+i}$ and the other 50 observations were randomly sampled from a Gaussian distribution with mean $\mu_i=5e_i-2.3e_{10+i}$, where e_i is an i^{th} basis vector and i=1, 2, . . . , 10. The first dataset should be separable into 10 distinct clusters. Within each big cluster, the first dataset should be classified into two subclusters or at least have a "dumbbell" shape due to the different mean values. All of the observations had covariance I_{20}. For each of four executions, k=10, $\alpha=1$, and b=0.5, 1, 2, 10, respectively. The UMAP method was also executed four times using k=10 and min_dist=0.001, 0.01, 0.1, 1, respectively. Initial values of the embedding were set to be the two eigenvectors with minimum eigenvalues of the normalized Laplacian, and the SGD with negative sampling algorithm was performed using 500 epochs. A Euclidean distance function was used.

Referring to FIGS. **3**A through **3**D, comparative clustering results are shown using transformation application **124** with b=0.5, 1, 2, 10, respectively, with the first dataset in accordance with an illustrative embodiment. Referring to FIGS. **3**A through **3**D, the big clusters were well separated from each other for all of the four values b=0.5, 1, 2, 10. In addition, when b=0.5 and 1, a majority of the big clusters were separated into two isolated subclusters. For the rest of the big clusters, the dumbbell shape was clearly visible as well. With the increasing values of b, the two subclusters within each cluster got closer and closer and eventually merged into one cluster. However, even with b=10, the dumbbell shape within each big cluster remained clearly visible.

Referring to FIGS. **4**A through **4**D, comparative clustering results are shown using the UMAP method with min_dist=0.001, 0.01, 0.1, 1, respectively, and with the first dataset in accordance with an illustrative embodiment. Referring to FIG. **4**A, even with min_dist=0.001, the subclusters within each big cluster are not well separated though the dumbbell shape is visible for some of the clusters. With increasing values of min_dist, the distances between different clusters decrease, and the dumbbell shape is lost within several clusters. There is further not much difference between FIGS. **4**A and **4**B.

The performance of transformation application **122** was compared to the UMAP method using four different real datasets. For each of the four real datasets, k=10, $\alpha=1$, and b=1, 2, 5, 10, respectively. The UMAP method was also executed four times using k=10 and min_dist=0.001, 0.01, 0.1, 1, respectively. Initial values of the embedding were set to be the two eigenvectors with minimum eigenvalues of the normalized Laplacian, and the SGD with negative sampling algorithm was performed using 500 epochs. A Euclidean distance function was used.

The performance of transformation application **122** was compared to the UMAP method on an image classification task using a second dataset known as the FASHION-MNIST dataset described in H. Xiao et al., *Fashion-MNIST: A Novel Image Dataset for Benchmarking Machine Learning Algorithms*, arXiv preprint, arXiv:1708.07747 (2017). The second dataset included 70,000 images of 10 classes of fashion items (clothing, footwear, and bags). Because the images were gray-scale images the feature dimension was 784 based on the 28×28 pixels size of each image.

Referring to FIGS. **5**A through **5**D, comparative clustering results are shown using transformation application **124** with b=1, 2, 5, 10, respectively, and with the second dataset in accordance with an illustrative embodiment. The legend indicates 0—t-short/top, 1—trouser, 2—pullover, 3—dress, 4—coat, 5—sandal, 6—shirt, 7—sneaker, 8—bag, and 9—ankle boot. Referring to FIGS. **5**A through **5**D, trousers (red) and bags (blue) always had the greatest distance from each other. In addition, shoes, bags, trousers, and other clothes (T-shirts, dresses, pullovers, shirts, and coats) were well separated when b=1 and 2. When b=5 and 10, bags and other clothes get much closer to each other and there are no longer distinct clusters. When b=1 and 2, a few subclusters were visible that were invisible when b=5 and 10. For example, a majority of the T-shirts (dark red) and dresses (orange) indicated by a first circle **500** were separated from coats (yellow), pullovers (vermilion), and shirts (light green) indicated by a second circle **502**. A majority of the sneakers (green), ankle boots (purple), and sandals (lemon) were separated as well. In addition, sandals approximately indicated by a third circle **504** and a fourth circle **506** were separated into two subclusters. A first subcluster approximately indicated by third circle **504** was close to sneakers, a second subcluster approximately indicated by fourth circle **506** was close to ankle boots. In addition, bags approximately indicated by a fifth circle **508** were separated into two subclusters.

To verify whether the subclusters were meaningful, 100 images were randomly sampled from each of the subclusters, and the images were compared. The comparison results are summarized in FIGS. **7**A through **7**F. Referring to FIGS. **7**A and **7**B, the separation of T-shirts and dresses from other clothing is due to long or short sleeves. Referring to FIGS. **7**C and **7**D, the separation of bags into two subclusters is due to one subcluster that includes a majority of the bags having handles showing at the top of the image, and another subcluster that either includes bags without a handle or where the handle is not showing at the top of the image. Referring to FIGS. **7**E and **7**F, the images of sandals also show that the majority of the sandals in one subcluster have middle or high heels; whereas, the sandals in the other subcluster were relatively flat. These image comparisons clearly show that the subclusters revealed by b=1 and 2 define meaningful subclusters that provide additional insight into the second dataset.

Referring to FIGS. **6**A through **6**D, comparative clustering results are shown using the UMAP method with min_dist=0.001, 0.01, 0.1, 1, respectively, and with the second dataset in accordance with an illustrative embodiment.

The performance of transformation application **122** was compared to the UMAP method on an image classification task using a third dataset known as the MNIST dataset described in Y. Lecun and C. Cortes, *The MNIST Database of Handwritten Digit Images for Machine Learning Research*, IEEE Signal Processing Magazine 29:141-142 (2012). The third dataset included 70,000 images of the handwritten digits 0-9. Because the images were gray-scale images the feature dimension was 784 based on the 28×28 pixels size of each image. The legend indicates the handwritten digit.

Referring to FIGS. **8**A through **8**D, comparative clustering results are shown using transformation application **124** with b=1, 2, 5, 10, respectively, with the third dataset in accordance with an illustrative embodiment. Referring to FIG. **8**A, the clusters have the largest separation. For example, all the digits were separated into distinct clusters. With increasing values of b, the distances between different digits became smaller and smaller. Some digits, such as 4, 7, and 9, and 3, 5, and 8, eventually joined together into clusters. Based on the embeddings and using k-means clustering to perform classification, the smallest error of 4.4% resulted when b=1 and 2.

Referring to FIGS. **9**A through **9**D, comparative clustering results are shown using the UMAP method with min_dist=0.001, 0.01, 0.1, 1, respectively, with the third dataset in accordance with an illustrative embodiment.

The performance of transformation application **122** was compared to the UMAP method on an image classification task using a fourth dataset known as the Turbofan dataset described in A. Saxena and K. Goebel, *Turbofan Engine Degradation Simulation data set*, NASA Ames Prognostics Data Repository, NASA Ames Research Center, Moffett Field, Calif. (2008). The fourth dataset describes engine degradation data simulated under different combinations of operational conditions. The fourth dataset included 21 sensor measurements for 260 engines under six operational conditions recorded until the engine failed. All of the engines were assumed to operate normally at the beginning of the data collection. The fourth dataset included 53,759 observations.

Referring to FIGS. **10**A through **10**D, comparative clustering results are shown using transformation application **124** with b=1, 2, 5, 10, respectively, with the fourth dataset in accordance with an illustrative embodiment. A flight condition indicator was removed from the fourth dataset. Using the readings from only the 21 sensors, the fourth dataset was clustered or classified into six operational categories with high accuracy. For each cluster, readings taken close to a fault point were approximately on an edge of the embedding (blue color). The colors show the relative life cycle of the engine when each reading is recorded. Each reading is one observation in the fourth dataset.

To further investigate the engine degradation process, the impact of different flight conditions was removed by subtracting the average reading measurement for each sensor at each flight condition and re-executing transformation application **124** with b=1, 2, 5, 10. Referring to FIGS. **10**E through **10**H, clustering results are shown using transformation application **124** with b=1, 2, 5, 10, respectively, with the modified fourth dataset in accordance with an illustrative embodiment. The cluster results clearly show that the sensor readings in the early stage of the study mainly concentrate on one side of the graph and the readings close to the fault points mainly concentrate on the other side of the graph with the tail. Referring to FIG. **10**E, with b=1, the readings recorded at a similar stage of an engine's life cycle tended to concentrate together.

Referring to FIGS. **11**A through **11**D, comparative clustering results are shown using the UMAP method with min_dist=0.001, 0.01, 0.1, 1, respectively, with the fourth dataset in accordance with an illustrative embodiment.

The performance of transformation application **122** was compared to the UMAP method on an image classification task using a fifth dataset known as the COIL-**20** dataset described in S. A. Nene et al., Columbia Object Image Library (1996). The fifth dataset included 1,440 gray-scale images of 20 objects for 72 rotations spanning 360 degrees. Because the images were gray-scale images the feature dimension was 784 based on the 28×28 pixels size of each image. The legend indicates the object.

Referring to FIGS. **12**A through **12**D, comparative clustering results are shown using transformation application **124** with b=1, 2, 5, 10, respectively, with the fifth dataset in accordance with an illustrative embodiment. The results show good separation between all 20 clusters for all values of b. With increasing values of b, a between-class distance for different objects becomes smaller and smaller, which can cause problems for data clustering. However, a circular structure of each object becomes more discernible with a higher value of b. Object 1 was classified into three subclusters **1200** (light blue color). Some of the object 1 images were randomly sampled from each of the three subclusters. The subclusters were formed mainly based on a direction of the arrow (downward, upward, and horizontally).

Referring to FIGS. **13**A through **13**D, comparative clustering results are shown using the UMAP method with min_dist=0.001, 0.01, 0.1, 1, respectively, with the fifth dataset in accordance with an illustrative embodiment. The legend indicates the object.

In general, the UMAP method generated good cluster visualizations for each dataset with the majority of the clusters well separated. However, the UMAP method failed to separate some clusters that were very similar to each other and failed to reveal the subtle subclusters discussed above with any value of min_dist. As a result, adjusting min_dist is insufficient to obtain a finer cluster structure.

There are applications for transformation application **122** in many areas such as process control and equipment health monitoring, image processing and classification, data segmentation, data analysis, voice processing and recognition, etc. The presented results demonstrate improved identification of meaningful subclusters that were similar but had distinguishable characteristics. The explosion of digital data is generating many opportunities for big data analytics, which in turn provides many opportunities for training cluster models to capitalize on the information contained in the data—to make better predictions that lead to better decisions.

The word "illustrative" is used herein to mean serving as an example, instance, or illustration. Any aspect or design described herein as "illustrative" is not necessarily to be construed as preferred or advantageous over other aspects or designs. Further, for the purposes of this disclosure and unless otherwise specified, "a" or "an" means "one or more". Still further, using "and" or "or" in the detailed description is intended to include "and/or" unless specifically indicated otherwise. The illustrative embodiments may be implemented as a method, apparatus, or article of manufacture using standard programming and/or engineering techniques to produce software, firmware, hardware, or any combination thereof to control a computer to implement the disclosed embodiments.

The foregoing description of illustrative embodiments of the disclosed subject matter has been presented for purposes of illustration and of description. It is not intended to be exhaustive or to limit the disclosed subject matter to the precise form disclosed, and modifications and variations are possible in light of the above teachings or may be acquired from practice of the disclosed subject matter. The embodiments were chosen and described in order to explain the principles of the disclosed subject matter and as practical applications of the disclosed subject matter to enable one skilled in the art to utilize the disclosed subject matter in various embodiments and with various modifications as suited to the particular use contemplated.

What is claimed is:

1. A non-transitory computer-readable medium having stored thereon computer-readable instructions that when executed by a computing device cause the computing device to:

(A) select an observation vector from a plurality of observation vectors, wherein each observation vector of the plurality of observation vectors includes a value for each variable of a plurality of variables, wherein the plurality of variables define a high-dimensional space;

(B) compute a distance between the selected observation vector and each observation vector of the plurality of observation vectors;

(C) select a plurality of nearest neighbors to the selected observation vector using the computed distances, wherein a number of the plurality of nearest neighbors is a predefined number, wherein each nearest neighbor of the plurality of nearest neighbors is one of the plurality of observation vectors that are closest to the selected observation vector;

(D) apply a first sigmoid function to compute a distance similarity value between the selected observation vector and each of the selected plurality of nearest neighbors based on the value of each variable of the plurality of variables of the selected observation vector and on the value of each variable of the plurality of variables of each of the plurality of nearest neighbors;

repeat (A) through (D) with each observation vector of the plurality of observation vectors selected as the observation vector in (A), wherein each of the computed distance similarity values computed in (D) are added to a first matrix;

compute an initial matrix from the plurality of observation vectors, wherein the initial matrix represents a transformation of each observation vector of the plurality of observation vectors into a low-dimensional space defined to include a predefined number of dimensions, wherein the predefined number of dimensions is less than a number of the plurality of variables;

execute an optimization method with the computed initial matrix, the first matrix, and a gradient of a second sigmoid function that computes a second distance similarity value between the selected observation vector and each of the plurality of nearest neighbors in the low-dimensional space, wherein the optimization method determines an optimized matrix that represents a transformation of each observation vector of the plurality of observation vectors into the low-dimensional space; and

output the optimized matrix.

2. The non-transitory computer-readable medium of claim **1**, wherein the computer-readable instructions further cause the computing device to present a visualization of the optimized matrix in a display.

3. The non-transitory computer-readable medium of claim **1**, wherein the computer-readable instructions further cause the computing device to train a clustering model with the optimized matrix to define a plurality of clusters in the low-dimensional space, wherein each observation vector of the plurality of observation vectors is assigned to a single cluster, and to present a visualization of the defined plurality of clusters in a display.

4. The non-transitory computer-readable medium of claim **1**, wherein the predefined number of dimensions is two or three.

5. The non-transitory computer-readable medium of claim **1**, wherein the first sigmoid function is

$$\delta_j = \frac{1}{1 + \frac{\max(0, dis_j - \rho)}{\sigma}},\ j = 1, \ldots, k,$$

where δ_j is the distance similarity value between a j^{th} nearest neighbor and the selected observation vector, dis_j is the distance computed between the j^{th} nearest neighbor and the selected observation vector, σ is a normalizing factor value, ρ is a distance to a closest nearest neighbor of the plurality of nearest neighbors, and k is the number of the plurality of nearest neighbors.

6. The non-transitory computer-readable medium of claim **5**, wherein the distance between the j^{th} nearest neighbor and the selected observation vector is computed using a Euclidean distance function.

7. The non-transitory computer-readable medium of claim **5**, wherein a binary search is used to compute a value for a for the selected observation vector.

8. The non-transitory computer-readable medium of claim **7**, wherein the binary search is based on solving

$$\sum_{j=1}^{k} \frac{1}{1+\frac{\max(0, dis_j-\rho)}{\sigma}} = \log_2 k.$$

9. The non-transitory computer-readable medium of claim **5**, wherein the first matrix is computed using $P_{ij}=P_{j|i}+P_{i|j}-P_{i|j}\odot P_{j|i}$, where $P_{j|i}=\delta_j$ when x_j is one of the plurality of nearest neighbors of the selected observation vector indicated as x_i, and is zero otherwise, $P_{i|j}=\delta_i$ when x_i is one of the plurality of nearest neighbors of x_j, and is zero otherwise, and $\odot$ indicates a component wise multiplication.

10. The non-transitory computer-readable medium of claim **1**, wherein the second sigmoid function is

$$Q(i,j) = \frac{1}{\left[1+\left(2^{\frac{1}{b}}-1\right)\|y_i-y_j\|_2^a\right]^b},$$

where α is a first predefined hyperparameter value, b is a second predefined hyperparameter value, y_i is an i^{th} observation vector transformed into the low-dimensional space, and y_i is a j^{th} observation vector transformed into the low-dimensional space.

11. The non-transitory computer-readable medium of claim **10**, wherein $\alpha=1$.

12. The non-transitory computer-readable medium of claim **10**, wherein the gradient of the second sigmoid function is computed using $\partial Q(i,j)/\partial y_i=-ab(1+(a^{1/b}-1)\|y_i-y_j|_2^{\alpha})^{-b-1}(2^{1/b}-1)\|y_i-y_j|_2^{\alpha-2}(y_i-y_j))$.

13. The non-transitory computer-readable medium of claim **10**, wherein a loss function optimized using the optimization method is $Loss=-\Sigma_{(x_i,x_j)\in E}P_{ij}\log Q(i,j)+\Sigma_{(x_i,x_j)\in E}\log(1-Q(i,j))$, where E is a collection of observation vectors (x_i, x_j) for which either x_i is one of the plurality of nearest neighbors of x_j or x_j is one of the plurality of nearest neighbors of x_j, x_i is an i^{th} observation vector of the plurality of observation vectors, and x_j is a j^{th} observation vector of the plurality of observation vectors, and P_{ij} is the first matrix.

14. The non-transitory computer-readable medium of claim **13**, wherein the first matrix is computed using $P_{ij}=P_{j|i}+P_{i|j}-P_{i|j}\odot P_{j|i}$, where $P_{j|i}=\delta_j$ when x_j is one of the plurality of nearest neighbors of the selected observation vector indicated as x_i, and is zero otherwise, $P_{i|j}=\delta_i$ when x_i is one of the plurality of nearest neighbors of x_j, and is zero otherwise, $\odot$ indicates a component wise multiplication, δ_j is the distance similarity value between a j^{th} nearest neighbor and the selected observation vector, and δ_i is the distance similarity value between the selected observation vector and the j^{th} nearest neighbor.

15. The non-transitory computer-readable medium of claim **14**, wherein the first sigmoid function is

$$\delta_j = \frac{1}{1+\frac{\max(0, dis_j-\rho)}{\sigma}},\ j=1, \ldots, k,$$

where dis_j is the distance computed between the j^{th} nearest neighbor and the selected observation vector, σ is a normalizing factor value, ρ is a distance to a closest nearest neighbor of the plurality of nearest neighbors, and k is a number of the plurality of nearest neighbors.

16. The non-transitory computer-readable medium of claim **15**, wherein the distance between the j^{th} nearest neighbor and the selected observation vector is computed using a Euclidean distance function.

17. The non-transitory computer-readable medium of claim **1**, wherein computing the initial matrix from the plurality of observation vectors comprises:

computing a weighted adjacency matrix from the plurality of observation vectors;

transforming the computed weighted adjacency matrix;

computing a degree matrix from the transformed computed weighted adjacency matrix;

computing a Laplacian matrix from the computed degree matrix;

decomposing the computed Laplacian matrix to define a plurality of eigenvectors; and

selecting a second plurality of eigenvectors from the defined plurality of eigenvectors, wherein a number of the second plurality of eigenvectors is the predefined number of dimensions,

wherein the selected second plurality of eigenvectors define the initial matrix.

18. The non-transitory computer-readable medium of claim **17**, wherein the weighted adjacency matrix is computed using

$$A = \begin{bmatrix} w_{11} & \ldots & w_{1N} \\ \vdots & \ddots & \vdots \\ w_{N1} & \ldots & w_{NN} \end{bmatrix},$$

where A is the weighted adjacency matrix, N is a number of the plurality of observation vectors,

$$w_{ij} = \frac{1}{1+\frac{\max(0, dis_j-\rho)}{\sigma}},\ i=1, 2, \ldots, N,\ j=1, 2, \ldots, N,$$

when a j^{th} observation vector x_i is one of the plurality of nearest neighbors of an i^{th} observation vector x_i, otherwise, $w_{ij}=0$; dis_j is a distance computed between the j^{th} observation vector x_j and the i^{th} observation vector x_i, σ is a normalizing factor value, ρ is a distance to a closest nearest neighbor of the plurality of nearest neighbors of the observation vector x_i.

19. The non-transitory computer-readable medium of claim **17**, wherein the weighted adjacency matrix is transformed using $B=A+A^T-A^{\circ}A^T$, where B is the transformed computed weighted adjacency matrix, A is the weighted adjacency matrix, T indicates a transpose, and $^{\circ}$ indicates a Hadamard product.

20. The non-transitory computer-readable medium of claim **17**, wherein the degree matrix is computed using

$$D = \begin{bmatrix} d_1 & & \\ & \ddots & \\ & & d_N \end{bmatrix},$$

where $d_j=\Sigma_{i=1}^{N}w_{ij}$, $j=1, 2, \ldots, N$, if i=j and $d_j\neq 0$ if $i\neq j$, and w_{ij} is an $(i,j)^{th}$ entry of the transformed computed weighted adjacency matrix.

21. The non-transitory computer-readable medium of claim 17, wherein the Laplacian matrix is computed using

$$L = D^{-\frac{1}{2}}(D - B)D^{-\frac{1}{2}},$$

where L is the Laplacian matrix, D is the degree matrix, and B is the transformed computed weighted adjacency matrix.

22. The non-transitory computer-readable medium of claim 17, wherein the selected second plurality of eigenvectors have smallest eigenvalues of the plurality of eigenvectors.

23. The non-transitory computer-readable medium of claim 1, wherein the optimization method is based on a stochastic gradient descent algorithm.

24. A computing device comprising:

a processor; and

a computer-readable medium operably coupled to the processor, the computer-readable medium having computer-readable instructions stored thereon that, when executed by the processor, cause the computing device to

(A) select an observation vector from a plurality of observation vectors, wherein each observation vector of the plurality of observation vectors includes a value for each variable of a plurality of variables, wherein the plurality of variables define a high-dimensional space;

(B) compute a distance between the selected observation vector and each observation vector of the plurality of observation vectors;

(C) select a plurality of nearest neighbors to the selected observation vector using the computed distances, wherein a number of the plurality of nearest neighbors is a predefined number, wherein each nearest neighbor of the plurality of nearest neighbors is one of the plurality of observation vectors that are closest to the selected observation vector;

(D) apply a first sigmoid function to compute a distance similarity value between the selected observation vector and each of the selected plurality of nearest neighbors based on the value of each variable of the plurality of variables of the selected observation vector and on the value of each variable of the plurality of variables of each of the plurality of nearest neighbors;

repeat (A) through (D) with each observation vector of the plurality of observation vectors selected as the observation vector in (A), wherein each of the computed distance similarity values computed in (D) are added to a first matrix;

compute an initial matrix from the plurality of observation vectors, wherein the initial matrix represents a transformation of each observation vector of the plurality of observation vectors into a low-dimensional space defined to include a predefined number of dimensions, wherein the predefined number of dimensions is less than a number of the plurality of variables;

execute an optimization method with the computed initial matrix, the first matrix, and a gradient of a second sigmoid function that computes a second distance similarity value between the selected observation vector and each of the plurality of nearest neighbors in the low-dimensional space, wherein the optimization method determines an optimized matrix that represents a transformation of each observation vector of the plurality of observation vectors into the low-dimensional space; and

output the optimized matrix.

25. A method of transforming high-dimensional data into low-dimensional data, the method comprising:

(A) selecting, by a computing device, an observation vector from a plurality of observation vectors, wherein each observation vector of the plurality of observation vectors includes a value for each variable of a plurality of variables, wherein the plurality of variables define a high-dimensional space;

(B) computing, by the computing device, a distance between the selected observation vector and each observation vector of the plurality of observation vectors;

(C) selecting, by the computing device, a plurality of nearest neighbors to the selected observation vector using the computed distances, wherein a number of the plurality of nearest neighbors is a predefined number, wherein each nearest neighbor of the plurality of nearest neighbors is one of the plurality of observation vectors that are closest to the selected observation vector;

(D) applying, by the computing device, a first sigmoid function to compute a distance similarity value between the selected observation vector and each of the selected plurality of nearest neighbors based on the value of each variable of the plurality of variables of the selected observation vector and on the value of each variable of the plurality of variables of each of the plurality of nearest neighbors;

repeating, by the computing device, (A) through (D) with each observation vector of the plurality of observation vectors selected as the observation vector in (A), wherein each of the computed distance similarity values computed in (D) are added to a first matrix;

computing, by the computing device, an initial matrix from the plurality of observation vectors, wherein the initial matrix represents a transformation of each observation vector of the plurality of observation vectors into a low-dimensional space defined to include a predefined number of dimensions, wherein the predefined number of dimensions is less than a number of the plurality of variables;

executing, by the computing device, an optimization method with the computed initial matrix, the first matrix, and a gradient of a second sigmoid function that computes a second distance similarity value between the selected observation vector and each of the plurality of nearest neighbors in the low-dimensional space, wherein the optimization method determines an optimized matrix that represents a transformation of each observation vector of the plurality of observation vectors into the low-dimensional space; and

outputting, by the computing device, the optimized matrix.

26. The method of claim 25, wherein the first sigmoid function

$$\delta_j = \frac{1}{1 + \frac{\max(0, dis_j - \rho)}{\sigma}}, j = 1, \ldots, k,$$

where δ_j is the distance similarity value between a j^{th} nearest neighbor and the selected observation vector, dis_j is the distance computed between the j^{th} nearest neighbor and the selected observation vector, σ is a normalizing factor value, ρ is a distance to a closest nearest neighbor of the plurality of nearest neighbors, and k is the number of the plurality of nearest neighbors.

27. The method of claim **26**, wherein the first matrix is computed using $P_{ij}=P_{j|i}+P_{i|j}-P_{i|j}\odot P_{j|i}$, where $P_{j|i}=\delta_j$ when x_j is one of the plurality of nearest neighbors of the selected observation vector indicated as x_i, and is zero otherwise, $P_{i|j}=\delta_i$ when x_i is one of the plurality of nearest neighbors of x_j, and is zero otherwise, and $\odot$ indicates a component wise multiplication.

28. The method of claim **25**, wherein the second sigmoid function is

$$Q(i, j) = \frac{1}{\left[1 + \left(2^{\frac{1}{b}} - 1\right)\|y_i - y_j\|_2^{\alpha}\right]^{b}},$$

where α is a first predefined hyperparameter value, b is a second predefined hyperparameter value, y_i is an i^{th} observation vector transformed into the low-dimensional space.

29. The method of claim **28**, wherein $\alpha=1$.

30. The method of claim **28**, wherein the gradient of the second sigmoid function is computed using $\partial Q(i,j)/\partial y_i=-\alpha b(\alpha^{1/b}-^{1})\|y_i-y_j\|)_2{}^{\alpha})^{-b-1}(2^{1/b}-1)\|y_i-y_j\|_2{}^{\alpha-2}(y_i-y_j))$.

* * * * *